

## Distribution Agreement

In presenting this thesis or dissertation as a partial fulfillment of the requirements for an advanced degree from Emory University, I hereby grant to Emory University and its agents the non-exclusive license to archive, make accessible, and display my thesis or dissertation in whole or in part in all forms of media, now or hereafter known, including display on the world wide web. I understand that I may select some access restrictions as part of the online submission of this thesis or dissertation. I retain all ownership rights to the copyright of the thesis or dissertation. I also retain the right to use in future works (such as articles or books) all or part of this thesis or dissertation.

Signature:

\_\_\_\_\_  
Daniel Chopyk

\_\_\_\_\_  
Date

Mechanisms of intestinal barrier disruption in acute and chronic liver injury

By

Daniel M. Chopyk  
Doctor of Philosophy

Graduate Division of Biological and Biomedical Sciences  
Immunology and Molecular Pathogenesis

---

Arash Grakoui, Ph.D.  
Advisor

---

Mark Czaja, M.D.  
Committee Member

---

Brian Evavold, Ph.D.  
Committee Member

---

Joshy Jacob, PhD  
Committee Member

---

Malú Tansey, Ph.D.  
Committee Member

Accepted:

---

Lisa A. Tedesco, Ph.D.  
Dean of the James T. Laney School of Graduate Studies

---

Date

Mechanisms of intestinal barrier disruption in acute and chronic liver injury

By

Daniel M. Chopyk  
B.S., Case Western Reserve University, 2012

Advisor: Arash Grakoui, Ph.D.

An abstract of  
A dissertation submitted to the Faculty of the  
James T. Laney School of Graduate Studies of Emory University  
in partial fulfillment of the requirements for the degree of  
Doctor of Philosophy  
in Graduate Division of Biological and Biomedical Sciences in  
Immunology and Molecular Pathogenesis  
2019

## Abstract

### Mechanisms of intestinal barrier disruption in acute and chronic liver injury By Daniel M. Chopyk

Enhanced intestinal permeability is recognized in various liver disease settings. The intestine houses a complex ecosystem of commensal microorganisms. Paramount to intestinal physiology is maintenance of homeostatic compartmentalization of these microbes by forming a tight, yet selectively permeable barrier. The gut barrier is composed of several constituent parts including epithelial, mucus, and immunological components. Compromise of any aspect of this barrier contributes to intestinal leakiness and bacterial translocation. Translocated microbes and their toxins gain immediate access to the liver via the portal circulation where they induce potent inflammatory reactions. Persistent hepatic inflammation driven by gut leakiness is thus thought to be a primary contributor to disease pathogenesis. In this dissertation, we sought to characterize underrecognized aspects of intestinal epithelial barrier dysfunction that contribute to chronic and acute liver injury.

We first explored the setting of alcoholic liver disease (ALD), a chronic condition of increasing clinical significance that remains without effective treatments. Using an *in vitro* system of intestinal epithelial monolayers, we identified the tight junction protein junctional adhesion molecule-A (JAM-A) as a potential target of ethanol-induced gut barrier collapse. Alcohol treatment brought a 30% reduction in JAM-A protein expression and was associated with perturbations in JAM-A signaling targets at earlier time points.

We next examined whether gut permeability contributes to the pathogenesis of acute liver injury using a model of acetaminophen (APAP) overdose. APAP toxicity remains the leading cause of acute liver failure in the western world. We found that intestinal permeability rapidly and markedly increases following APAP intoxication. Gut permeability coincided with marked intestinal apoptosis, which was strikingly limited to cells within the intestinal crypts. With the use of specialized reporter mice, we confirmed that APAP-sensitive cells were predominantly classified as *LGR5*<sup>+</sup> stem cells. This suggests that enterotoxicity during APAP intoxication has potentially long-lived consequences.

In summary, this dissertation adds significant knowledge to our understanding of gut barrier physiology by: 1) identifying new molecular targets of ethanol-induced gut barrier disruption; and 2) identifying a novel extrahepatic toxicity following high-dose APAP consumption. Moreover, this work identifies *LGR5*<sup>+</sup> stem cell death and dysfunction as a novel potential mechanism of intestinal barrier compromise.

Mechanisms of intestinal barrier disruption in acute and chronic liver injury

By

Daniel M. Chopyk  
B.S., Case Western Reserve University, 2012

Advisor: Arash Grakoui, Ph.D.

A dissertation submitted to the Faculty of the  
James T. Laney School of Graduate Studies of Emory University  
in partial fulfillment of the requirements for the degree of  
Doctor of Philosophy  
in Graduate Division of Biological and Biomedical Sciences in  
Immunology and Molecular Pathogenesis  
2019

## Acknowledgements

I would like to thank:

- Arash Grakoui, for his support and insightful scientific critique that helped push me past my limits that helped me develop confidence in my own abilities. I am especially grateful for his willingness to take direct mentorship over my training upon the announcement of Dr. Anania's resignation late into my training.
- My loving wife Krystal for her patience in supporting me through my research endeavors and all the associated stress that came along with it. I doubt anyone else could understand what I put her through on many nights, and no matter what she had always helped see me through my troubles in the end. I additionally thank her for all the time and effort she put into preparing finalized, professional versions of my figures, posters, and illustrations with her graphic design skills.
- All members of the Anania lab, especially Pradeep Kumar, who I shared the most time with in lab and who I consider a valuable mentor and friend. He always was there to hold me up when things looked down and offered valuable scientific critique.
- All members of the Grakoui lab, who welcomed me warmly into their research group during my fourth year of graduate studies. I felt that I have undergone tremendous professional growth under their guidance and friendship and will be forever grateful for this experience. I am especially grateful for Manoj Thapa for the direct mentorship he has provided me in both my independent projects and our collaborative efforts. I am also equally as grateful for Eduardo Salinas for his valuable scientific insight, friendship, and aid in supporting me through a number of personal and professional problems over the past year and a half.
- All of the close friends that I have come to make since moving to Atlanta, who have provided me with tremendous personal support in persisting through the challenges posed by graduate school. I am especially grateful for Toshihiro and Yuki Umehara, John DuConge', and Shunji and Rieko Sakamoto for their warmth, generosity, and understanding.
- My parents Vera and Michael Chopyk for their everlasting support of my educational endeavors, and in their personal support through personal hardship. I am also especially grateful for my mother-in-law Marie Williams for her equal love and support, which is far above what I believe myself to deserve.
- My grandparents Alexandra and George Mackiw, who believed in my capabilities and provided endless support as well. I dedicate much of this work in loving memory of Alexandra, who sadly left us just under a year ago. Few people on this earth can match her generosity, kindness, and personal strength.

## Table of Contents

### Chapter 1: Physiology of the gut barrier and its contribution to diseases of the

liver and other target organs -----

1. Introduction -----1

2. Components of the gut barrier-----3

2.1 Epithelial barrier -----3

2.2 Mucus barrier -----19

2.3 Immune barrier -----22

2.4 Microbial barrier -----27

3. Pathological derangements of gut barrier -----30

4. Highlights of gut permeability in specific diseases -----

4.1 Alcoholic liver disease -----33

4.2 Non-alcoholic fatty liver disease -----34

4.3 Drug-induced liver injury -----37

4.4 Primary sclerosing cholangitis -----39

4.5 Neurological and other disorders -----42

5. Summary and future directions -----44

6. Conclusion -----44

Figures -----46

### Chapter 2: Dysregulation of junctional adhesion molecule-A contributes to

ethanol-induced barrier disruption in intestinal epithelial cell monolayers -----51

Abstract -----52

Introduction -----54

<b>Materials and methods</b>	56
<b>Results</b>	66
<b>Discussion</b>	72
<b>Figures</b>	76
<b>Chapter 3: Acetaminophen intoxication rapidly induces apoptosis of intestinal crypt stem cells and enhances intestinal permeability</b>	91
<b>Abstract</b>	93
<b>Introduction</b>	94
<b>Experimental procedures</b>	97
<b>Results</b>	102
<b>Discussion</b>	107
<b>Figures</b>	111
<b>Chapter 4: Discussion</b>	120
<b>Tight junction dysfunction in ALD</b>	121
<b>Intestinal permeability and intestinal stem cell injury in APAP ALF</b>	124
<b>Final Reflections</b>	127
<b>References</b>	128

## **Chapter 1: Physiology of the gut barrier and its contribution to diseases of the liver and other target organs**

Over the past decade there has been an increasing appreciation amongst medical researchers for the need to study the body as an indivisible unit rather than organs in isolation. Most biological processes in both health and disease involve significant crosstalk between distant sites, and technological innovation has empowered us to more accurately analyze these intricate networks of cross-organ communication. In this rapidly evolving area of study, the intestine has been the subject of most excitement and attention owing to the increased recognition of enhanced intestinal permeability that occurs in a tremendously diverse array of pathological processes (1-5). Intertwined with this intestinal physiology is the recognition of dramatic health-modulating functions of the gut microbiome (1, 6). Astonishingly, our increased appreciation of intestinal permeability and the intestinal microbiome has provided answers to previously inexplicable variability observed throughout research literature even in studies conducted using genetically identical animals (7). While this appears true for virtually every disease process imaginable, disorders of the liver have been under particular focus due to the close anatomical and physiological connections between these two organs (1).

There is a myriad of reasons for the prominent role of intestinal physiology as a critical regular of health and disease. The gut represents the largest mucosal surface in the body which has the most amount of contact with our external environment. It is therefore unsurprising that the intestine houses the largest number of immune cells in our body, which has significant consequences for host immunity and vaccine design (8).

Further, the intestinal tract is colonized by countless bacteria that far outnumber our own cellular content by a factor of at least ten to one (9). This complex network of microbes can have dramatic effects on host health and is maintained in a delicate balance that is determined in part by host genetics and dietary factors (1, 6). A tightly regulated barrier is critical in proper compartmentalization of these bacterial populations (10). Once any aspect of this barrier is compromised, the gut environment offers several methods of entry for systemic dissemination of microbes and toxins. Most relevant to liver physiology is entrance into the hepatic portal circulation (1). While this is the most well-studied method of gut-liver crosstalk, the intestinal lamina propria is also highly enriched in lymphatic vessels for quick and easy access to the mesenteric lymph nodes and eventual drainage into the systemic venous circulation (1, 11). Finally, it is also important to remember that the gut is innervated by several hundred million neurons. While certainly a less understood and less conventional route for dissemination, retrograde traffic along the enteric nervous system neurons is yet another option for dissemination of pathogens which leak through the intestinal barrier (12).

The importance of a healthy intestinal barrier cannot be overemphasized. The gut must maintain a tightly regulated barrier that allows selective passage of nutrients while remaining occlusive to the countless species of bacteria within the lumen (10). Further, the intestine also plays an active part in regulation of the luminal microbial content, which itself can modulate health and disease (13). Thus, a comprehensive understanding of intestinal barrier physiology is necessary in order to better understand what functional derangements occur either as a cause or consequence of disease. Each individual component of the intestinal barrier will be reviewed in detail in the

following sections of this chapter. Next, general mechanisms of pathological derangement of the gut barrier will be discussed. Finally, examples on the role of intestinal permeability and the gut microbiome in specific disease processes will be provided, with a particular focus on various liver disorders.

## **2. Anatomical and physiological components that comprise the intestinal barrier**

The intestinal barrier is formed by several different constituent parts that can be generally broken down into physical, immunological, and microbial components. The physical barrier can be further broken down into epithelial and mucus components (**Figure 1**). This section will provide a primer on each aspect of the gut barrier, with an emphasis on the epithelial components which have been the most characterized.

### **2.1 Epithelial barrier:**

#### *A. Tight junctions (TJs) and their primary structural components:*

The physical component of the gut barrier is primarily sustained by an epithelial sheet of only a single cell in thickness. The remarkable selective strength of the intestinal epithelium is owed to the formation of incredibly resilient and occlusive cell-cell junctions known as the tight junction (TJ). The TJ, sometimes also referred to as the *zonula occludens*, was discovered in a landmark study in 1963 by Farquhar and Palade who described TJ as a belt-like structure between cells in the most apical portion of the basolateral (14). Electron microscopic analysis indicated that these structures formed at

regions of fusion of adjacent cell membranes with “complete obliteration” of the intercellular space (14). Evidence that the TJ was the basis for epithelial barrier function was also provided by the observation that this complex was found to restrict the passage of hemoglobin (14). Freeze-fracture electron microscopy (EM) techniques further characterized the TJ as a branching and anastomosing network of strands or grooves, the patterns of which were noted to differ amongst epithelia of different tissue origins (15). At the same time scientists were becoming increasingly aware that differing epithelia did not share equal features of paracellular permeability (16, 17). Despite these observations, it was initially thought that TJ is a static structure. However, it is now known the TJ is an extremely dynamic structure comprised of a diverse set of proteins that regulate epithelial and endothelial permeability with respect to size and charge of molecules (18, 19). Over the past three decades tremendous strides have been made to elucidate the molecular components that comprise the TJ (20). The basic components of the TJ can be categorized into the integral membrane proteins (occludin, claudins, and junctional adhesion molecule, hereafter, JAM) and the peripheral membrane scaffolding proteins, which anchor the integral membrane proteins to the cellular cytoskeleton (**Figure 2**) (20). A brief history and description of these components with respect to biological structure and function will be provided in the following subsections.

*The tight junction transmembrane protein constituents: Occludin, Claudin, and Junctional Adhesion Molecules (JAMs):*

*Occludin*

Occludin was the first integral membrane protein constituent of TJs to be described and is the most well-studied (21, 22). Sequence analysis demonstrated that this protein has a cytoplasmic amino-terminus, four transmembrane domains in the amino-terminal half, and a long cytoplasmic carboxy-terminal tail (~250 residues) with a predominance of charged residues (21). A key 150 amino acid-long sequence of the carboxy-terminus with a high degree of interspecies conservation was demonstrated to be responsible for binding of occludin to the amino-terminal half of zonula occludens-1 (ZO-1), an important scaffolding protein which acts as a link to the actin cytoskeleton (22-24). Additionally, occludin is highly enriched in tyrosine and glycine residues (~60% of sequence) within its first extracellular loop (22). The unique amino acid composition of this region was found to contribute to the formation of homophilic interactions that occurs during the extracellular binding of occludin in *trans* (i.e., between adjacent cells) (25, 26).

Several early studies highlighted the importance of occludin in normal TJ architecture. For example, occludin co-localizes with ZO-1 and -2 at points of cell-to-cell contact (23), and it was found by immunolabelling and freeze-fracture EM to be directly localized at TJ strands (27). Later studies confirmed that, following translation, occludin is first targeted to the basolateral cell membrane, after which it traffics to the TJ under regulation by phosphorylation events in serine and threonine residues at the carboxy terminus (28-30). For occludin to begin its journey to the TJ, it most likely uses ZO-1 (which first accumulates at *adherens* junctions) as an initial targeting signal to TJs (23, 25). The importance of this interaction between occludin and ZO-1 was underscored by

the observation that occludin confers adhesiveness to fibroblast cell lines lacking TJs, but only if they co-expressed ZO-1 and *adherens* junction components (25).

Numerous observations also suggest that occludin is an important regulator of epithelial barrier function by modulating transepithelial electrical resistance (TEER; ion flux) and paracellular flux of organic solutes. However, the specific role that occludin plays in these physiological functions remains unclear. For instance, overexpression of occludin in filter-grown Madin-Darby Canine Kidney (MDCK) monolayers resulted in increased TEER, but also increased [<sup>3</sup>H]mannitol flux. It was speculated that the enhancement of paracellular flux was a result of exogenous occludin molecules outnumbering the cellular supply of ZO-1 (25, 31, 32). These studies provided the first evidence that suggested a potential regulatory dissociation between electrical resistance and paracellular permeability functions based upon ZO-1-independent and ZO-1-dependent interactions, respectively. It was also shown that the carboxy terminus of occludin is important for TJ “fence” function, which refers to the ability of TJ to limit intramembrane diffusion and maintain distinct lipid and protein composition of apical vs. basolateral membranes (32). Furthermore, *in vitro* treatment of cultured epithelial monolayers with synthetic peptides correlating to the sequences of the extracellular loops of occludin reduced TEER by selectively removing occludin from TJs without altering overall TJ morphology (33).

Further evidence in support of an accessory role of occludin in TJs was provided by phenotypic analyses of mice deficient in occludin protein expression (*occludin*<sup>-/-</sup>) (34). Surprisingly, TJs were observed in the *occludin*<sup>-/-</sup> mice that were virtually indistinguishable from wild-type (WT) controls, and there were no differences in

epithelial and sub-epithelial resistances in both the small and large intestine. However, these animals displayed various other phenotypic abnormalities, including, but not limited to: calcium deposition in the cerebellum and basal ganglia starting at 9-weeks of age; gastritis and thickening of the gastric mucosal folds; loss of chief cells and reduced parietal cell population in gastric glands; reduced cortical bone thickness; premature atrophy of the seminiferous tubules at ~60-weeks of age; and alteration of the sexual behavior of male *occludin*<sup>-/-</sup> mice (34). Nevertheless, these studies raised questions about the existence of potential variants of occludin or entirely different integral membrane proteins that also localize to TJs.

Occludin is now recognized as belonging to a family of proteins each containing a tetra-spanning MARVEL (MAL and related proteins for vesicle trafficking and membrane link) domain (35), collectively referred to as tight-junction associated MARVEL proteins (TAMPS). The TAMP family consists of occludin, tricellulin (36), and marvelD3 (37, 38), the latter of which is expressed as two splice variants. While occludin and both marvelD3 splice variants predominantly accumulate at both bicellular and tricellular junctions, tricellulin specifically accumulates at tricellular contacts (36, 38). Knockdown of any one of these TAMPs is associated with a similar decrease in TEER, and the reduction is further exacerbated by simultaneous knockdown of multiple TAMPs (38). These observations suggest that the TAMP family proteins have both distinct and overlapping functions (38). Future investigations should focus on elucidating the structural and functional relationships between TAMPs and with other TJ proteins. Of critical importance is filling in the gaps in knowledge in how these molecules sense

stimuli and transduce these events as signals within the cell, which is a feature of TJ proteins that is far underappreciated (20, 34).

### *Claudins*

The realization that occludin plays only an accessory role in TJ formation fueled new efforts that led to the subsequent identification of both claudin-1 and -2 (39). The claudins, both ~22-23 kDa in size, were found to have 38% amino acid sequence identity with each other but shared no sequence identity with occludin. However, both claudin-1 and claudin-2 were predicted by hydrophilicity analysis to have cytoplasmic amino- and carboxy- termini, four transmembrane domains, and a hydrophobic first extracellular loop, and thus have a similar overall structure to that of occludin (39). It was soon recognized that claudins represent a diverse multigene family, and there are currently now at least 27 claudin family members identified (40). Interestingly, although the amino acid sequence of the carboxy-terminus is quite diverse among claudin family members, many contain a carboxy-terminal -Y-V sequence, which was later shown to be responsible for mediating binding to the first post-synaptic density protein 95, *Drosophila* disc large tumor suppressor, and zonula occludens-1 protein (PDZ) domains of ZO-1, ZO-2, and ZO-3 (41, 42). All other known claudins, except claudin-12, possess a carboxy-terminal PDZ binding motif to mediate claudin-ZO binding interactions (20).

Transfection of mouse L fibroblasts, which normally do not form TJs, with either claudin-1 or claudin-2 alone resulted in accumulation of the transfected proteins at cell-cell contact sites that resembled TJ-like strands and conferred adhesiveness in a Ca<sup>2+</sup>-

independent manner (43, 44). Moreover, Furuse *et al.* observed that TJ strand morphology between claudin-1 transfectants and claudin-2 transfectants was quite distinct. Considering these findings, and that expression patterns of each claudin species is quite varied among and within tissues (41, 45-48), it was speculated that TJ morphology and barrier properties are determined primarily by each cell or tissue's distinct claudin expression profile. Later *in vitro* work confirmed this hypothesis (49), and a few individual claudin species have been linked to specific TJ architectural features *in vivo*, such as claudin-11 with the parallel arrays of TJ strands in brain and testis (48, 50), and claudin-5 with the extremely distinct TJ strands of endothelial cells (51). Additional complexity arises from the ability of separate claudin species to bind *in cis* to form heteropolymers within TJ strands on the same cell, as well as forming heterophilic interactions in TJ strands across adjacent cells *in trans*. There are, however, some restrictions on heterophilic interactions in *trans* between certain claudin species, such as the inability of claudin-1 strands to interact with claudin-2 strands (49).

The most telling data regarding the critical role that claudins play in contributing to the TJ barrier structure-function relationships came from observations in claudin-1 deficient (*claudin-1<sup>-/-</sup>*) mice (52). Unlike *occludin<sup>-/-</sup>* mice, all *claudin-1<sup>-/-</sup>* mice rapidly died within 24-hours after birth. This was later attributed to rapid water loss through the skin owing to epidermal barrier dysfunction, enabling the passage of solutes up to ~600 Da in size. These findings were particularly surprising as TJs were previously thought to be of little importance in stratified epithelial tissues, and there were no apparent morphological differences in TJs of the deepest layer of the epidermis, the *stratum basale*, in the mutant mice (52). However, mechanistic understanding of claudin function in controlling

paracellular permeability came through studies conducted on clusters of patients with familial renal hypomagnesemia. Through this work, Simon *et al.* discovered paracellin-1/occludin-16 and made the striking observation that it acts as a  $Mg^{2+}$  (and to a lesser extent,  $Ca^{2+}$ ) selective pore (46). This unique ability of claudins to act as ion-selective pores was soon verified in complementary *in vitro* studies using separate strains of MDCK cells that differed in their claudin expression profiles and monolayer resistance properties (53-55). High claudin-2 expression was associated with a dramatic reduction in monolayer resistance (53), whereas high claudin-4 expression was found to dramatically enhance TEER by causing a selective reduction in paracellular  $Na^+$  permeability (54).

It is now recognized that the ion selectivity of each claudin, their contribution to TEER, their overall classification as either “tight” (such as claudins-1, 3, 4, 5, 11, 14, and 19) or “leaky” (such as claudins-2, 10, 15, and 17), but not their contribution to TJ strand morphology appears to be determined by their extracellular domains, particularly the overall charge of the first extracellular loop (56-58). Thus, ion conductance and possibly overall “leakiness” to small organic solutes such as the bacterial derived N-formyl-L-methionyl-L-leucyl-L-phenylalanine (fMLP; 438 Da) (59) can be differentially regulated by expression of distinct claudin species. Furthermore, expression of the claudins can be dynamically regulated by inflammatory and other stimuli (58, 60), perhaps providing a mechanistic explanation for divergent regulation of ion flux (i.e., TEER) and paracellular permeability to all but the smallest solutes. As is the case with occludin, further studies focused on elaborating the non-structural functions of the claudin family will likely prove critical in broadening our understanding of normal and pathological epithelial function.

### *Junctional Adhesion Molecules*

At the same time as the identification of the claudins, Martín-Padura *et al.* discovered a third integral membrane protein that localized to epithelial TJs, which they named Junctional Adhesion Molecule (JAM-1, also JAM-A and F11R; hereafter referred to as JAM-A) (61, 62). Unlike both occludin and claudins, JAM-A was identified as a 36-41 kDa type I integral membrane protein, with an extracellular amino-terminus, a single transmembrane domain, and a cytoplasmic carboxy-terminal tail. Sequence analysis identified JAM-A as an immunoglobulin superfamily member with two V-type immunoglobulin (Ig) domains with intrachain disulfide bonds in its extracellular amino-terminus (61). Like the TAMPs and claudins, a family of JAM proteins was eventually recognized, which includes JAM-A (61, 62), JAM-B (also VE-JAM and JAM-2) (63, 64), and JAM-C (also JAM-3) (65, 66), which all share around 35% amino acid sequence identity and have short cytoplasmic tails that contain a class II PDZ binding motif (67). The JAM family also includes a subgroup of related members encompassing JAM-4, JAM-Like (JAM-L) protein, endothelial cell-selective adhesion molecule (ESAM), Coxsackie and adenovirus receptor (CAR), and CAR-like membrane protein (CLMP) that instead have a long cytoplasmic carboxy-terminal tail that, except for JAM-L and CLMP, ends in a class I, rather than class II, PDZ binding motif (67, 68). However, for the purposes of this review, JAM-A will be the focus for the remainder of this discussion on JAMs as it is the most well-studied and is the only classical JAM (ie, JAM-A, -B, and -C) known to be expressed on mucosal epithelial cells (67).

Similar to occludin and unlike the claudins (43), transfection of JAM-A alone into L fibroblasts was not associated with TJ strand formation (69). However, it was later observed that JAM-A can dimerize via homophilic interactions both *in cis* and *in trans* (70, 71). These interactions are mediated by the membrane distal Ig domain, and oligomerization of JAM-A leads to a platform of concentrated PDZ-binding motifs that likely aids in signal transduction processes (72). Furthermore, numerous studies have reported that JAM-A binds to several scaffolding proteins including ZO-1 (73, 74), ZO-2 (75), AF-6/afadin (73, 75), and cingulin (73). These interactions are all dependent upon the carboxy-terminal PDZ binding motif of JAM-A (20, 73, 74). However, unlike the claudins, which bind to ZO-1, -2, and -3 at their first PDZ domain, JAM-A binds to the third PDZ domain of ZO-1, and this binding interaction is also dependent upon the Src homology 3 (SH3) domain of ZO-1 (76). Together, these unique characteristics of JAM-A suggest that, like occludin, this molecule appears to play an accessory role in determining TJ architecture; yet, the unique structural properties of JAM-A are highly supportive of signaling functions.

Despite its apparent accessory role in TJ structure, both *in vitro* and *in vivo* studies have demonstrated that JAM-A contributes to regulation of TJ barrier function. Transfection of Chinese hamster ovary (CHO) cells with JAM-A resulted in a ~50% decrease in paracellular permeability to 40-kDa FITC-dextran (61). Furthermore, JAM-A deficient (*JAM-A*<sup>-/-</sup>) mice have baseline defects in intestinal barrier function as indicated by a reduced mucosal TEER and increased paracellular permeability to 4-kDa FITC-dextran (77). *JAM-A*<sup>-/-</sup> mice also have increased colonic neutrophil infiltration and large lymphoid aggregates compared to WT animals. Moreover, *JAM-A*<sup>-/-</sup> mice are more susceptible to

dextran sulfate sodium (DSS)-induced colitis (77). However, though *JAM-A*<sup>-/-</sup> mice developed more severe colitis by clinical parameters, histological injury was surprisingly worse in WT animals (77). This apparent contradiction may be explained by the enhanced intestinal epithelial proliferation observed with JAM-A deficiency.

A recent study suggests that JAM-A may regulate intestinal barrier function via a unique signal transduction pathway involving ZO-2, afadin, PDZ-guanine nucleotide exchange factor 1 (PDZ-GEF1), and Ras-related protein 2c (Rap2c) (75). Monteiro *et al.* propose that JAM-A induced activation of Rap2c inhibits activation of Ras homolog gene family member A (RhoA). RhoA inhibition, in turn, leads to a reduction in myosin light chain (MLC) phosphorylation, ultimately resulting in decreased contraction of the apical actomyosin ring and closure of the paracellular space (75). Because JAM-A appears to regulate paracellular permeability through active control of cytoskeletal contractility, it is thought to predominantly modulate non-selective “leak” pathway flux across epithelial barriers (75). Therefore, JAM-A could provide a molecular basis for controlling the paracellular diffusion of relatively large molecules such as bacterial lipopolysaccharide (LPS). This hypothesis provides unique functional niche of JAM-A that distinguishes it from the claudin family, which instead regulate “pore” pathway flux of ions and small solutes in a charge-and size-selective manner (18, 75).

JAM-A has also been implicated in establishing cell polarity and is a regulator of cell migration, including leukocyte transendothelial migration (20, 61, 67, 69, 71, 78-81). Specifically, JAM-A has been shown to regulate  $\beta$ 1 integrin expression and cell migration via Rap1 (82). Different signaling modules are likely triggered by JAM-A based off its binding status within the cellular environment. For example, in JAM-A

expressing epithelial cells under subconfluent conditions, most JAM-A molecules are present as dimers *in cis* on individual cells. As cells become more confluent and come in contact with each other, more JAM-A molecules will bind between adjacent cells *in trans*, thus potentially triggering new signal transduction pathways (83). In support of this, *trans*-, but not *cis*-dimerization, was associated with increased Rap2 activity. Thus, once epithelial cells reach confluence, JAM-A molecules dimerize *in trans* and trigger signals to induce formation and maintenance of a tight barrier (75, 82, 84). Determining the similar regulatory nuances of the remaining TJ proteins will prove critical in expanding our understanding of TJ physiology.

#### *Scaffolding proteins: Zonula Occludens, Afadin, and cingulin*

\*Note: there is a tremendous amount of diversity in TJ scaffolding proteins and the following section is a brief summary of those best studied to date. For a more comprehensive listing see (20).

#### *ZO-1, -2, and -3*

ZO-1 was the first TJ associated protein discovered and is the most well studied (85). ZO-1, and the closely related ZO-2 and ZO-3 (86-88), are members of the membrane-associated guanylate kinase (MAGUK) protein family. Additional members of this family include the PSD-95/SAP and the *Drosophila* discs large tumor suppressor gene product (89). All members of this family are multidomain proteins that are characterized by three amino-terminal PDZ domains (named after the first letters of the three proteins above),

a central SH3 domain, followed by a region with homology to guanylate kinase (GUK) (88). The ZO proteins were localized by immune-gold labeling to cytoplasmic regions surrounding the membrane contacts of the TJ complex (85, 87, 88), which led to their correct identification as peripheral membrane proteins. ZO proteins can bind to the carboxy-termini of occludin, the claudins, and JAM-A through interactions mediated by distinct domains: PDZ1 binds claudins, PDZ3 plus some of the SH3 domain binds JAM-A, and the GUK domain binds occludin (24, 42, 76). Additionally, ZO-1/ZO-2 and ZO-1/ZO-3 heterodimers can form via PDZ2/PDZ2 interactions (42). All three ZO proteins can also bind actin directly via their carboxy-terminal halves (90). Thus, these proteins provide stability to the TJ complex by anchoring the integral membrane proteins to the cytoskeletal complex. ZO-1, -2, and -3 can additionally bind other actin binding proteins, providing a secondary means of linking the TJ to the cytoskeleton [see (20) and (91)]. However, the three ZO proteins are not entirely functionally redundant, at least *in vivo*. For instance, ZO-3 deficient mice are born with no apparent abnormal phenotype (92), whereas ZO-2 knockout results in early embryonic lethality (93). Nonetheless, the unique characteristics of each ZO species are still not fully appreciated, and more work is required to gain better insight into their specific functional niches.

### *Cingulin*

Cingulin is an  $\alpha$ -helical coiled-coil peripheral membrane protein (94). It is visible by electron microscopy as an elongated, rod-like molecule, often with curves or kinks, suggesting it has some degree of flexibility. Interestingly this protein's structure resembles that of brush-border myosin, and it was discovered serendipitously while

attempting to make anti-brush-border myosin antibodies (94). Cingulin binds with ZO-1 via its amino-terminus (95), and its known to have both structural and signaling functions (74, 96-98). For instance, knockdown of cingulin in MDCK cells was associated with increased RhoA activity, which resulted in increased cell proliferation and increased expression of claudin-2 and ZO-3 (96). Therefore, cingulin inhibits RhoA activation and signaling under normal conditions, which contributes to maintaining a “tight” barrier.

#### *AF-6/Afadin*

Afadin is a single PDZ domain-containing protein that localizes at both cadherin-based adherens junctions as well as TJs (99, 100). It is known to interact with components of the cell polarity complex, and its expression may be required for proper positioning of the TJ relative to the adherens junction (20, 101). Afadin is able to bind to F-actin and ZO-1, and it also interacts with JAM-A (99, 100, 102). Interestingly, afadin’s ZO-1 binding domain is located in close proximity to a Ras binding domain, such that activated Ras molecules can displace afadin from ZO-1 (100). Thus, the Ras-Afadin-ZO-1 axis may represent one pathway by which activated Ras can disrupt cell-cell contacts. Similar to *JAM-A*<sup>-/-</sup> mice (77), conditional intestine-specific afadin deficient mice also display enhanced gut permeability and greater susceptibility to DSS –induced colitis (103).

#### *B. Adherens junctions:*

Though the TJ is the primary cellular structure responsible for regulating paracellular permeability, several additional junctional complexes also exist including *adherens junctions*, gap junctions, and desmosomes (104). *Adherens junctions* are cadherin and nectin based structures located below the TJ (104, 105). While a detailed discussion of these structures is beyond the scope of the current review, they broadly are responsible for regulating cell-cell adhesion. *Adherens junctions* do not play a large role in direct regulation of paracellular permeability, but they do facilitate the formation of functional TJ strands (104, 105). Therefore, *adherens junctions* form part of a complex network with the TJ, and thus modulation of this structure often times can lead to disruption of the TJ itself (104).

### *C. Physiological cell turnover:*

The intestinal epithelium must be able to withstand considerable mechanical forces as fecal content is moved towards the rectum. As the epithelial lining of the gut is only a single-cell thick, many cells die during this process. In fact, it is estimated that the human gastrointestinal tract sheds as many as  $10^{11}$  epithelial cells per day (106). While the maintenance of continuous TJs during this controlled process of cell sloughing remains critical for barrier function, it also necessitates a continuous and well-regulated source of cell renewal. A collection of various adult stem cell populations localized within the intestinal crypts is responsible for this high demand of cell division, and results in complete turn-over of the entire intestinal epithelium ever 3-5 days of life (106, 107). Therefore, although these populations of cells are most often the center of

discussions on embryological and wound healing processes, they should also be considered a critical component of the gut barrier.

While the existence of intestinal stem cells has been known for decades, expansion of our knowledge has been limited due to a lack of clearly identifiable surface markers and reagents to study these relatively rare cellular populations. However, recent advancements in the past 5 to 10 years have identified a number of putative surface markers that has poised the field for a massive renaissance of discovery (106, 108). The most well-studied of these markers is leucine-rich repeat-containing G-protein coupled receptor 5 (*LGR5*), which is a marker expressed by a subset of rapidly-dividing crypt base columnar cells that were found to give rise to all major categories of intestinal epithelial cells (106, 109). Critically, single isolated *LGR5*<sup>+</sup> cells are capable of forming self-renewing organoids with complete crypt-villus architecture *in vitro* (110). It is generally agreed upon that this population of cells is most critical for maintaining homeostatic renewal of intestinal epithelial cells *in vivo* (106). However, due to their rapidly dividing nature, *LGR5*<sup>+</sup> cells are also susceptible to radiation-induced injury and cytotoxic drugs (111, 112). The long-term effects of *LGR5*<sup>+</sup> stem cell depletion are currently unclear, but it has been demonstrated that one or several populations of typically quiescent stem cells can compensate for their loss in the short-term and potentially eventually repopulate the *LGR5*<sup>+</sup> cell niche (106, 112, 113). The exact phenotype of these quiescent cells remains somewhat elusive, though a strong candidate population is a subset of crypt cells that express the marker *Bmi1* (106, 112, 113). However, it is important to note that these topics remain incompletely characterized and significant controversy exists (106, 114, 115). Furthermore, while

antibody reagents remain limited for these makers, fluorescent protein reporter mice have proven a useful tool in propelling intestinal stem cell studies forward. This field is likely to see rapid progress in the coming years with increasing relevance on gut barrier studies.

## **2.2 Mucus barrier:**

Within the intestinal epithelial monolayer reside specialized cells referred to as goblet cells that are responsible for producing a sizable mucus layer that serves as an additional physico-biochemical barrier, as well as a lubricant for luminal contents during peristalsis (116). The number and function of these goblet cells, and accordingly the structure and character of the mucus layer, varies along different segments of the gastrointestinal tract. Generally, the abundance of goblet cells and the thickness of the mucus layer increases with increasing presence of colonized microbiota, with the greatest abundance of goblet cells being in the colon (117). Within the colon the mucus layer additionally changes from a single phase of loose mucus (as is the case in the small intestine) to a dynamic dual phase system consisting of an inner, dense mucus layer and an outer loose mucus layer (118). In this way, the mucus barrier limits contact between the luminal microbiota and the intestinal enterocytes. This phenomenon is also exemplified by studies in germ-free mice, which were shown to have fewer intestinal goblet cells and a thinner mucus layer than conventionally housed animals. However, mucus production in the germ-free mice normalized to the level of conventionally housed animals following treatment with bacterial molecules such as LPS (119).

Structurally the intestinal mucus barrier is formed by a collection of highly glycosylated glycoproteins referred to as mucins (MUC) that are produced and secreted by the goblet cells. Up to 20 mucin family members have been discovered to date, which are subdivided into either secreted mucins (e.g., MUC2, MUC5AC, MUC5B, MUC6) and membrane-associated mucins (e.g., MUC1, MUC3, MUC4, MUC13, MUC17) (117). The secreted mucins form the bulk of the mucus layer throughout the intestine, with MUC2 being by far the most predominant (120). Conversely, the membrane-associated mucins anchor the secreted mucins to the epithelial glycocalyx to form the dense inner mucus layer of the colon (117, 120).

The synthesis and structure of secreted versus membrane-associated mucins differs in a few notable ways. Secreted mucins are translated in the endoplasmic reticulum (ER) and are dimerized at their C-terminal cysteine knot (CK) domains via disulfide bonds. The dimerized proteins are transported to the Golgi apparatus for O-glycosylation, which starts with the addition of N-acetyl galactosamine (GalNAc) residues to which more complex oligosaccharides are assembled upon. Further processing events results in N-terminal trimerization of the dimers upon exposure to low pH and high calcium concentrations within secretory vesicles of goblet cells. Upon their release, the dense mucus granules become hydrated and expand in volume by up to 3,000-fold (117, 120). Conversely, membrane associated mucins are synthesized as single transmembrane proteins in the ER that undergo autocatalytic cleavage at the membrane-adjacent portion of their extracellular domains. However, this newly cleaved fragment still strongly binds to the remaining transmembrane fragment of the mucin molecule. Thus, the purpose of this fragmentation is hypothesized to facilitate shedding of the

transmembrane mucins from the cell surface to prevent cellular damage caused by mechanical stress during peristalsis. Furthermore, unlike secreted mucins, glycosylation of the membrane-associated mucins initiates with *N*-glycosylation events within the ER. Further *O*-glycosylation of the membrane-associated mucins is carried out within the Golgi apparatus prior to their export and insertion into the plasma membrane (117, 120).

The most obvious functions of the intestinal mucus layer are acting as a physical barrier to protect the epithelium from the luminal microbiota and as a lubricant to promote the movement of luminal contents during peristalsis while protecting the epithelium from the associated mechanical stress. However, intestinal mucus plays many more critical physiological roles that are relevant to the collective barrier function of the intestine. For instance, as a rich source of carbohydrates, the intestinal mucus can act as an important source of food for a large number of commensal microorganisms (121-123). These microbes, in turn, can produce metabolites that are utilized by the enterocytes and promote general health of the epithelium (116). The mucins glycoproteins can also contribute directly to epithelial cell health. Some membrane associated mucins, such as MUC3 in mice, inhibit epithelial cell apoptosis, and promote the aggregation and migration of the enterocytes (124). Finally, the gel-like structure of the mucus supports additional functions of the intestinal epithelial and immune cells. Due to its viscosity, the mucus traps various antimicrobial peptides (AMPs) and immunoglobulins (Igs) such that a gradient is formed with the highest concentrations being present in the mucus regions closest to the epithelium. Moreover, oxygen, which facilitates the optimal function of some AMPs, diffuses out of the blood to form a similar concentration gradient in the mucus (117). Together these conditions result in exquisite control of microbial growth

and colonization and contribute to maintaining the relative sterility of the inner mucus layer within the colon. These and various other mediators of the immune system will be the topic of the following section.

### **2.3 Immune barrier:**

The intestine houses the largest collection of immune cells in the body and acts as a vital component of the host immune system (8, 125). The gut is continuously exposed to innumerable antigens from the colonized microbiota and dietary materials. In health, an intricate, dynamic equilibrium between the luminal microorganisms, dietary compounds, and the mucosal immune system keeps these conditions in check in order combat potential pathogens and limit the growth of commensals organisms while also allowing for tolerance of necessary nutrients. This highly demanding regulatory role demands a complex network within the mucosal immune system comprised of various secretory and cellular components. Epithelial cells, as well as the typical populations of myeloid and lymphoid immune cells all contribute to this balance (126). Importantly, as a testament to the unique demands of the gut mucosal niche, numerous populations of unconventional immune cells, including type-I interferon producing plasmacytoid dendritic cells (pDCs) (126), all subgroups of innate lymphoid cells (ILCs) (127), mucosa associated invariant T cells (MAIT) (128), and  $\gamma\delta$ -T cells (129), are all highly enriched in the intestine compared to elsewhere in the body. Our understanding of this intertwined network of gut-resident immune cells is incomplete but rapidly evolving. While the functions of many of these specialized subpopulations of cells remain unclear (8), it is important to appreciate the complexity of the mucosal immune system to better

understand the barrier and immunomodulatory functions of the intestine. However, for the purpose of this review on gut barrier physiology, the focus of this section will be on the role of secreted antimicrobial peptides and immunoglobulin A (IgA), both of which contribute important functional components to the intestinal barrier.

*Antimicrobial peptides – Defensins, Lectins, and Cathelicidins, and others:*

Antimicrobial peptides (AMPs) are several classes of small proteins secreted predominantly at epithelial surfaces with microbicidal activities (130). Within the gut, the largest producers of these proteins are another class of specialized epithelial cells called Paneth cells. Paneth cells are located at the base of the intestinal crypts, intercalated between the *LGR5*<sup>+</sup> stem cells, where they secrete large quantities of digestive zymogens, stem-cell growth factors, and AMPs (131). Due to their role in AMP production these cells can be considered as significant contributors to innate immune defense.

AMPs of different classes utilize diverse mechanisms of antimicrobial functions, though in general they target disruption of the bacterial cell wall or membrane (130). Some, such as lysozyme and secretory phospholipase A2 (sPLA<sub>2</sub>) actively enzymatically destroy their targets. Lysozyme hydrolyzes the 1,4- $\beta$ -glycosidic within the bacterial peptidoglycan cell wall, while sPLA<sub>2</sub> instead penetrates the cell wall and hydrolyzes phospholipids within the bacterial membrane (130, 132). Meanwhile, defensins, C-type lectins, and cathelicidins, the three of the major classes of intestinal AMPs that have been best characterized, non-enzymatically kill their targets via separate nuanced

mechanisms of bacterial membrane disruption (130). However, each of these AMP classes utilize positively charged residues to preferentially bind to and insert themselves into bacterial membranes, which have a net negative charge due to their enrichment with acidic phospholipids such as cardiolipid and phosphatidylglycerol (13, 130). The following paragraphs will briefly describe the archetypal molecules in each group.

Defensins are subdivided into three groups as  $\alpha$ -,  $\beta$ -, and  $\theta$ -defensins based upon structural differences arising from differential disulfide bond arrangement.  $\alpha$ -defensins are only expressed by the Paneth cells of the small intestine, whereas  $\beta$ -defensins are found in both the large and small intestine.  $\theta$ -defensins are only expressed by Old World monkeys and are not found in humans (130, 133). Within the small intestine  $\alpha$ -defensins are some of the most abundantly expressed AMPs (13). They are secreted in propeptide forms and are activated by enzymatic cleavage by matrix metalloproteinase-7 (MMP-7) in mice and trypsin in humans. Once activated,  $\alpha$ -defensins dimerize and insert into the bacterial membrane forming aqueous pores that cause membrane disruption and death (130, 133).

The regenerating islet-derived protein 3 (REG3) family are the best characterized C-type lectins with REG3 $\gamma$  in mice and its human ortholog REG3 $\alpha$  being the most studied. These proteins are also secreted by Paneth cells of the small intestine and specifically target gram-positive bacteria due to a requirement of peptidoglycan surface binding to elicit their antimicrobial activity (13, 130). REG3 $\gamma$  and REG3 $\alpha$  are also produced in inactive forms and are proteolytically activated by trypsin, which enables high-affinity binding to the long carbohydrate chains of bacterial peptidoglycan. The initial binding

reaction of REG3 $\gamma$ /REG3 $\alpha$  to the peptidoglycan surface allows it to these proteins to oligomerize and form hexameric pores within the bacterial membrane, leading to membrane disruption and bacterial death (134).

Cathelicidins are expressed by epithelial cells in both the small and large intestine as a single gene that generates a precursor peptide that can be cleaved into several active AMPs (130). The best characterized cathelicidins are LL-37 in humans and cathelin-related antimicrobial peptide (CRAMP) in mice (135, 136). These AMPs are broadly active against both gram-positive and gram-negative bacteria as well as some fungi (136, 137). They have a disordered structure in aqueous solution but convert to an  $\alpha$ -helical structure upon binding to bacterial membranes via charge-charge interactions. The LL-37/CRAMP helices are then able to insert into the bacterial membrane and form toroidal-shaped pores, leading to membrane disruption and cell death (138).

Each of these classes of AMPs and others contribute to the control of commensal intestinal microorganism growth and limit the colonization of potentially pathogenic microbes (130). Some AMPs such as lysozyme and SPLA<sub>2</sub> are constitutively expressed, whereas the expression of others such as REG3 $\gamma$  is either substantially upregulated or entirely dependent upon sensing of bacterial products by Toll-like receptor receptors (TLRs) on epithelial cells (130, 139). Interestingly, the expression of REG3 $\gamma$  has also been particularly linked to separation of the microbiota from the host epithelium (139, 140). Furthermore, due to the diverse range of expressed AMPs and their targeting of the bacterial membrane resistance to these proteins is a rare occurrence (130).

### *Immunoglobulin A:*

In addition to the innate AMPs, large amounts of IgA, around 3g per day in humans, are secreted by adaptive immune cells into the intestinal lumen to add to the barrier function of the gut (141). The majority of IgA within the intestine is produced by plasma cells within Peyer's patches and the lamina propria, though some amount is contributed by the hepatic plasma cells that secrete IgA into bile (142). Lamina propria plasma cells secrete IgA as a polymeric molecule consisting of two IgA molecules link by a J-chain molecule. The secretory IgA (sIgA) binds to the polymeric Ig receptor (pIgR) on the basolateral surface of intestinal epithelial cells, which then uptake and transport the sIgA-pIgR complex onto their apical surface. The sIgA complex is then released into the intestinal lumen by proteolytic cleavage of the pIgR, which leaves a fragment of the receptor referred to as secretory component still attached to the sIgA complex (13, 141).

The multivalent nature of sIgA is an important structural aspect that facilitates its proposed protective functions. For instance, sIgA can bind multiple bacteria at a time which leads to non-covalent crosslinking of the intestinal microbiota (143). Such crosslinking of intestinal microbes facilitates their entrapment by mucus. Potential binding interactions between secretory component within sIgA and mucus glycoproteins further strengthen the entrapment of intestinal bacteria (143, 144). Mucus entrapment both limits the potential interaction of intestinal microbes with the epithelium and aids in their clearance via fecal excretion. The entire process of cross-linking/agglutination, mucus entrapment, and clearance of intestinal bacteria is referred to as "immune exclusion" (13, 143, 145). Surprisingly, it was also recently demonstrated that some beneficial commensal organisms such as *Bacteroides fragilis* actually utilize IgA binding

as a means of favoring their colonization within the host (146). However, aside from directly binding pathogens themselves, sIgA is able to bind and neutralize secreted bacterial toxins as yet another mechanism of host protection (13, 141, 147).

Although sIgA is abundantly produced and elicits several protective mechanisms of action, IgA deficiency is not associated with any adverse clinical features under normal circumstances in both mice and humans (where IgA deficiency is relatively common) (141, 148, 149). A potential explanation for this observation is that an increase in IgM secretion, which follows a similar route of production to yield secretory-component linked Ig pentamers, is able to compensate for the loss of IgA (149). However, IgA-deficient mice harbor a qualitatively different microbiome than wild-type animals and are more susceptible to certain infectious diseases (142, 150, 151). Humans with IgA deficiency are also more likely to develop allergies, celiac disease, and gastrointestinal infections (141, 142, 148). Furthermore, mice deficient for activation-induced cytidine deaminase (AID), which are unable to perform somatic hypermutation or Ig class switch recombination, develop intestinal bacterial overgrowth with an increased level of gut translocation into the mesenteric lymph nodes (152). Therefore, although the specific functional roles of IgA continue to be under characterization, sIgA, and to a lesser extent sIgM, contribute significantly to overall intestinal barrier function.

#### **2.4 Contribution of commensal microbiome to gut barrier function:**

The primary function of the intestinal barrier is to maintain homeostatic separation of the intestinal microbiome from the host interior while also permitting adequate absorption of

dietary nutrients and fluids. However, as was mentioned above, for a healthy human the host cells are outnumbered by our colonized bacteria by a factor of nearly ten to one (9). Intestinal colonization with commensal microorganisms is in fact a necessary contributor to host health in a variety of ways, including reinforcement of the gut barrier via both direct and indirect mechanisms (6, 9). Host commensals provide a direct barrier to colonization of potential pathogenic microbes by competition for space and host- and diet-derived nutrients, a phenomenon referred to as colonization resistance (10, 153, 154). Moreover, our commensals provide continuous stimulation of pathogen recognition receptors (PRRs) such as TLRs on enterocytes and Paneth cells to increase the production of MUCs and AMPs (116, 130). Mucosal adherent commensal bacterial populations, such as the mucolytic *Akkermansia muciniphila*, are particularly important for such homeostatic epithelial cell stimulation (6, 155, 156). Mucosal adherent bacteria are notably less abundant than luminal bacteria and represent a qualitatively different population of organisms (6). Furthermore, commensal microorganisms “educate” our immune cells by providing low-levels of immunostimulation to enhance IgA production and modulate baseline cytokine production in favor of anti-inflammatory signals that promote maintenance of the epithelial barrier and TJs (6, 141). Finally, many commensal bacterial strains produce short chain fatty acids (SCFAs) such as butyrate from the metabolic breakdown of insoluble fiber and other luminal carbohydrates which serve as a primary nutrient for enterocytes that promotes their health, regeneration, and TJ barrier function and maintenance (6, 9, 157).

As was excellently explained by Hiippala *et al.* in a recent review, extreme caution must be taken in attempting to generalize certain protective and beneficial functions

associated with specific commensal bacterial species due to highly strain- and disease-specific observations (6). However, even with this in mind, a common observation is that bacteria of the phyla *Bacteroidetes* and *Firmicutes* are generally associated with promoting health whereas an overabundance of *Proteobacteria* phylum members, which are normally present in lower frequencies in the human intestine, is typically associated with inflammation and disease (6). One hypothesized reasoning for this trend is that most *Proteobacteria*, as gram-negative bacteria, express a highly immunogenic hexa-acylated form of LPS which likely is a cause for increased intestinal inflammation in their overabundance (6, 158, 159). Exceptions to this observation exist, and several gram-negative commensals of other phyla have been associated with health promoting functions, such as the aforementioned *A. muciniphila* (6). However, in the healthy human gut, *Bacteroidetes* and *Firmicutes* represent up to 90% of the intestinal luminal bacterial load (9). Some notable members of these phyla which have been particularly associated with health-promoting functions include *Faecalibacterium prausnitzii* and *Bacteroides* spp. (160). *F. prausnitzii* by itself represents up to 15% of the intestinal bacterial load and is a substantial producer of butyrate by carbohydrate fermentation (6, 161).

Interestingly, *F. prausnitzii* can also utilize metabolites produced by other commensal bacterial strains for butyrate production. This sort of intersection of metabolic pathways between multiple organisms within the gut is referred to as “cross-feeding” and further elaborates the level of complexity that is involved within microbiome research (6, 162). There is estimated to be at least 1000 distinct species of bacteria within the gut, most of which are unable to be cultured by conventional means. There are, however,

commensal viruses, fungi, and even parasites present within our microbiome, which are far less understood (6, 9). Our knowledge is only at the tip of the iceberg when it comes to the role of commensal microorganisms in regulating the intestinal barrier and thus systemic health. Due to the sheer complexity of interactions involved in the host-microbiome network, robust systems biology, metabolomic, and microbiological analyses will be critical to unraveling the full mutualistic nature of this ecosystem.

### **3. Pathological derangements of intestinal barrier function that contribute to liver and other diseases:**

Homeostatic compartmentalization of the microorganisms residing within the intestine is perhaps the most important physiological function of the gut for regulating systemic health aside from nutrient absorption. When any aspect of this barrier fails, even bacteria that generally promote health can wreak havoc and contribute to disease development and injury. A strong example of this is the pathobiont *B. fragilis*, which although is a member of the health-promotion phylum *Bacteroidetes*, has also been found to be a significant contributor to infections and abscess formation whenever it “escapes” containment in the gut (163). However, regardless of the cause and organisms involved, the resultant enhancement of intestinal permeability upon barrier compromise leads to an influx of highly immunostimulatory pathogen associated molecular patterns (PAMPs) directly into the internal systemic body environment (1). As stated, this has been found to cause far reaching consequences even on organs such as the brain and kidney (164, 165), but the organ that is typically the most pathologically impacted is the liver (1). The liver and gut share a close anatomical link between the

portal circulation, through which the nutrient rich venous blood from the gut is perfused through the liver for absorption prior to returning to the heart and lung for reoxygenation. In the case of a leaky gut, the portal blood would also contain the highest concentration of PAMPs which would be first encountered by the immune cell populations of the liver (**Figure 3**) (1). As a result, these PAMPs such as LPS and bacterial and viral RNA will trigger activation of PRRs such as TLR4 on Kupffer cells (liver resident macrophages) and other immune cells, triggering a violent inflammatory response. The resulting hepatic inflammation poses a threat to the liver and is a strong contributor to liver injury and disease (1, 11).

The precise mechanisms of intestinal leakiness are varied and incompletely understood. As should be now evident from reviewing intestinal barrier physiology, the gut barrier is highly complex with many constituent parts in a delicate balance. For instance, disruptions at the epithelial level can be due to physical trauma, TJ disruption, and alterations in epithelial cell turn over within the stem cell niche, among other causes (10). Reductions in the mucus layer thickness or changes in its character and quality additionally can contribute to intestinal bacterial translocation (122). Furthermore, deficiencies in either innate or adaptive immune control of microbial populations, including the secreted AMPs, can contribute to gut microbial translocation (10, 166). Finally, overgrowth and alterations in the diversity of the intestinal bacterial populations (referred to as dysbiosis) can lead to intestinal inflammation and gut barrier compromise (1, 9). For this reason, the mutual yet competitive relationship between different intestinal commensal strains is critical as the nature of this competition normally maintains this ecosystem in relative stability (167).

The scenarios presented above discuss the most widely-accepted paradigm in that intestinal leakiness leads to liver inflammation, and thus disease progression. In general, but not always, gut leakiness involves intestinal inflammation and injury as the link between liver injury and bacterial translocation (1). However, in reality, the cause and consequences of each of these factors in any particular disease condition may not be so clear. Communication between the gut and liver is bi-directional (1). Though the portal circulation from gut to the liver has been most heavily emphasized, the liver “communicates” back to the gut via hepatic bile flow and the release of soluble mediators into the systemic circulation (1). Therefore, it is not always evident whether the gut leakiness and dysbiosis that is typically present in liver disease is a cause or itself a consequence of the liver pathology. Contributing to this uncertainty is that factors which affect liver function (age, gender, diet, etc.) also have profound effects on intestinal physiology and gut microbial diversity (6, 9, 10).

Whether gut leakiness and/or intestinal dysbiosis is among the first triggers of liver injury, or if it occurs later as a consequence of altered liver function, is a question with answers that likely varies based upon the particular disease. This question is important to answer for mechanistic insight, but the answer is relatively inconsequential in considering the contribution of gut leakiness and dysbiosis to liver injury. Substantial evidence exists that gut leakiness almost universally contributes to systemic inflammation and disease progression, if not causation (10, 168). In the following sections, the seminal and recent findings regarding the role of gut leakiness in several different liver diseases will be discussed. Furthermore, a brief highlight of gut leakiness in extra-hepatic diseases will additionally be presented.

## 4. Specific highlights of gut barrier dysfunction in liver disease and beyond

### 4.1 Alcoholic liver disease (ALD)

Alcohol use was attributed to 3-million deaths globally (5.3% of total deaths) in 2016 (169). ALD accounts for a significant proportion of these deaths, and nearly half of liver cirrhosis-related mortality is due to alcohol abuse (169). Evidence regarding a critical, and likely early, role of gut permeability is substantial. Increased endotoxin levels in the serum from ALD patients was observed over several decades ago, and it has been demonstrated that even a single binge of alcohol can induce transient endotoxemia in healthy subjects (170-172). Alcohol consumption is also associated with intestinal bacterial overgrowth and dysbiosis. Amongst human ALD patients it was found that those with the most severe alcoholic hepatitis had higher relative proportions of *Bifidobacterium*, *Streptococci*, and *Enterobacteria* in their feces (173). This associated dysbiosis seems to contribute to both the disease susceptibility and progression (173, 174). Importantly, antibiotic-treated animals are protected from alcohol-induced liver injury (175, 176). However, germ-free (GF) mice, which lack the protective benefits and immune system education provided by commensal bacteria from during development, were found to be more susceptible to alcohol. GF mice were also found to metabolize the ethanol at a faster rate than conventionally housed animals, which can account for their increased susceptibility (177).

The mechanisms by which alcohol consumption causes gut leakiness are broad and overlapping. Ethanol and particularly its metabolite acetaldehyde are particularly strong disruptors of epithelial TJs. This appears to affect multiple levels of the junctional proteins, including ZO-1, occludin, claudins, and several associated signaling molecules such as myosin light chain kinase (MLCK) (178, 179). For example, occludin protein expression is drastically reduced in the intestines of alcohol-fed mice (175).

Furthermore, mice deficient in occludin expression are more susceptible to alcoholic liver injury (180). However, Chen *et al.* demonstrated that this reduction in occludin could be reversed by non-absorbable antibiotic treatment (175). It was also demonstrated that alcohol-fed mice have reduced expression of the AMP REG3 $\gamma$  in the intestine, and mice deficient in REG3 $\gamma$  were developed more severe ALD (181, 182).

Several recent lines of evidence have also shown a potential role of altered intestinal epithelial stem cell function and direct epithelial injury in ALD. For instance, Cho *et al.* reported increased intestinal apoptosis alongside TJ protein degradation in alcohol-fed rodents (179). Moreover, Lu *et al.* observed a decrease in intestinal stem cell markers *LGR5* and *Bmi1* in the small intestines of alcohol-fed mice (183).

#### **4.2 Non-alcoholic fatty liver disease (NAFLD)**

NAFLD refers to a spectrum of lipid-associated liver disorders ranging from simple steatosis, non-alcoholic steatohepatitis (NASH), fibrosis, cirrhosis, and eventually cancer (184). NAFLD is a leading cause of chronic liver disease and is a fast-growing global health concern. It is currently estimated that the global prevalence of NAFLD is

about 25% (185). The largest risk factors for NAFLD/NASH are obesity and metabolic syndrome, and it is estimated that 39% of the adult population worldwide is overweight and 13% is obese (185). Though they remain distinct entities, NAFLD/NASH and ALD share similarities in their mechanisms of pathogenesis. The current line of thought around NAFLD/NASH is a so called “two-hit” hypothesis that initiates in altered lipid metabolism and insulin resistance/metabolic syndrome which leads to the development of hepatic steatosis. A second-hit that promotes persistent liver inflammation, such as intestinal dysbiosis and excessive gut-leakiness, is thought to contribute to the progression of NAFLD to NASH, fibrosis, and cirrhosis (184, 186). As mentioned above this is likely an oversimplification, and the two categorical factors of this hypothesis (altered lipid metabolism, gut leakiness, and hepatic inflammation) likely work together to both initiate and progress fatty-liver diseases.

There has been a growing appreciation of the role of intestinal dysbiosis and gut leakiness in NAFLD pathogenesis over the past twenty-years. The observations of endotoxemia and TJ dysfunction in alcohol-fed animals and ALD patients discussed above led similar investigations into the effects of obesity and high-fat diets (HFDs) on intestinal permeability. These efforts uncovered that obese rodents similarly have disrupted intestinal TJs due in part to re-localization and reduced expression of ZO-1 and occludin (187). Furthermore, it was shown prior that the livers of obese rats are more sensitive to LPS stimulation and that their Kupffer cells demonstrated reduced phagocytic function (188). NAFLD patients were also found to have higher prevalence of small intestinal bacterial overgrowth and gut leakiness compared to lean controls. Interestingly, the degree of hepatic steatosis, but not the presence of NASH, correlated

with the level of gut leakiness and the presence intestinal bacterial overgrowth (189). More recently it was demonstrated that mice deficient in JAM-A developed more severe steatohepatitis than control animals when placed on a high-fat, high-cholesterol, and high-fructose diet (190). NAFLD/NASH was prevented in the mutant mice by treatment with either antibiotics or with sevelamer hydrochloride, a bile acid-binding resin that was demonstrated to have LPS-binding activity (190). Though these are similar observations as reported in ALD studies, it is not clear whether or how the mechanisms of TJ disruption differ between ethanol exposure and HFD. Furthermore, while alterations in intestinal microbial populations are observed in NAFLD/NASH, the specific alterations that occur between phyla and species are less defined than in ALD literature (174, 191). These inconsistencies likely arise from diet-specific effects of particular nutrients and metabolites. Moreover, modalities for diagnosing NAFLD in humans often differ between studies (i.e., ultrasonography, MRI, biopsy, etc.) (174, 191). However, it appears that the most common findings are that gram-negative bacteria are enriched while gram-positive bacteria are reduced in the setting of NAFLD/NASH, and in particular the abundance butyrate-producing bacteria is reduced (174, 191, 192). Coincidentally, treatment of mice with sodium-butyrate was found to alleviate HFD-induced steatohepatitis and endotoxemia (193). Endotoxemia alone was found to increase the risk for obesity and metabolic syndrome in mice (194). However, GF mice have been found to be both more- and less-susceptible to NAFLD/NASH development depending on the particular mouse strain and diets used (174). Thus, it remains uncertain to what extent intestinal dysbiosis contributes to each stage of NAFLD as disease progresses from simple steatosis to NASH, fibrosis, and cirrhosis.

### 4.3 Drug-induced liver injury (DILI)

DILI is a common cause of liver injury and is one of the most frequent reasons for drug non-approval or withdrawal. The term DILI encompasses both predictable, dose dependent injury of known hepatotoxins and unpredictable/idiosyncratic injury (iDILI) (195). Practically any drug can be capable of inducing iDILI, and there are over 1000 drugs that have currently been linked to this phenomenon. iDILI tends to occur after a longer latency of drug use in only a small subset of exposed at-risk persons, and while it poses a significant health concern, its unpredictability of occurrence and broad range of phenotypes makes it a difficult topic to study (195, 196). Therefore, this section will instead focus on DILI due to the known hepatotoxic effects of acetaminophen (APAP), a commonly used antipyretic and analgesic in both the clinic and in over-the-counter drug formulations. APAP intoxication represents the leading cause of acute liver failure in the western world. Its use is widespread due to its favorable side-effect profile compared to non-steroidal anti-inflammatory drugs and opiates. The metabolic breakdown of APAP by hepatic cytochrome P4502E1 generates a highly reactive, toxic metabolite N-acetyl-p-benzoquinone imine (NAPQI) (197). At therapeutic doses NAPQI is reduced by the hepatic antioxidant glutathione and typically safely tolerated. However, with either large single ingestions of APAP or too frequent dosing at the therapeutic threshold results in depletion of hepatic glutathione, leading to formation and accumulation of protein adducts and widespread liver necrosis (197).

The onset of APAP-induced liver injury occurs in a predictable and dose-dependent manner, but the later stages of injury are less understood. There is evidence that

suggests that secondary immune-mediated injury occurs within the liver, indicating that targeting causative agents of the inflammatory response may make for an attractive and effective therapeutic intervention (197, 198). This hypothesis has brought some interest of gut-liver interactions and intestinal permeability to the field, though the research here is still newly developing. It was previously shown that APAP-treated mice experience transient portal endotoxemia and the inhibition of LPS binding protein by a synthetic peptide, but not its genetic deficiency, alleviated APAP hepatotoxicity (199, 200). Furthermore, Yang *et al.* demonstrated increased intestinal permeability to 4 kDa fluorescein isothiocyanate (FITC)-dextran and evidence of bacterial translocation into the mesenteric lymph nodes following APAP intoxication (201). Interestingly, neutralization of the cellular damage marker High mobility group box 1 (HMGB1) limited bacterial translocation but did not reduced FITC-dextran permeability (201). The mechanism behind APAP-induced gut permeability is still unclear, and though Yang *et al.* suggested a potential role gut mucosal injury following APAP-toxicity, there has been a lack of convincing data to demonstrate such (201). However, a similar hypothesis was also suggested by Possamai *et al.* after they had observed an increase in serum apoptosis markers in the portal veins relative to blood collected via the hepatic veins of APAP-induced acute liver failure patients undergoing transplantation (202). Specifically, it was speculated that this observation in serum apoptosis markers was due to APAP-induced apoptosis of enterocytes, similar to what is seen in sepsis patients (202). Some *in vitro* experiments have demonstrated modest intestinal epithelial death in response to high doses APAP concentrations, but convincing *in vivo* data to address Possamai's proposal are lacking (203, 204).

Roles that the intestinal microbiota may play to contribute to APAP acute liver injury aside from potential translocation-induced hepatic inflammation have also been proposed. For instance, the contribution of microbial metabolism of APAP was thought as a potential source of variation of clinical phenotypes amongst APAP hepatotoxicity patients. To that end, in a separate study Possamai *et al.* utilized GF mice to demonstrate that in the extent of early liver injury within 8-hours after APAP intoxication was equivalent to conventionally housed animals. However, GF mice had a modestly improved clinical phenotype compared to the conventionally housed mice, so it is possible that GF animals could experience less liver injury at later time points post intoxication (205). Conversely, a recent study demonstrated an intriguing mechanistic link between diurnal variation in commensal microbiota populations and susceptibility to APAP intoxication (206). In this study, variations in microbial populations and an increase in cecal concentration of the microbial metabolite 1-phenyl-1,2-propanedione (PPD) was observed at the start of the active cycle relative to the resting cycle of mice. Increased amounts of PPD exacerbated APAP hepatotoxicity in these animals, whereas gut sterilization with antibiotic pre-treatment prevented APAP liver injury (206). Therefore, it is most likely that additional aspects of the gut microbiota and the gut-liver aspect have modulatory impact on APAP-induced hepatic injury and possible on various etiologic agents of iDILI.

#### **4.4 Primary sclerosing cholangitis (PSC)**

PSC is a chronic idiopathic cholestatic liver disease that involves progressive sclerosis (scarring) of the biliary tree. The disease is marked by persistent biliary inflammation that

results in periductal fibrosis and eventually destruction of the bile ducts and liver cirrhosis (207, 208). PSC is most common in individuals of Northern European ancestry and the prevalence is nearly twice as high in men than in women (207). By definition as a disease of cholestasis, PSC involves the build-up and regurgitation of toxic bile salts that promote liver inflammation and injury. However, the factors which trigger biliary inflammation at the onset of PSC are unclear but appear multifactorial. Genetic, immunological, and environmental factors including diet appear to contribute to PSC risk and pathogenesis (207). There is also a strong contribution of intestinal inflammation, leakiness, and dysbiosis, as approximately 75% of PSC patients have comorbid inflammatory bowel disease (IBD) (209). However, only about 7-8% of IBD patients have comorbid PSC (207, 209). Interestingly, the majority of PSC-IBD involves colonic inflammation, and PSC-IBD appears to have a microbial signature that more closely resembles PSC than isolated IBD (209-211). Therefore, a strong case for gut leakiness and intestinal dysbiosis in PSC pathogenesis is made from these epidemiological observations alone. It was also demonstrated two-decades ago that LPS is detected within the cholangiocytes in the liver biopsies of PSC patients (212). Since then enhanced gut leakiness in the PSC population has been recognized by several clinical studies, which also found that the degree of gut leakiness correlated with worse disease outcomes (213, 214).

Much less is known about the mechanisms that induce PSC-associated gut barrier dysfunction than ALD and NAFLD. However, a recent study that used bile-duct ligation in mice as a model of cholestatic liver injury demonstrated that gut leakiness was associated with increased intestinal endoplasmic reticulum stress, intestinal epithelial

cell apoptosis, and reduced expression of epithelial stem cell marker *LGR5* (215). An elegant study by Nakamoto *et al.* demonstrated an enrichment of *Klebsiella pneumoniae* in the fecal content of PSC patients with ulcerative colitis. Colonization of mice with the patient-derived fecal microbiota demonstrated a pathogenic association with specific strains of *K. pneumoniae* that were able to induce pore formation within epithelial monolayer and enhance gut leakiness (210). Furthermore, the same study demonstrated that intestinal permeability was associated with a hepatic T<sub>H</sub>-17 mediated immune response that contributed to liver injury (210). A separate mechanistic study conducted by Tedesco and Thapa *et al.* in a genetic model of PSC instead found that an enrichment of intestinal *Lactobacillus gasseri* and its subsequent translocation to the liver induced IL-17 mediated inflammatory injury orchestrated instead by hepatic V $\gamma$ 6+  $\gamma\delta$ -T cells (216). This observation underscores the fact that even commensal organisms typically associated with health such as *L. gasseri* are capable of mediating deleterious immune reactions once homeostatic compartmentalization is compromised. Another recent study by Liao *et al.* reinforced these findings by demonstrating a role for dysbiosis-driven intestinal inflammation and gut leakiness via the NLRP3 inflammasome in a mouse model of PSC (208). This study also revealed that PSC-animals have reduced intestinal expression of ZO-1 and MUC2 (208). Though a full discussion is beyond the scope of this review, it is also worth mentioning that the pathophysiology of PSC is further entwined in intestinal physiology via the enterohepatic circulation of bile acids and altered bile acid metabolism (217). Thus, the advancements in our mechanistic understanding of the role of intestinal dysbiosis and gut leakiness in PSC and other cholestatic liver diseases is undergoing rapid advancements.

#### 4.5 Neurological and other disorders

Though anatomically the liver is the closest neighbor to the intestine, it is becoming increasingly clear that the intestine and its microbial content can have profound impacts on a diverse range of pathologies across multiple other target organs. Thus, while focusing on the gut-liver axis is convenient for the advancement of liver research, it is too limiting when trying to present the full significance of intestinal barrier physiology. For example, recent work is uncovering a role for gut barrier dysfunction and dysbiosis in cardiac diseases and renal diseases (4, 5, 164, 165). However, what is perhaps the most intriguing realization is that there is a clear and exciting influence of the gut on the pathophysiology neurological disorders (3, 12). Since the brain is considered a strictly sterile environment owing to the more restrictive blood-brain barrier (BBB), the influence of bacterial toxins or even live, translocated gut bacteria on brain physiology is an enticing, yet somewhat unsettling possibility. While enhanced BBB permeability has been reported under certain contexts due in part to reduced TJ protein expression such as claudin-5 (218), the influence of gut microbial populations on the brain need not be so direct. Gut microbiota educate the systemic immune system, and thus alter immune cell responsiveness and cytokine profiles (3, 219). Indeed, one study demonstrated that antibiotic treatment reduced brain injury in an ischemic stroke model by limiting an a small intestinal  $\gamma\delta$  T cell immune response (220). Furthermore, studies in GF mice have revealed that in the healthy animal, the presence of commensal microbial population facilitates enteric nervous system development (ENS) and dampens the hypothalamic-pituitary-adrenal (HPA) axis stress response. Conversely, monocolonization with a

strain of enteropathogenic *Escheria Coli* (EPEC) enhanced the HPA stress response (221).

Associations of gut permeability and altered microbiota have become apparent with a wide spectrum of neurological disorders, including autism spectrum disorders, depression, and amyotrophic lateral sclerosis (ALS) (3, 12). Parkinson's disease (PD) research has seen perhaps the strongest interest in gut-brain physiology (2). A likely reason for this focus is the early recognition that constipation owing to slowed gastrointestinal motility is an incredibly common comorbidity in the PD patient population, affecting between 50-80% of those with PD (2, 222). Moreover, constipation was found to commonly precede development of motor symptoms by up to 15-years (222). It was actually rather recently that the first evidence for a potential role of gut leakiness and intestinal inflammation in PD patients was demonstrated (223). However, a recent study by Sampson *et al.* provided some mechanistic insight into the role of intestinal bacteria in PD pathogenesis (224). In this work, mutant mice that are genetically susceptible to develop PD that were either treated with antibiotics or housed under GF conditions were found to be protected from the development of disease-related motor symptoms. Interestingly SCFA-feeding alone, without microbial recolonization, in GF PD-susceptible mice was sufficient to induce motor symptom development (224). Though SCFAs promote intestinal health, these metabolites were found to promote microglial activation, inflammation, and pathology. Thus, mechanistic insight is only beginning to be unraveled in the realm of the gut-brain axis, and it is likely that further metabolomic studies will push the field forward.

## **5. Summary and future directions**

Our knowledge on gut permeability and the intestinal microbiome is only in its infancy. In order to move forward we need more studies to move beyond simple associative observations and begin identifying mechanistic causes of gut barrier loss and links to the microbiota. While this is an extremely daunting task, we are beginning to see some of these efforts come to fruition (210, 216, 220, 224). As technology progresses, these types of study designs become easier and quicker to perform. However, our newfound appreciation of the profound effects of gut microbes emphasizes the need to strive for further experimental control considerations such as littermate controls in animal studies. Once more in-depth mechanistic understanding is gained, we will be able to leverage this knowledge for new therapeutics targeted at gut permeability, inflammation, and the microbiome. Experimental manipulation of these axes by probiotics, antibiotics, and occasionally interceptive interventions such as with sevelamer hydrochloride already hint at exciting possibilities that one day could be achieved in humans with the proper technological advancements (175, 190, 206, 225, 226). Furthermore, even with the associative knowledge that we are rapidly accumulating, we are able to identify novel biomarkers and assays for more timely disease recognition and more accurate patient risk stratification (227).

## **6. Conclusion**

It is an incredibly exciting time for gut barrier research, with vast opportunities available to expand our knowledge of whole-body health modulation by intestinal physiology and

the microbiome. There is a place, and indeed a need, for nearly all fields of biological sciences in the academic study of the gut barrier. The mysteries of the basic cell biology of the TJ remain to be fully elucidated. Microbiological analyses that unweave the metabolic functions and competitive niches of gut microbes are of paramount importance. Complementary studies on how these microbes interact with and direct the host immune system continue to expand our knowledge of fundamental immunology and disease pathogenesis. Stem cell biology as it pertains to gut homeostasis and barrier function is a newly rejuvenated field as new tools and mouse strains have been generated. Even so, these topics are likely only the tip of the iceberg. Major advancements in therapeutic development are anticipated through investigating these realms of the gut-liver axis and beyond. Thus, we must strive for collaborative, integrative approaches across these fields of study to bring about a new era of holistic, whole-body, and host-microbe discovery.

### **Acknowledgements**

We acknowledge the contribution of graphic designer Krystal Chopyk in generating the infographic summary figures for this chapter.

**Figure 1. Components of the gut barrier.** The intestinal barrier is comprised of mucus, microbial, epithelial, and immunological components. Within the colon the mucus forms two distinct layers – a looser, outer layer where most of the intestinal bacteria reside, and a dense, inner layer that is comparatively sterile. The commensal microbiota reinforce the gut barrier by providing colonization resistance to potential pathogens and by producing useful metabolites such as short chain fatty acids (SCFAs) that promote epithelial health and integrity. Goblet cells are scattered through the intestinal epithelial monolayer and are responsible for mucus production. Additional specialized cellular populations are found within the bases of the intestinal crypts. Here, *LGR5*<sup>+</sup> stem cells are a source of continuous cell renewal to maintain epithelial integrity. These stem cells also give rise to differentiated Paneth cells, which remain at the base of the crypts and produce large amounts of antimicrobial peptides (AMPs) and growth factors. Plasma cells within the lamina propria also secrete dimeric immunoglobulin A that is transported across epithelial cells and contributes to immune exclusion of the luminal microbiota. MUC2, mucin 2; sIgA, secretory immunoglobulin A.

**Figure 2. Architecture of intestinal epithelial tight junctions.** The intestinal epithelial tight junction is composed of three classes of transmembrane proteins which associate with various scaffolding proteins that act as linkers to the actin cytoskeleton. The transmembrane proteins include occludin and other tight junction associated MARVEL proteins (TAMPs), claudins, and junctional adhesion molecule-A (JAM-A). Occludin and claudin proteins have cytoplasmic N- and C-termini and four transmembrane domains. Junctional adhesion molecule-A instead has a cytoplasmic C-terminus and two extracellular V-type immunoglobulin domains. Importantly, JAM-A can dimerize both *in*

*cis* (molecules on the same cell) and *in trans* (molecules on adjacent cells). ZO-1/2, zonula occludens-1/2.

**Figure 3. Mechanisms of gut barrier dysfunction and routes for systemic entry of translocated bacteria and toxins.** Various conditions such as dysbiosis, inflammation, and tight junction (TJ) dysfunction can contribute to enhanced gut permeability.

Translocated bacteria and microbial toxins can gain access to distant sites via various routes upon gut barrier collapse. Most importantly, a large concentration of bacteria and pathogen associated molecular patterns (PAMPs) can enter the portal circulation and gain immediate access to the liver. The liver contains large populations of immune cells which respond to these various stimuli by triggering potent inflammatory reactions. A portion of these bacteria, PAMPs, and metabolites pass through the liver where they gain access to the systemic circulation. In parallel, a number of translocated bacteria and PAMPs from the intestine gain access to the lymphatic vasculature, where they first pass through the mesenteric lymph nodes (MLNs). Similarly, a portion of these intralymphatic toxins will enter the systemic circulation. Intestine-derived bacteria, PAMPs, toxins, and metabolites can thereafter influence the function of distant organ sites such as the heart, kidney, and brain. Translocated gut pathogens may additionally influence the brain via retrograde transport along fibers of the vagus nerve that contribute to the myenteric plexus. AMPs, antimicrobial peptides.

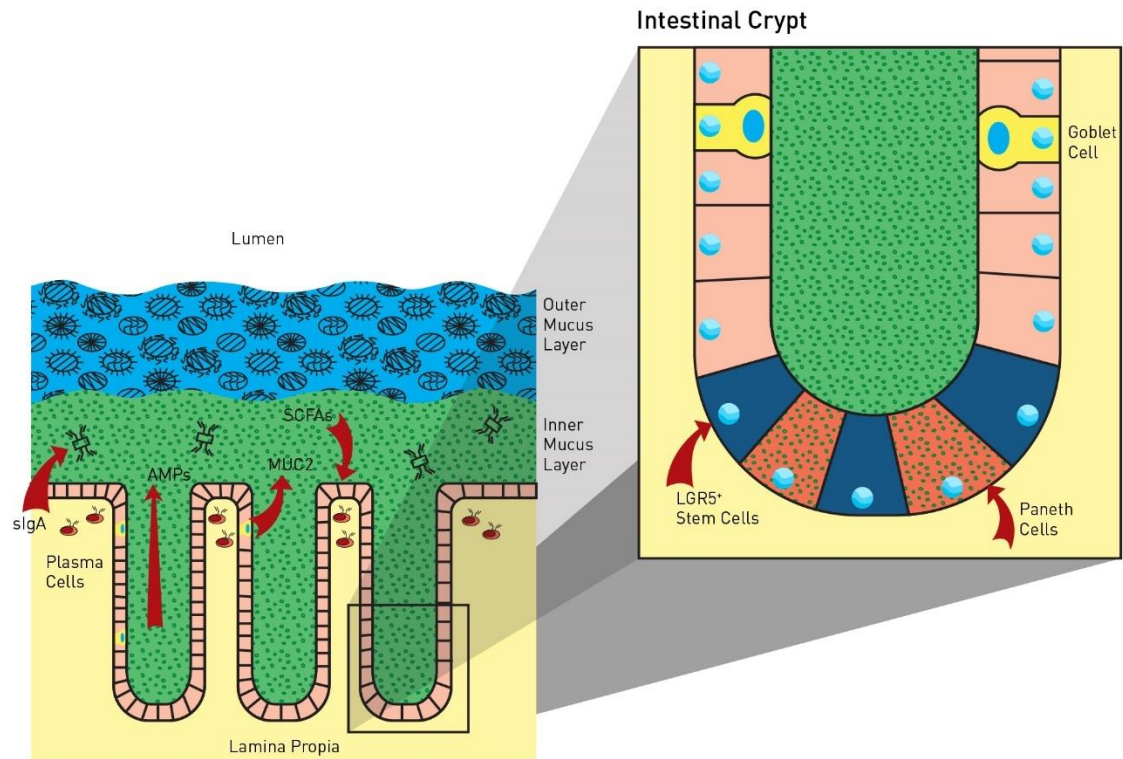


Figure 1

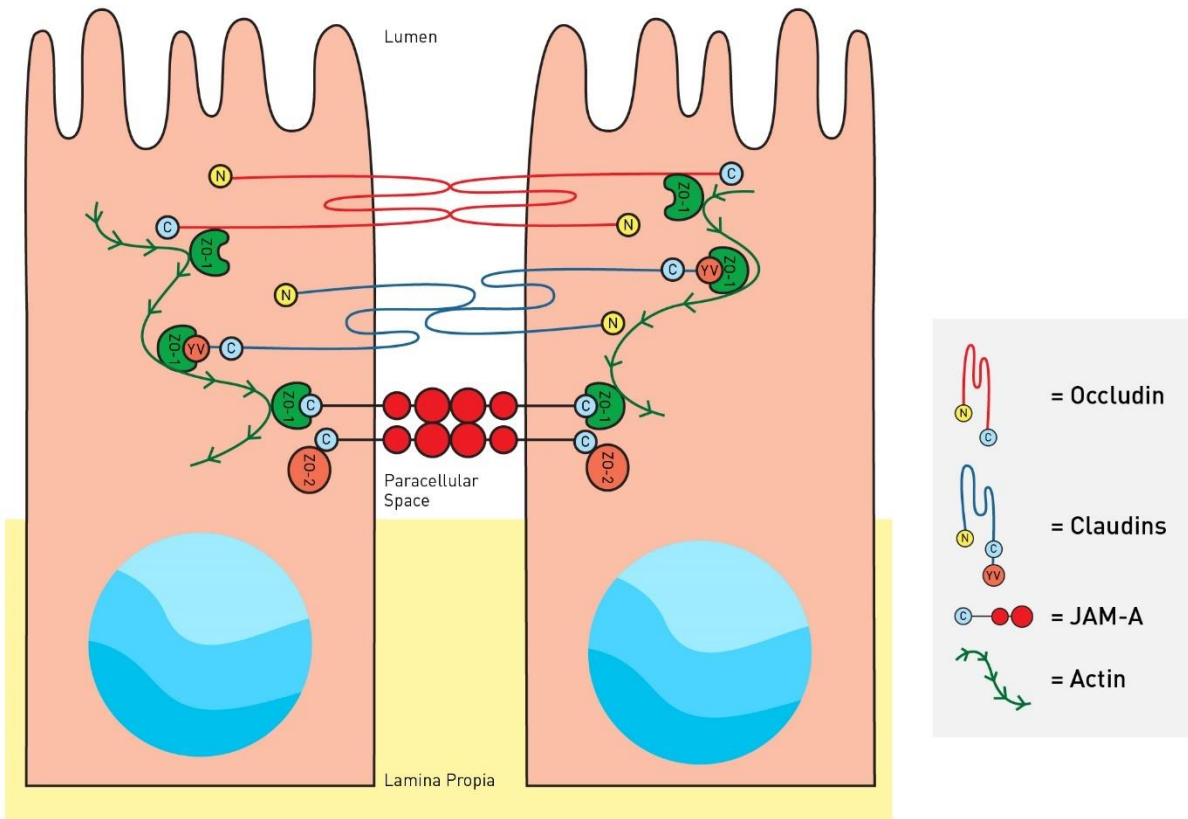
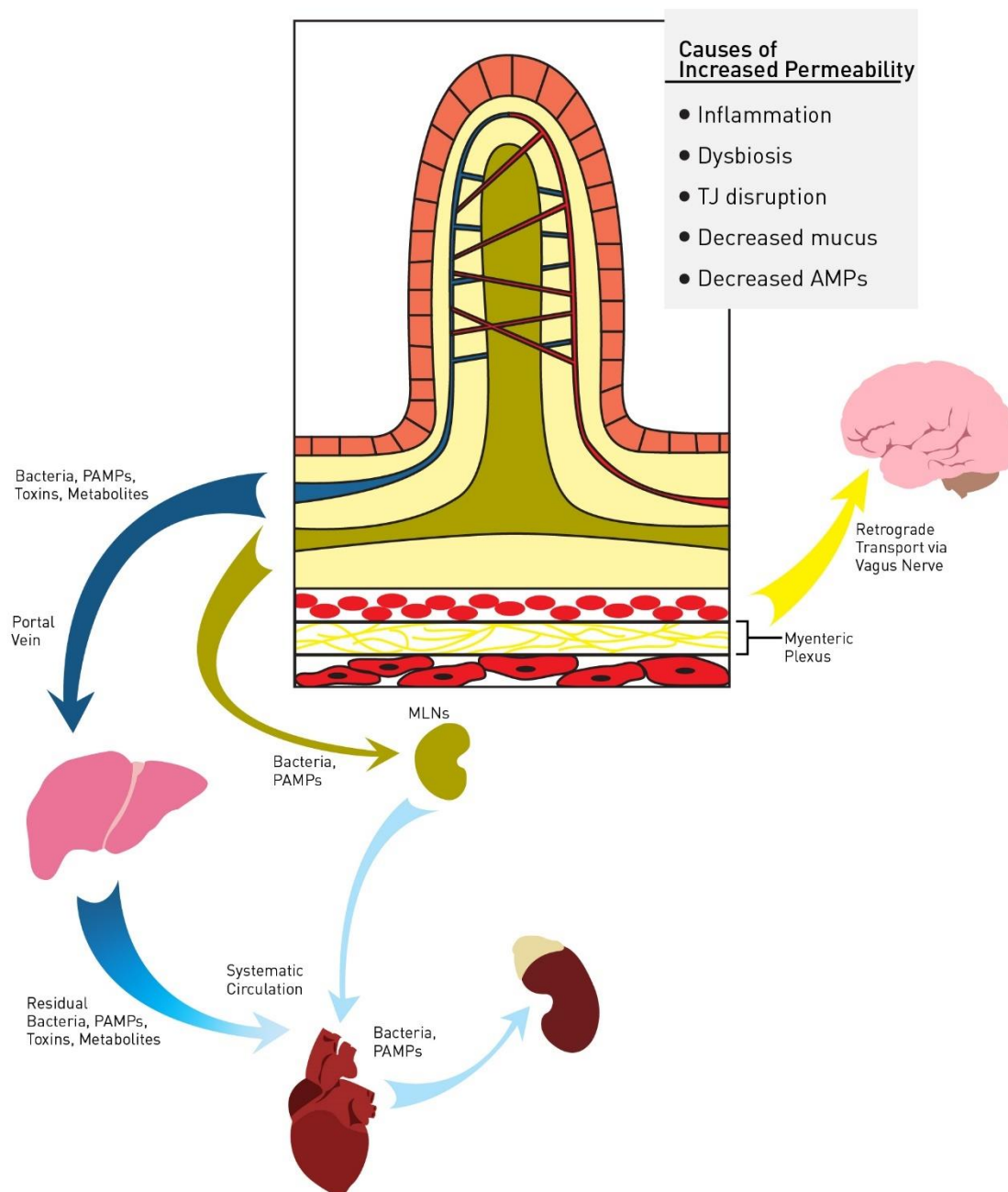


Figure 2



**Figure 3**

## **Chapter 2: Dysregulation of junctional adhesion molecule-A contributes to ethanol-induced barrier disruption in intestinal epithelial cell monolayers**

Daniel M. Chopyk<sup>1\*</sup>, Pradeep Kumar<sup>1</sup>, Reben Raeman<sup>1</sup>, Yunshan Liu<sup>1</sup>, Tekla Smith<sup>1</sup>, Frank A. Anania<sup>1</sup>

### **Author contributions**

D.M.C., P.K., R.R., and F.A.A. conception and design of research; D.M.C. performed experiments and analyzed data; Y.L., T.S. provided aid in maintenance of transduced and transfected Caco-2; D.M.C., P.K., R.R., and F.A.A. interpretation of results; D.M.C. drafted manuscript; D.M.C. prepared figures; D.M.C., P.K., R.R., F.A.A. edited and revised manuscript; F.A.A. approved final version of manuscript

### **Affiliations**

<sup>1</sup>Emory University School of Medicine, Department of Medicine, Division of Digestive Diseases, 615 Michael Street NE, Suite 201, Atlanta, GA 30322

### **Running Head**

### **JAM-A in ethanol induced epithelial barrier dysfunction**

### **\*Corresponding Author**

Daniel M. Chopyk

Published in *Physiological Reports*, 2017 Dec.; 5(23) PMID: 29208693

Department of Medicine, Division of Digestive Diseases, 615 Michael Street NE, Suite 265, Atlanta, GA 30322, USA. Phone: +1(404)-727-2862. Fax: +1(404)-727-5767

E-mail: [dchopyk@emory.edu](mailto:dchopyk@emory.edu)

## **Abstract**

Alcohol consumption promotes loss of intestinal barrier function. However, mechanisms by which ethanol affects the tight junction (TJ), the cellular structure responsible for maintaining the gut epithelial barrier, are not well understood. Three classes of transmembrane proteins comprise TJs: occludin, claudins, and junctional adhesion molecules (JAMs). It has recently been postulated that JAM-A (F11R), the most abundant JAM expressed in intestinal epithelium, regulates “leak” pathway flux, a paracellular route for the non-selective permeation of large solutes. Since transluminal flux of many gut-derived antigens occurs through this pathway, we investigated the role of JAM-A in ethanol-induced disruption of the intestinal epithelial barrier. Using Caco-2 and SK-CO15 monolayers, we found that ethanol induced a dose- and time-dependent decrease in JAM-A protein expression to about 70% of baseline levels. Alcohol also reduced Ras related protein 2 (Rap2) activity, and enhanced myosin light chain kinase (MLCK) activity, changes consistent with impaired JAM-A signaling. Stable overexpression and shRNA-mediated knockdown of JAM-A were employed to investigate the role of JAM-A in paracellular-mediated flux following alcohol exposure. The paracellular flux of 40-kDa fluorescein isothiocyanate (FITC)-dextran following ethanol treatment was decreased by overexpression of JAM-A; conversely, flux was enhanced by JAM-A knockdown. Thus, we conclude that ethanol-mediated control of JAM-A expression and function contributes to mechanisms by which this chemical induces intestinal epithelial leakiness.

## **Keywords**

Junctional adhesion molecule-A; ethanol; intestinal epithelial barrier; Caco-2; Rap2; myosin light chain kinase

**New & Noteworthy**

In this study, we present new evidence suggesting that dysregulation of the tight junction protein JAM-A may contribute to the mechanisms by which ethanol disrupts intestinal epithelial barrier integrity and function. Ethanol exposure was found to reduce JAM-A protein expression in Caco-2 monolayers, as well as result in impaired signaling activity of JAM-A signaling molecules Rap2 and MLCK.

## Introduction

The most recent World Health Organization data reports that alcohol use accounts for approximately 3.3 million annual deaths globally, a large proportion of which are the result of alcoholic liver disease (ALD) (228). Approximately 50% of deaths attributable to cirrhosis are the result of alcohol abuse (228). Recently, it has become clear that alcohol exposure causes impaired intestinal barrier function (178, 229), leading to elevated serum endotoxin (170, 230-232). Since blood from the intestines drains into the venous portal system, it is the liver that first encounters elevated levels of lipopolysaccharide (LPS) and other gut-derived pathogen associated molecular patterns (PAMPs) (178, 233). A growing body of evidence suggests that the resulting liver inflammatory response, primarily driven via LPS-Toll-Like Receptor-4 (TLR-4) interactions on liver-resident Kupffer cells, promotes ALD pathogenesis (11, 234).

Alcohol causes profound physiological changes to epithelial cells lining the gut (178). Of particular interest are the effects of ethanol on the tight junction (TJ), the structure responsible for the formation, maintenance, and regulation of epithelial paracellular barrier function (14). TJs consist of three groups of transmembrane proteins: occludin, claudins, and junctional adhesion molecules (JAMs) (20). Though TJ proteins share some functional redundancy, each molecule has several unique roles (20, 38, 235). For example, the claudin family of proteins has been demonstrated to regulate permeability to ions and small solutes in a charge selective manner (235, 236). However, the individual functions of occludin and JAMs are much less understood.

Numerous studies have demonstrated that ethanol, its metabolites, and alterations of the gut microbiome suppress intestinal occludin expression (175, 180, 237). Moreover, occludin knockout (KO) mice were recently found to be more susceptible to ethanol-induced gut barrier

dysfunction and liver injury (180). However, the lack of a pronounced intestinal phenotype in occludin KO mice in the absence of alcohol suggests that this protein may play an accessory role in regulating epithelial barrier function (34). Similarly, mice lacking JAM-A (F11R), the prominent JAM expressed in the intestine, were demonstrated to have elevated serum endotoxin levels compared to wild-type (WT) littermates after 8-weeks of high-fat diet (190). This finding supports the proposed functional role that JAM-A regulates paracellular permeability to macromolecular solutes via regulating the contractile tone of the apical cytoskeleton through modulation of myosin light chain kinase (MLCK) (75). Ethanol has been demonstrated to enhance MLCK activity at least in part via activation of the Ras homolog gene family member A (RhoA), another proposed signaling partner of JAM-A (75, 238-240).

Despite the demonstration of an important role of JAM-A for TJ function, and that ethanol exposure interferes with molecules associated with JAM-A signaling, the role of JAM-A in ethanol-induced gut barrier dysfunction has been left understudied.

Here, we hypothesized that dysfunction of JAM-A contributes to ethanol-induced epithelial barrier disruption and provide multiple approaches demonstrating that ethanol reduces JAM-A protein expression, and disrupts its downstream signaling partners. Additionally, we provide evidence that directly associates JAM-A expression with enhanced barrier function in the context of alcohol exposure.

## **Materials and Methods**

### **Chemical Reagents:**

Cell culture reagents including antibiotics were purchased from Corning (Corning, NY) and Sigma-Aldrich (St. Louis, MO), except for fetal bovine serum which was purchased from Atlanta Biologicals (Flowery Branch, GA). Fluorescein isothiocyanate (FITC)-dextran 4-kDa and 40-kDa were purchased from Sigma-Aldrich. Hanks Balanced Salt Solution with  $\text{Ca}^{2+}/\text{Mg}^{2+}$  without phenol red (HBSS+) was purchased from Sigma-Aldrich. Two hundred-proof ethanol was purchased from Decon Labs (King of Prussia, PA) and was sterile filtered with Thermo Fisher Nalgene™ bottle-top vacuum filters (Waltham, MA).

### **Antibodies:**

Mouse monoclonal anti-human JAM-A was purchased from NovusBio (Littleton, CO; #H00050848-M01). Goat polyclonal anti-human JAM-A (#AF1033) and goat polyclonal anti-mouse JAM-A (#AF1077) were both purchased from R&D Systems (Minneapolis, MN). Mouse monoclonal anti-occludin, mouse monoclonal anti-zonula occludens-2 (ZO-2), and donkey polyclonal anti-goat IgG (H+L)-Alexa Fluor® 488 were purchased from Thermo Fisher (#33-1500, #37-4700, and #A-11055). Mouse monoclonal anti- $\beta$ -actin and mouse monoclonal anti-myosin light chain kinase (MLCK) were purchased from Sigma-Aldrich (#A5441 and #M7905). Mouse monoclonal anti-FLAG (Sigma-Aldrich #F1804) was a kind gift from Dr. Chris Yun (Emory University, Atlanta, GA). Goat anti-mouse IgG-HRP was purchased from Santa Cruz (Dallas, TX; #sc-2005).

### **Cell culture:**

Caco-2, SK-CO15, and HEK293T cells were originally purchased from American Type Culture Collection (ATCC, Manassas, VA). Caco-2 and SK-CO15 cells were empirically pre-treated for mycoplasma with plasmocin. All cells were maintained in DMEM supplemented with 10% FBS

and 1% penicillin-streptomycin, and 1 mM sodium pyruvate additionally added for Caco-2 cultures. Cells were split every 3 to 5 days.

#### **Caco-2 cell transfection and generation of stable clones overexpressing JAM-A:**

JAM-A overexpression was achieved by transfection of Caco-2 cells with a pCMV6-F11R-MycDDK plasmid purchased from OriGene (Rockville, MD; #RC221478). The plasmid was first expanded in NEB-5 $\alpha$  competent *E. Coli* purchased from New England BioLabs (Ipswich, MA; #C2988J) by heat shock transformation. Transformed bacteria were selected by overnight incubation at 37°C on Lysogeny Broth (LB) agar plates with 25  $\mu$ g/mL kanamycin (Sigma-Aldrich). Selected colonies were expanded in 25  $\mu$ g/mL kanamycin LB broth incubated at 37°C and 250 RPM for 16-hr. Plasmid DNA was isolated using a QIAprep Spin Miniprep Kit (Qiagen; Hilden, Germany). The equivalent empty pCMV6 vector control plasmid (OriGene #PS100001) was previously expanded in a similar fashion.

One day before transfection, actively dividing Caco-2 cells were seeded on a 6-well plate in antibiotic-free DMEM. Cells were 60-70% confluent the next morning, and media was replaced with Opti-MEM™ reduced serum growth media (Thermo Fisher). The cells were then transfected with 3  $\mu$ g DNA of either plasmid, and 9  $\mu$ l Lipofectamine® 2000 (Thermo Fisher) per well. Opti-MEM™ was changed with complete growth media 6-hr post-transfection. Transfected cells were split 48-hr post-transfection, and were grown in increasingly higher concentrations of G418 up to ~700  $\mu$ g/mL (Sigma-Aldrich) over several weeks. Selected clones were perpetually maintained in 700  $\mu$ g/mL G418 thereafter. Cells from passage 20 to 32 were used for transwell experiments.

#### **Generation of shRNA plasmid lentiviral vectors and Caco-2 transduction:**

Bacterial stocks expressing plasmids encoding JAM-A specific shRNA (Cat. #TRCN0000431967), pLKO.1 control shRNA, pLTR-G envelope, and PCD/NL-BH4 packaging

plasmid were purchased from Sigma-Aldrich. All bacterial stocks were expanded as described above using either 100 µg/mL ampicillin (Sigma-Aldrich) or 50 µg/mL kanamycin (pLTR-G only). Plasmid DNA was isolated as described above.

For generation of pseudoviral particles, actively dividing HEK293T cells were seeded in T75 flasks (Corning) in antibiotic-free media and were cultured overnight. Subconfluent cultures (90%) were transfected with shRNA target (pLKO.1 or JAM-A), helper plasmid (PCD/NL-BH4), and envelope plasmid (pLTR-G) DNA in an 8 µg : 6 µg : 4 µg ratio using 30 µL of lipofectamine<sup>®</sup> LTX reagent and 30 µL PLUS<sup>™</sup> reagent (Thermo Fisher) in serum-free DMEM. Viral supernatants were harvested 48-hr post-transfection and were cleared by centrifugation for 5-min at 931 x *g* at 25°C and filtered through a 0.45 µm pore PVDF syringe tip filter (Millipore; Billerax, MA). Viral stocks were aliquoted and frozen at -80°C until use.

For viral transduction, Caco-2 cells at passage 30 were seeded on 6-well plates and were grown to 100% confluence over 7-d. On day 7, cells were incubated in a 1:1 dilution of media plus crude viral supernatant with polybrene (Santa Cruz) at a final concentration of 10 µg/mL. Viral supernatants were replaced with fresh complete growth medium after 24-hr. After an additional 24-hr, the transduced cells were split onto new plates using media supplemented with 10 µg/mL puromycin (Sigma-Aldrich). Selection media was changed every 48-hr over 10-d. The selected colonies present on day 10 were split into T75 flasks using 10 µg/mL puromycin, and were continuously expanded and maintained under these conditions thereafter. Cells between passages 34 to 39 were used for transwell experiments.

**Transwell seeding and maintenance:**

Corning 24-mm 6-well and 6.5-mm 24-well 0.4 µm pore polyester membrane transwell inserts were coated with 10 µg/cm<sup>2</sup> growth area rat tail collagen Type 1 (Sigma-Aldrich) diluted in 70% ethanol. Transwells were left to dry under UV light overnight and were washed once with PBS

and once with complete growth media. Actively dividing Caco-2 or SK-CO15 cells were split and seeded at an approximate density of  $2 \times 10^4$  cells/cm<sup>2</sup> growth area ( $1 \times 10^5$  cells per 6-well insert,  $6.67 \times 10^3$  per 24-well insert). Media was changed 6-hr after seeding, and every 48-hr thereafter. Experiments were carried out between days 15 and 20 after seeding (7-12 days post-confluence).

### **Modified high-density transwell seeding for transfected and transduced Caco-2**

#### **experiments:**

Stable clones of transfected and transduced Caco-2 cells exhibited greatly reduced growth rates compared to non-transformed cells due to the presence of selection antibiotics. To compensate, these cells were seeded on transwells at about  $2.6 \times 10^5$  cells/cm<sup>2</sup> growth area ( $1.3 \times 10^6$  cells per 6-well insert,  $8.5 \times 10^4$  per 24-well insert) to achieve confluence overnight. Media was changed 24-hr after seeding, and every 48-hr thereafter. Experiments were carried out between days 7 and 8.

#### **Ethanol Treatment:**

Except for inserts used for FITC-dextran and resistance studies, epithelial cell monolayers were prepared 24-hr in advance by individually separating monolayers into new 6-well plates according to each condition (i.e., ethanol or control) with subsequent treatment with media to achieve 94% of the planned final volume. After overnight incubation at 37°C, monolayers were treated with media, sterile-filtered 200-proof ethanol (6% v/v), or a 1:1 mixed solution of both (3% v/v) to the final volume. These concentrations were based on previously published *in vitro* and *in vivo* studies (239, 241, 242). All plates were sealed with parafilm to minimize the loss of ethanol as vapor during the treatment period (243). It has been previously shown that sealing plates did not result in a significant in change in pH or cell viability within the prescribed treatment time frames (243).

**Transepithelial Electrical Resistance (TEER) and FITC-Dextran Flux:**

Only 6.5-mm 24-well transwell inserts were used for measuring TEER. Caco-2 cells were washed twice with HBBS+, and were then incubated in fresh HBSS+ for 1-hr at 37°C. Next, 4-kDa or 40-kDa FITC-dextran was pipetted into the apical compartment at a final concentration of 1 mg/mL, immediately followed by the addition of HBSS+, ethanol, or a 1:1 mixture of both, to both the apical and basal chambers (0, 3%, 6% v/v final concentrations of ethanol). Resistance was measured immediately after treatment ( $t = 0$ ) and following 3-hr incubation using an EMD Millipore Millicell-ERS Volt-Ohm meter (Millipore; Model #MERSSTX01). Basal fluid fluorescence at 485 nm excitation and 525 nm emission was measured after the 3-hr incubation using a BioTek® Synergy2 microplate reader with Gen5 software (Winooski, VT). Empty cell-free collagen coated transwells were used to normalize monolayer resistances and record maximal FITC-dextran flux. Only monolayers with minimum baseline TEER values consistent with confluence were used for analysis ( $\geq 250 \Omega \times \text{cm}^2$  for unmanipulated Caco-2;  $\geq 80 \Omega \times \text{cm}^2$  for pCMV6-transfected Caco-2). Inclusion of shRNA transduced Caco-2 monolayers in data analysis was based solely on confluence by microscopic inspection.

**Protein Lysate collection and Western Blot Analysis:**

Epithelial cell monolayers were washed with ice-cold PBS (Corning) twice and were lysed with ice-cold RIPA lysis buffer (Alfa Aesar; Haverhill, MA) with cOmplete™ and PhosSTOP™ protease/phosphatase inhibitor cocktails (Roche; Basel, Switzerland). Lysates were sonicated and cleared by centrifugation at  $9.3k \times g$  for 10-min at 4°C. Protein quantifications were made by bicinchoninic acid assay (BCA assay; Thermo Fisher). Equal amounts of protein were then aliquoted in reducing LDS sample buffer using RIPA lysis buffer as diluent. Samples were reduced by heating at 95°C for 5- to 7-min.

Unless otherwise stated, 20  $\mu\text{g}$  of protein was loaded in either NuPAGE™ 4-12% Bis-Tris protein gels (Thermo Fisher) run in 3-(N-morpholino)propanesulfonic acid (MOPS) buffer (Thermo Fisher) or in 12% polyacrylamide gels made with Protogel® run in Tris-Glycine SDS buffer (National Diagnostics; Atlanta, GA). All gels were transferred to PVDF membranes by electro-transblotting. Blots were blocked with 5% non-fat milk in TBST for 1-hr at 25°C. All primary antibody incubations other than anti- $\beta$ -actin (1:10,000 for 1-hr at 25°C) were overnight at 4°C at the following dilutions in 5% BSA TBST: anti-human JAM-A (NovusBio) 1:500, anti-occludin 1:1000, anti-MLCK 1:10,000, anti-ZO-2 1:1000, anti-mouse JAM-A 1:2000. Anti-FLAG antibodies were used 1:1000 in 3% non-fat milk in TBST for overnight incubation at 4°C. Secondary antibody incubation was applied for 1-hr at 25°C using goat anti-mouse-IgG-HRP diluted to 1:5,000 in 5% non-fat milk in TBST. All blots were developed using ECL solution made in-house and autoradiographic imaging (VWR; Radnor, PA). Densitometry was measured using VisonWorks®LS UVP Image Acquisition and Analysis software version 8.1.2. Densitometry measurements for each target were normalized to respective  $\beta$ -actin bands.

#### **Immunoprecipitation and Kinase Activity Assay:**

Protein lysates were collected from Caco-2 monolayers as described above except T-per™ Tissue Protein Extraction Reagent (Thermo Fisher) was used to preserve enzymatic function. Lysates were quantified and snap-frozen in liquid nitrogen on the day of harvest, and were thawed in water baths (25°C) on the day of immunoprecipitation (IP) and analysis. Smooth muscle/non-muscle myosin light chain kinase (MLCK) was immunoprecipitated from 400  $\mu\text{g}$  of total protein lysate using magnetic SureBeads™ (Bio-Rad; Hercules, CA) coated with 1  $\mu\text{g}$  mouse anti-MLCK (Sigma-Aldrich #M7905). IP was subsequently performed as outlined in Bio-Rad's protocol. Kinase activity of the immunoprecipitated complexes was directly measured without elution using an ADP-Glo™ kinase assay kit (Promega; Madison, WI) and synthetic

peptide substrate MRCL3 (SignalChem; Richmond, British Columbia, Canada). Briefly, the MLCK-SureBeads™ complexes were magnetized and all wash buffer was aspirated. The bead complexes were fully resuspended in 10  $\mu$ L of 1X kinase reaction buffer (40 mM Tris-HCl pH 7.5, 20 mM MgCl<sub>2</sub>, 0.1 mg/mL BSA) and were divided into two-5  $\mu$ L aliquots each that were measured in duplicate. A 20  $\mu$ L mixture of MRCL3 peptide and ATP was added to the beads for a final concentration of 50  $\mu$ M ATP and 0.4  $\mu$ g/mL MRCL3. The reaction mixtures were incubated at 25°C for 60-min before the kinase reaction was stopped by addition of 25  $\mu$ L of ADP-Glo™ reagent. The samples were incubated for another 40-min at 25°C and then 50  $\mu$ L of kinase detection reagent was added. Luminescence was measured with the kinase-Glo protocol on a GlowMax® 20/20 Luminometer (Promega) after a final 30-min incubation at 25°C. All sample measurements were adjusted for the luminescence of antibody-coated SureBeads™ alone.

#### **Rap2 Activation Pulldown Assay:**

Active Rap2 was analyzed via a RalGDS RBD Agarose bead pulldown assay kit according to the manufacturer's instructions (Cell BioLabs; San Diego, CA). Rap2 pulldown was conducted using 500 to 750  $\mu$ g of protein, and in some experiments lysates from Caco-2 monolayers treated in duplicate were pooled. Western blots were performed as described above on the pulled down, active Rap2 and respective total protein samples using the respective antibodies at their recommended concentrations. Densitometric measurements for active Rap2 were normalized to the total Rap2/ $\beta$ -actin ratio.

#### **Lactate Dehydrogenase (LDH) Assay:**

Caco-2 monolayers were washed twice with HBSS+ and were divided into separate, clean 6-well plates according to planned treatment (0%, 3%, or 6% v/v ethanol). Cells were then incubated in HBSS+ at 94% of the planned final volume for 1-hr at 37°C, after which the

remaining volume was added as HBSS+, 200-proof ethanol, or a 1:1 mixture of both as described above. After 6-hr incubation at 37°C, apical solutions were collected and cleared by centrifuged at 9.3k x g for 10-min at 4°C. LDH activity was measured in triplicate using a cytotoxicity detection kit (Roche). Absorbance at 490 nm and 620 nm was measured using a BioTek® Synergy2 microplate reader with Gen5 software. Results were normalized according to wells containing HBSS+ alone.

### **Immunofluorescence confocal microscopy:**

Caco-2 monolayers were washed with 0.05% Triton X-100 (Thermo Fisher) in PBS (PBST) and were fixed by 20-min RT incubation in 3.7% paraformaldehyde (Electron Microscopy Sciences; Hatfield, PA) in 0.05% PBST. Cells were then permeabilized with 0.1% PBST for 20-min at RT followed by blocking with 5% BSA and 5% donkey serum in 0.05% PBST for 30-min at RT. Monolayers were then excised from their inserts and were stained overnight at 4°C with goat anti-human JAM-A (R&D Systems) 1:40 in 3% BSA diluted in 0.05% PBST. Secondary staining was done by 1-hr RT incubation in donkey anti-goat IgG (H+L)-Alexa Fluor® 488 1:1000 in 1% BSA diluted in 0.05% PBST. Samples were then mounted using Prolong™ Gold with DAPI (Thermo Fisher). Samples were visualized with an Olympus IX81 inverted microscope (Olympus Scientific Solutions Americas, Inc.; Waltham, MA).

Frozen sections of mouse ileum were thawed at RT for 10 min and were rehydrated with 0.05% PBST. Tissue was fixed with incubation in 100% methanol at -20°C for 10 min., followed by permeabilization in 0.3% PBST for 15 min at RT. Samples were blocked with 5% BSA and 5% donkey serum in 0.3% PBST for 1-hr at RT. Tissue was then stained overnight at 4°C with goat anti-mouse JAM-A 1:100 in 1% BSA in 0.3% PBST. An additional tissue sample was incubated in 1% BSA in the absence of primary antibodies was included as a negative control. All samples

were next stained with donkey anti-goat IgG (H+L)-Alexa Fluor® 488 1:1000 in 1% BSA diluted in 0.3% PBST for 1-hr at RT. Samples were mounted and imaged as described above.

**Mice and chronic plus binge ethanol in high-fat diet model and in vivo assessment of gut permeability:**

All mouse work was outsourced to the Southern California Research Center for ALPD and Cirrhosis Animal and Morphology Core facilities. Eight-week old wild-type male C57BL/6 mice were fed a modified high-fat, high-cholesterol Lieber-DeCarli diet containing 1.26 g/kg cholesterol, 12.5% calories derived from milk-fat, 16.7% calories derived from lard, and 8.4% calories derived from corn oil (Dyets, Inc.; Bethlehem, PA; Cat. #710383 and #710384). Mice were fed ethanol by an escalated dose (%v/v) of 1.45% for 3d, 2.9% for 4d, and 4.35% (~23.3% total calories). A cohort of control mice was pair-fed an equivalent isocaloric diet without ethanol. Additionally, mice were given a once-per-week binge of ethanol starting at a dose of 3.5 g ethanol per kg body weight. The binge dosage was increased by an additional 0.5 g ethanol per kg body weight each consecutive week to a final dose of 6.0 g ethanol per kg body weight. Control mice were given an isocaloric glucose binge.

The sixth and final ethanol or glucose binge was conducted 1-d prior to sacrifice. Prior to sacrifice, mice were additionally gavaged with 600 mg/kg 4-kDa FITC-dextran in PBS. Serum samples from each mouse were collected by facial vein bleeds 4-hr post FITC-dextran gavage. Mice were then euthanized while under isoflurane anesthesia and serum was collected by cardiac puncture. Remaining blood was removed from livers prior to harvest by gentle perfusion with ice-cold PBS by a butterfly needle inserted via the portal vein. Ileum samples were cleaned of associated fat, cut longitudinally, and gently washed in ice-cold PBS to remove luminal contents. Short segments of distal ileum (~1 cm) were cut and flash frozen in liquid nitrogen for analysis by western blot. Remaining ileum segments were rolled using a flat toothpick and were frozen in Tissue-Tek OCT compound (Sakura Finetek USA, Inc.; Torrance, CA) for sectioning.

**Histology:**

Liver tissue was fixed in 10% phosphate buffered formalin (Thermo Fisher) and embedded in paraffin. After sectioning, samples were stained with hematoxylin and eosin and were visualized using a Nikon® Eclipse E600 light microscope (Nikon Instruments, Inc.; Melville, NY)

**Statistical Analyses:**

All data are reported as means  $\pm$  SEM. Data were all analyzed using GraphPad Prism® 7.0a software (GraphPad Software; La Jolla, CA). Differences among multiple groups were analyzed by one-way ANOVA followed by Dunnett's multiple comparison test. Experiments involving only two treatment groups were analyzed by students *t*-test. Statistical significance was set at  $p < 0.05$  for all analyses.

## Results

### **Ethanol induces a dose-dependent reduction in Caco-2 monolayer barrier function without affecting cell viability**

We employed the well-established *in vitro* system of Caco-2 monolayers to study the direct effects of ethanol on the intestinal epithelial TJ. Prolonged culture of this human colon adenocarcinoma cell line on transwell inserts results in their differentiation and permits development of mature TJs and brush border microvilli (241, 244). In agreement with previous studies, we observed a dose-dependent reduction in monolayer TEER within 3-hr of ethanol treatment (**Fig. 1A, B**) (239, 241). Ethanol doses below ~1% v/v (~171 mM) did not result in significant reductions in monolayer TEER (data not shown). Because TEER is only a measure of ionic flux, we also assessed the paracellular permeability of the monolayers using both small (4-kDa) and large (40-kDa) FITC-dextran. Permeability of both sizes of FITC-dextran was significantly increased by 6% ethanol exposure (**Fig. 1 C, D**;  $2.72 \pm 0.29$ -fold 6% vs 0% 4-kDa;  $4.38 \pm 0.36$ -fold 6% vs 0% 40-kDa). Furthermore, ethanol dosages as high as 6% did not cause significant changes in cellular viability as measured by LDH release, even after 6-hr treatment (**Fig. 2**).

### **Expression of JAM-A, but not occludin or ZO-2, was reduced in Caco-2 and SK-CO15 monolayers after prolonged ethanol exposure**

The effect of ethanol on JAM-A protein expression in Caco-2 monolayers was investigated by dose response in which cells were exposed to 3% or 6% ethanol for 6-hr. A significant reduction in JAM-A protein expression compared to controls was observed after 6% ethanol treatment (**Fig. 3A**;  $0.75 \pm 0.08$ -fold change 6% vs 0%), while 3% ethanol exposure resulted in a non-significant trend towards reduced expression ( $p=0.16$ ). Similar changes in occludin expression

were also observed at both 3% and 6% ethanol, but no significant change was observed in ZO-2 protein expression at either concentration (**Fig. 3A**). We also performed a time course of 6% ethanol treatment to examine the time frame of JAM-A protein reduction in Caco-2 monolayers. Our data demonstrate that prolonged exposure to ethanol for at least 6-hr was required to cause a significant reduction in JAM-A and occludin protein expression (**Fig. 3B**). Consistent with dose response analysis, we did not observe any significant change in ZO-2 protein levels. We also found that at 9-hours JAM-A protein expression was reduced but neither ZO-2 nor occludin levels were reduced (data not shown). SK-CO15 monolayers were also treated with ethanol to test further applicability of these findings beyond Caco-2 cells. As with Caco-2, protein expression of both JAM-A and occludin, but not ZO-2, was significantly reduced by 6% ethanol treatment for 6-hr (**Fig. 3C**;  $0.62 \pm 0.04$ -fold change in JAM-A 6% vs 0%). We further hypothesized that the reduction in JAM-A expression would be accompanied by disruption of its subcellular localization. Surprisingly, imaging of Caco-2 monolayers by confocal immunofluorescence microscopy revealed that JAM-A localization was unaltered after 6% ethanol treatment for 6-hr (**Fig. 4**).

### **Treatment of Caco-2 monolayers with ethanol alters the activation status of JAM-A signaling partners Rap2 and MLCK**

Because JAM-A contributes to maintenance of intestinal epithelial barrier function through both structural and signaling functions (75), we hypothesized that ethanol exposure would result in perturbations of JAM-A signaling partners MLCK and Rap2. Corroborating previously published observations (239-241), MLCK immunoprecipitation from Caco-2 monolayer lysates followed by *in vitro* kinase activity analysis revealed a significant upregulation of MLCK activity within 3-hr of 6% ethanol treatment, which began to normalize within 6-hr (**Fig. 5A**). This increase in MLCK phosphorylation activity (~4-fold) was observed without significant changes in total MLCK

protein expression though there was a trend toward diminished MLCK expression (**Fig. 5B**). Interestingly, activation of the small GTPase Rap2, an upstream inhibitor of MLCK proposed to be regulated by JAM-A (75), was significantly reduced by acute (30-min) exposure to 6% ethanol (**Fig. 5C**;  $0.58 \pm 0.16$ -fold 6% vs 0%).

### **Overexpression of JAM-A in Caco-2 monolayers is associated with increased TEER and protects against ethanol-induced barrier dysfunction**

Because ethanol exposure reduced JAM-A protein expression and shifted the activation status of JAM-A signaling partners towards states that promoted epithelial barrier disruption, we were interested in examining whether manipulating JAM-A expression would result in alteration of monolayer response to ethanol. To address this question, we selected stable lines of Caco-2 cells transfected with plasmids expressing a pCMV6 driven Myc-DDK tagged JAM-A (F11R) or empty vector. JAM-A overexpression in the pCMV6-F11R-MycDDK, but not empty vector, transfected cells was confirmed by anti-FLAG western blot (**Fig. 6A**). Compared to controls, cells overexpressing the Myc-DDK tagged JAM-A formed monolayers with a near 2-fold increase in resistance in the absence of alcohol (**Fig. 6B**,  $126.4 \pm 13.09$  vs  $260 \pm 23.95 \Omega \times \text{cm}^2$ ). Treatment of monolayers overexpressing JAM-A with 6% was associated with a significant reduction in resistance versus untreated cells (**Fig. 6B**). There was no significant difference in monolayer TEER between empty vector and F11R-MycDDK transfected Caco-2 monolayers following 6% ethanol treatment (**Fig. 6B**,  $41.66 \pm 2.12$  vs  $66.55 \pm 3.37 \Omega \times \text{cm}^2$ ). Surprisingly, the resistance of Caco-2 monolayers overexpressing MycDDK-tagged JAM-A that were treated with ethanol also did not significantly differ from cells transfected with the empty pCMV6 vector that were not exposed to ethanol (**Fig. 6B**). Therefore, to better understand if JAM-A overexpression might protect against ethanol-induced epithelial barrier loss, we assessed the

paracellular permeability of the transfected Caco-2 monolayers by using 40-kDa FITC-dextran as in **Fig. 1D**. We calculated the FITC-dextran concentration of the basal solution 3-hr post 6% ethanol treatment by standard curve for more detailed analysis. In the absence of alcohol, overexpression of JAM-A caused non-significant trend towards reduced monolayer permeability (**Fig. 6C**,  $2.25 \pm 0.26$  vs  $1.40 \pm 0.30$   $\mu\text{g/mL}$ ). However, 40-kDa FITC-dextran permeability following ethanol treatment was significantly reduced by about 50% in monolayers overexpressing JAM-A compared to empty-vector transfected cells (**Fig. 6C**,  $4.57 \pm 0.31$  vs  $2.60 \pm 0.12$   $\mu\text{g/mL}$ ). Interestingly, the FITC-dextran permeability of ethanol treated pCMV6-F11R-MycDDK transfected Caco-2 monolayers did not significantly differ from empty-vector monolayers that were not treated with ethanol. Together, these TEER and FITC-dextran observations suggest that overexpression of JAM-A in Caco-2 monolayers was associated with a “tighter” barrier even after ethanol exposure.

### **Knockdown of JAM-A in Caco-2 monolayers is associated with exacerbated disruption of barrier function induced by ethanol exposure**

Since our observations suggested that overexpression of JAM-A serves to protect against ethanol-induced barrier loss we sought to test the converse hypothesis, that is whether JAM-A knockdown would result in impaired barrier function. To address this question, we employed shRNA-mediated knockdown of JAM-A. Western blots performed on 7-day old monolayers from pLKO and JAM-A shRNA transduced Caco-2 cells revealed virtually complete knockdown of JAM-A protein levels (**Fig. 7A**). Knockdown of JAM-A caused a dramatic reduction in Caco-2 monolayer TEER (**Fig 7B**,  $202.62 \pm 22.17$  vs  $55.46 \pm 5.29$   $\Omega \times \text{cm}^2$ ). Furthermore, TEER of monolayers expressing JAM-A targeted shRNA was not significantly reduced by ethanol, nor did their resistance significantly differ from pLKO-transduced monolayers that were treated with

ethanol. Paracellular permeability of 40-kDa FITC-dextran was also dramatically increased by JAM-A knockdown (**Fig. 7C**). FITC-dextran concentrations collected from ethanol-naïve monolayers with JAM-A knockdown were significantly greater than those collected from ethanol-treated pLKO-transduced Caco-2 (**Fig. 7C**,  $14.75 \pm 0.70$  vs  $10.82 \pm 0.98$   $\mu\text{g/mL}$ ). Ethanol treatment significantly enhanced the paracellular permeability of JAM-A shRNA transduced Caco-2 monolayers to FITC-dextran despite the relatively modest effects ethanol treatment had on TEER in these cells (**Fig. 7C**,  $14.75 \pm 0.70$  vs  $21.71 \pm 1.36$   $\mu\text{g/mL}$ ). Together, these results suggest that JAM-A plays a pivotal role in maintenance of intestinal epithelial barrier function as measured by both electrical resistance and paracellular permeability to inert solutes.

#### **Chronic plus binge ethanol disrupts subcellular localization of JAM-A, but not its total expression, in the ileum of high-fat, high-cholesterol Lieber-DeCarli diet fed mice**

In order to relate our *in vitro* observations to an *in vivo* model of ethanol feeding, we employed the services of Southern California Research Center for ALPD and Cirrhosis Animal and Morphology Core. Through these services, 8-week old C57BL/6 WT mice were subjected to 6-weeks of a modified high-fat, high-cholesterol Lieber-DeCarli diet plus once per week ethanol binge. Ethanol-fed mice suffered greater liver injury as measured by histologic assessment, liver/body weight ratio, and elevated serum ALT (**Fig. 8A-C**). Prior to sacrifice, mice were gavaged with a 4-kDa FITC-dextran solution to measure intestinal epithelial permeability as described previously (190). As shown in **Fig. 8D**, serum FITC-dextran concentration was significantly higher in the ethanol fed mice, suggesting that ethanol increased intestinal epithelial permeability of these animals. Though ileum occludin expression was dramatically reduced in ethanol-fed mice, we observed no effect on total protein expression of JAM-A (**Fig. 9A**). Because many cell types other than enterocytes express JAM-A, such as endothelial cells and leukocytes (67), we employed confocal immunofluorescence imaging to visualize JAM-A

expression in the intestinal mucosa. Our data demonstrate relocalization of JAM-A from the junctions between enterocytes of ethanol-fed mice (**Fig. 9B**).

## Discussion

In the present study, Caco-2 monolayers were used to reaffirm past observations that ethanol causes a significant disruption of monolayer barrier function (239, 241). Enhanced permeability of relatively large 40-kDa FITC-dextran particles reported here supports the hypothesis that “leak” pathway regulators such as JAM-A are involved in the mechanisms by which ethanol disrupts the intestinal epithelial barrier, and corroborates observations from other published studies (245-247). By western blot we observed a consistent reduction in JAM-A expression with no alteration in its subcellular localization following ethanol exposure in both a dose- and time-dependent manner *in vitro*. This observation was apparently a consequence of prolonged exposure to ethanol, as the reduction in JAM-A protein levels was not observed until at least 6-hr of treatment. We observed similar reductions in occludin protein levels, which corroborates previously published observations, as well as our *in vivo* results reported here (175, 180, 237, 239, 240). Surprisingly, in contrast to our Caco-2 observations, JAM-A expression in the ileum was unaltered in chronic plus binge ethanol-fed mice. Instead, possible JAM-A dysfunction was noted by disruption of its subcellular localization of JAM-A in enterocytes. This discrepancy might be explained by the metabolism of ethanol to acetaldehyde and other metabolites that occurs *in vivo*, but not in Caco-2 cells, which lack expression of alcohol dehydrogenase (248). Moreover, mice in the current study were sacrificed ~24-hr post final ethanol gavage, while it has been noted that the maximal amount of liver damage following a single ethanol binge occurs at ~9-hr (249). Therefore, it is possible that total intestinal JAM-A protein content might change in a similar time frame, and thus JAM-A expression, but not its localization, may recover within 24-hr acute ethanol binge. We also found that ethanol *in vitro* did not result in significant changes in expression of ZO-2, a TJ scaffolding protein that associates with JAM-A (75). Therefore, it is likely that the observations we have made are due to a direct regulatory effect of

ethanol or acetaldehyde on JAM-A, rather than a secondary effect caused by disruption of the other complexed partner molecules.

Although JAM-A protein expression in epithelial monolayers was reduced to about 70% of baseline levels, observed after 6-hr ethanol treatment, reductions in monolayer TEER occurred within an acute time frame, 3 hr. Therefore, we were interested in whether JAM-A signaling dysfunction may precede alterations in its expression. Monteiro *et al.* recently suggested that JAM-A contributes to intestinal epithelial barrier function through regulation of MLC phosphorylation via the Rap2c-RhoA-MLCK signaling axis, in **Figure 10** (75). Hence, in the absence of JAM-A, MLC phosphorylation increases leading to apical actomyosin contraction and expansion of the paracellular space, resulting in a leakier monolayer (75). Here we reported that ethanol exposure induced a significant increase in MLCK phosphorylation activity within 3-hr of ethanol treatment. Our findings corroborate previous *in vitro* and *in vivo* observations that ethanol enhances phosphorylation of MLC in intestinal epithelial cells (175, 238-241). Importantly, two of these studies performed by independent groups linked MLCK activation to upstream activation of RhoA (238, 240). Although inducible nitric oxide synthase (iNOS) was proposed as one potential regulator of RhoA (238), we questioned whether ethanol-induced perturbations in Rap2 would also contribute to RhoA regulation. In the present study, we provide the first evidence that ethanol causes an acute reduction in Rap2 activation. Therefore, we propose a novel paradigm by which ethanol induces a reduction in active Rap2, which contributes to activation of RhoA, and ultimately leads to enhanced MLCK activity and MLC phosphorylation. While additional studies will be necessary to solidify this hypothesis, it is tempting to speculate the possibility that inhibition of Rap2 is mediated through ethanol-mediated disruption of JAM-A signaling function (**Fig. 10**).

We also found that JAM-A overexpression nearly doubled Caco-2 monolayer TEER. However, this difference was abolished by ethanol treatment. In contrast, monolayers overexpressing JAM-A displayed significantly less permeability to 40-kDa FITC-dextran in the presence, but not the absence, of alcohol. Together these parallel observations suggest several possible conclusions, all of which raise interesting questions for future studies: 1) Though they are often associated together, epithelial TEER and paracellular permeability to inert solutes might be under distinct, sometimes divergent mechanisms of regulation; 2) JAM-A contributes to monolayer TEER, but may play a minimal role in the mechanisms by which ethanol reduces TEER; and 3) the greater baseline TEER of monolayers overexpressing JAM-A indicated a sufficiently “tighter” barrier that was maintained throughout enough of the 3-hr treatment duration to result in a lower net flux of FITC-dextran. While many of these questions need be addressed by future studies, near complete knockdown of JAM-A alone abolished monolayer TEER to levels similar to those of ethanol-treated controls. However, since ethanol exposure clearly does not induce profound downregulation of JAM-A protein, the direct contribution of JAM-A, independent of other TJ structural members, to the regulation of epithelial TEER remains unclear. Nevertheless, the dramatic enhancement of FITC-dextran flux across Caco-2 monolayers that results as a consequence of JAM-A deficiency, both in the presence and absence of alcohol, provides solid evidence for the critical role that JAM-A plays in regulating paracellular permeability.

In conclusion, we demonstrated that prolonged exposure of intestinal epithelial cells to ethanol diminishes JAM-A protein expression *in vitro*, and potentially disrupts its subcellular localization *in vivo*. Acute exposure of Caco-2 cells to alcohol was associated with perturbations of Rap2 and MLCK activity, signaling molecules regulated downstream of JAM-A. Thus, our data raise the possibility that JAM-A signaling dysfunction and reduction of its protein content contributes

to ethanol-induced intestinal epithelial barrier loss. Through both knockdown and overexpression studies, we demonstrate a critical role of JAM-A in regulation of paracellular permeability both in the absence and presence of ethanol. However, further studies will be required to discriminate any potentially divergent regulatory mechanisms of monolayer TEER versus permeability to solutes, and to further elucidate the effects that ethanol consumption has on JAM-A *in vivo* and the timing at which they occur.

### **Acknowledgements**

The authors would like to thank Dr. Jason Matthews (Emory University, Atlanta, GA) for providing Caco-2 cells and Dr. Peijian He (Emory University, Atlanta, GA) for providing SK-CO15 and HEK293T cells, as well as for providing for providing pLTR-G and PCD/NL-BH4 plasmids and technical aid in preparing lentiviral vectors. The authors additionally thank Dr. Chris Yun (Emory University, Atlanta, GA) for usage of EMD Millipore Millicell-ERS Volt-Ohm meter. This research project was supported in part by the Emory University Integrated Cellular Imaging Microscopy Core of the Emory and Children's Pediatric Research Center. We also acknowledge the Animal and Morphology Core facilities of the NIAAA-supported Southern California Research Center for ALPD and Cirrhosis (P50 AA011999) for providing support in designing mouse diets and in carrying out all animal ethanol feeding studies.

### **Grants**

This work was supported by NIH grant F31AA024960 to DMC; NIH grants DK062092, DK113147, and DK111678 to FAA; and NIH grant DK110264 to RR. A portion of this work was also supported by funds provided by Emory University.

### **Disclosures**

The authors have no conflicts of interest.

## Figure Legends

**Figure 1: Ethanol induces a dose-dependent reduction in transepithelial electrical resistance (TEER) associated with an increase in paracellular flux of FITC-dextran in Caco-2 monolayers.** Caco-2 monolayers were incubated in HBSS+ at 37°C for 1-hr. FITC-dextran of either 4-kDa or 40-kDa in size was added to the apical compartments of the transwell plates at 1 mg/mL, followed by treatment of both apical and basal compartments with 0% (HBSS+ alone), 3%, or 6% v/v ethanol. TEER was measured immediately and again after 3-hr incubation. Fluorescence of the basal solutions following 3-hr incubation was measured and compared to solution collected from equivalently treated cell-free transwell inserts. TEER readings are reported both as the normalized values after 3-hr incubation (**A**), and as the percent change from baseline (**B**). Flux of FITC-dextran 4-kDa (**C**), and 40-kDa (**D**), were normalized to blank inserts and reported as fold-change relative to monolayers treated with 0% ethanol. All data are representative means  $\pm$  SEM of at least 4 individual monolayer inserts from 2 independent experiments. Data analyzed by one-way ANOVA, \* $p < 0.05$ , \*\* $p < 0.01$ , \*\*\* $p < 0.001$ , \*\*\*\* $p < 0.0001$ .

**Figure 2: Ethanol up to 6% v/v does not increase Caco-2 monolayer cell death.** After incubating Caco-2 monolayers in HBSS+ at 37°C for 1-hr, apical and basal compartments of the transwell plate were treated 0% (HBSS+ alone), 3%, or 6% v/v ethanol. LDH activity within apical extracellular media was measured after 6-hr incubation. Data are representative of means  $\pm$  SEM of at least 3 individual monolayers from 2 independent experiments. Data analyzed by one-way ANOVA.

**Figure 3: Ethanol induces a dose- and time-dependent decrease in JAM-A and occludin, but not ZO-2, protein expression in Caco-2 and SK-CO15 monolayers.** Caco-2 monolayers 15-d after seeding were incubated overnight followed by treatment with 0% (medium), 3%, or

6% v/v ethanol for an additional 6-hr incubation (A). Additional transwell plates were exposed to 6% ethanol in staggered fashion for 0- (medium alone), 3-, or 6-hr (B). SK-CO15 monolayers were also treated with 0%, 3%, or 6% v/v ethanol for 6 hours (C) Total protein lysates were collected and analyzed by western blot. Images are representative of results of at least 6 (A), 4 (B), and 3 (C) independent experiments. Densitometry results are reported as the fold-change in target protein expression (normalized to  $\beta$ -actin) relative to monolayers treated with medium alone. Densitometry data reported as means  $\pm$  SEM and analyzed by one-way ANOVA, \* $p$ <0.05, \*\*\* $p$ <0.001.

**Figure 4: Subcellular localization of JAM-A is not altered by ethanol exposure.** Caco-2 monolayers 15-d after seeding were incubated overnight followed by treatment with 0% (medium) or 6% v/v ethanol for an additional 6-hr incubation. Monolayers were then fixed with paraformaldehyde, excised from their inserts, and stained with primary and fluorophore conjugated secondary antibodies. Images are representative of  $n = 4$  monolayers per treatment.

**Figure 5: Ethanol exposure is associated with a transient increase in myosin light chain kinase (MLCK) phosphorylation activity as well as a decrease in Rap2 activation.** Equal amounts of protein collected from Caco-2 monolayers treated with 6% v/v ethanol for 0- (medium only), 3-, or 6-hr, were incubated with antibody coated magnetic protein beads to immunoprecipitate MLCK over 1-hr. MLCK phosphorylation activity was measured directly on these bead complexes by Promega ADP-Glo™ kinase assay kit using 50  $\mu$ M ATP and 0.4  $\mu$ g/mL synthetic peptide substrate MRCL3. (A) MLCK phosphorylation activity in relative luminescence units (RLU) is reported as means  $\pm$  SEM. (B) Total MLCK expression was not significantly different among samples; data representative of 2 independent experiments and was analyzed by one-way ANOVA, \* $p$ <0.05. Rap2 activity was analyzed by pulldown of lysates collected from monolayers treated with 6% v/v ethanol for 0 or 30-min (C). Rap2 western blot

and densitometry are representative of 3 independent experiments. Data analyzed by students  $t$ -test,  $*p < 0.05$ .

**Figure 6: JAM-A overexpression in Caco-2 monolayers is associated with increased TEER and enhanced barrier function.** Transfected Caco-2 monolayers with stable expression of Myc-FLAG tagged JAM-A (F11R) or pCMV6 empty vector were incubated in HBBS+ at 37°C for 1-hr. FITC-dextran 40-kDa was added to the apical compartments of the transwell plates, followed by treatment of both apical and basal compartments with 0% (HBSS+ alone) or 6% v/v ethanol. TEER was measured immediately and again after 3-hr incubation. Expression of the tagged-JAM-A in the differentiated monolayers was confirmed by western blot (**A**). TEER values (**B**), and FITC-dextran concentration (**C**), of basal solutions after 3-hr incubation are reported as means  $\pm$  SEM. Western blot representative of 2 independent experiments. All other data are representative of multiple individual monolayer inserts from 2 independent experiments. Data analyzed two-way ANOVA,  $*p < 0.05$ ,  $**p < 0.01$ ,  $***p < 0.001$ ,  $****p < 0.0001$ .

**Figure 7: JAM-A deficiency is associated with decreased Caco-2 monolayer TEER and enhanced paracellular permeability.** Transduced Caco-2 monolayers with either JAM-A specific shRNA or scrambled control (pLKO) were incubated in HBBS+ at 37°C for 1-hr. FITC-dextran 40-kDa was then added to the apical compartments of the transwell plates, followed by treatment of both apical and basal compartments with 0% (HBSS+ alone) or 6% v/v ethanol. TEER was measured immediately and again after 3-hr incubation. Knockdown of JAM-A in the differentiated monolayers was confirmed by western blot (**A**). TEER values (**B**), and FITC-dextran concentration (**C**), of basal solutions after 3-hr incubation are reported as means  $\pm$  SEM. Western blot representative of 2 independent experiments. All other data are representative of multiple individual monolayer inserts from 3 independent experiments. Data analyzed two-way ANOVA,  $*p < 0.05$ ,  $**p < 0.01$ ,  $***p < 0.001$ ,  $****p < 0.0001$ .

**Figure 8: Chronic plus binge ethanol feeding exacerbates liver injury and increases intestinal permeability in mice fed a high-fat, high-cholesterol liquid diet.** Eight-week old wild-type C57BL/6 mice were fed a modified high-fat, high-cholesterol Lieber-DeCarli diet with or without ethanol plus once per week ethanol or glucose binge for 6-weeks. Liver injury was assessed by comparing hematoxylin and eosin stained liver sections (**A**), liver to body weight ratios (**B**) and serum AST and ALT levels (**C**). Additionally, prior to sacrifice, intestinal permeability was assessed by measuring serum concentration of 4-kDa FITC-dextran. Mice were gavaged with 600 mg/kg 4-kDa FITC-dextran and serum samples were collected by cheek bleed after 4-hr. All data are representative of  $n = 4$  ethanol-fed mice and  $n = 5$  pair-fed controls. Data analyzed by students  $t$ -test,  $*p < 0.05$ ,  $**p < 0.01$ .

**Figure 9: Chronic plus binge ethanol feeding disrupts JAM-A subcellular localization, but not its overall protein expression, in the ileum high-fat, high-cholesterol liquid diet fed mice.** Eight-week old wild-type C57BL/6 mice were fed a modified high-fat, high-cholesterol Lieber-DeCarli diet with or without ethanol plus once per week ethanol or glucose binge for 6-weeks. Total protein lysates (30  $\mu$ g per sample) of distal ileum tissue were analyzed by western blot. Depicted image is from non-adjacent wells ran on the same gel (**A**). Densitometry data is representative of  $n = 3$  mice per group and was analyzed by students  $t$ -test,  $**p < 0.01$ . Additionally, subcellular localization of JAM-A within ileum was assessed by confocal immunofluorescence microscopy (**B**). Immunofluorescence images are representative of  $n = 4$  ethanol-fed mice and  $n = 5$  pair-fed controls.

**Figure 10: JAM-A Barrier Promoting Signaling Pathway and Perturbations Induced by Ethanol.** JAM-A associates directly with ZO-2, which forms a complex with Afadin and the guanine-nucleotide exchange factor PDZ-GEF1. This complex activates Rap2c by promoting GTP binding. Active Rap2c inhibits RhoA-mediated activation of MLCK and downstream MLC phosphorylation which promotes barrier function. Ethanol exposure disrupts upstream targets,

disinhibiting RhoA, and resulting in enhanced MLC phosphorylation. Contraction of the apical actomyosin ring follows, leading to an expanded paracellular space and increased solute flux. Perturbations induced by ethanol depicted as red lightning bolts. Arrows indicate activation, whereas bar-headed lines indicate inhibition.

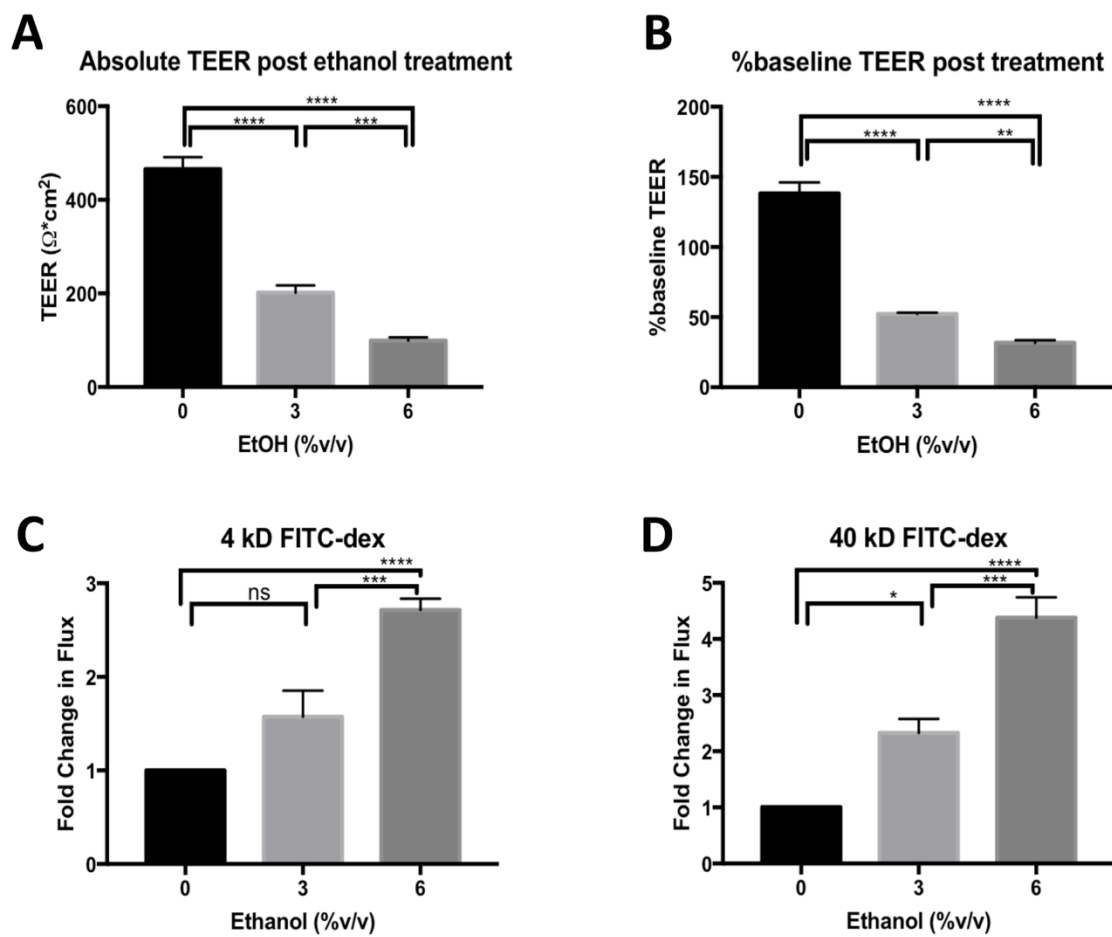
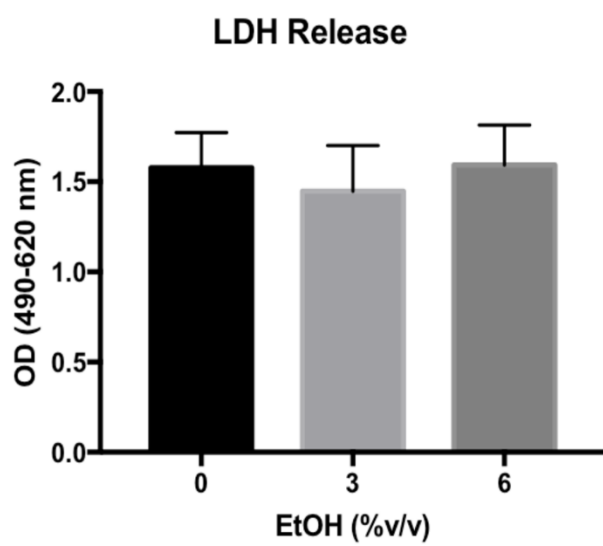


Figure 1



**Figure 2**

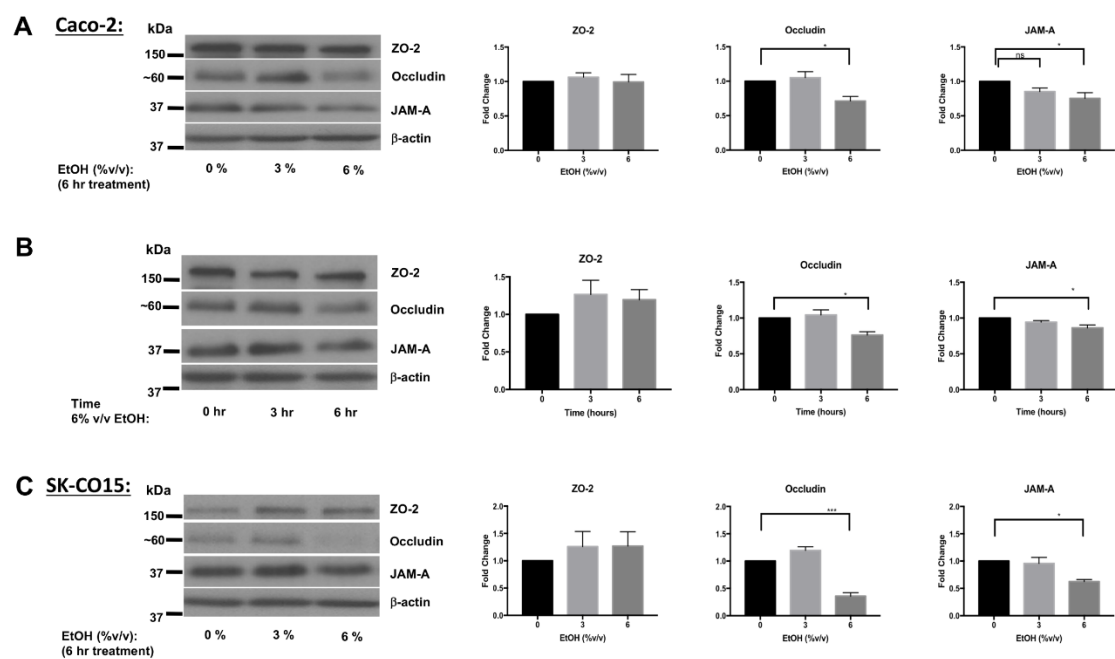
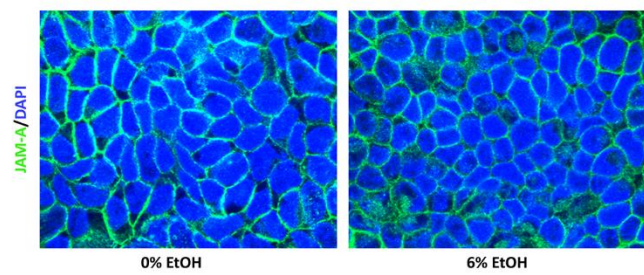


Figure 3



**Figure 4**

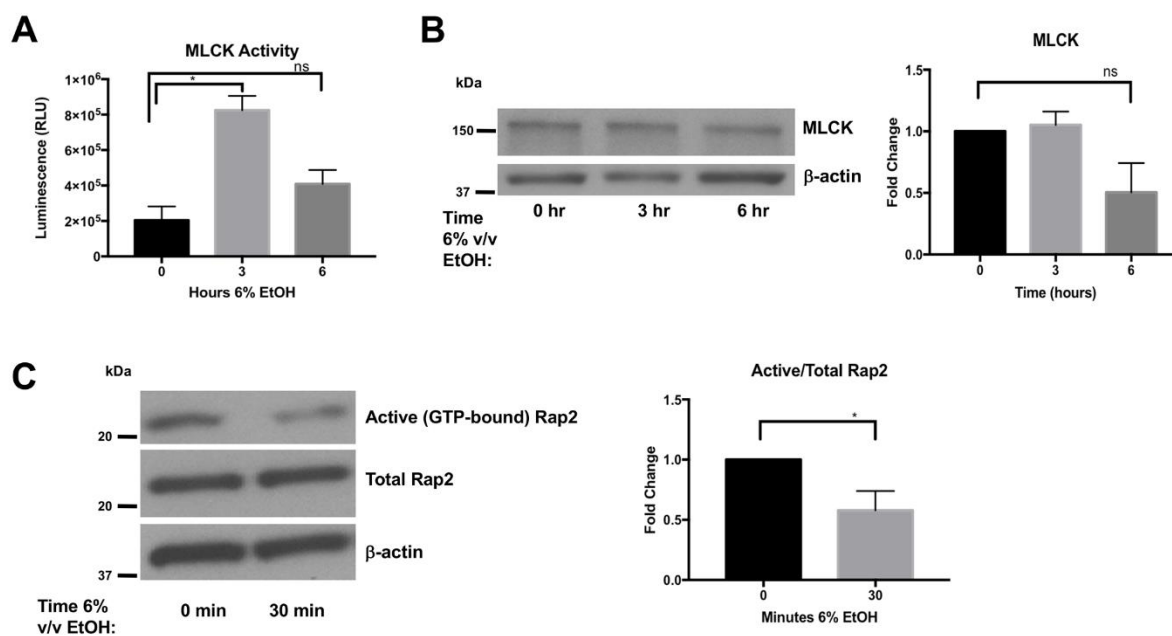


Figure 5

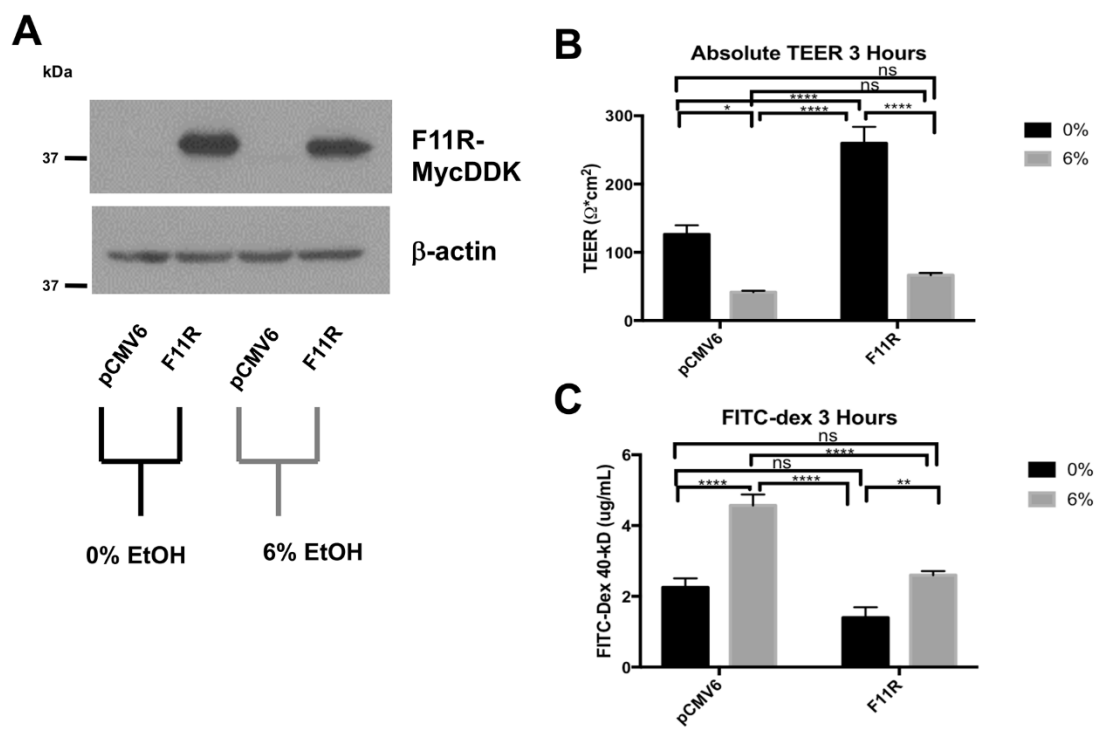


Figure 6

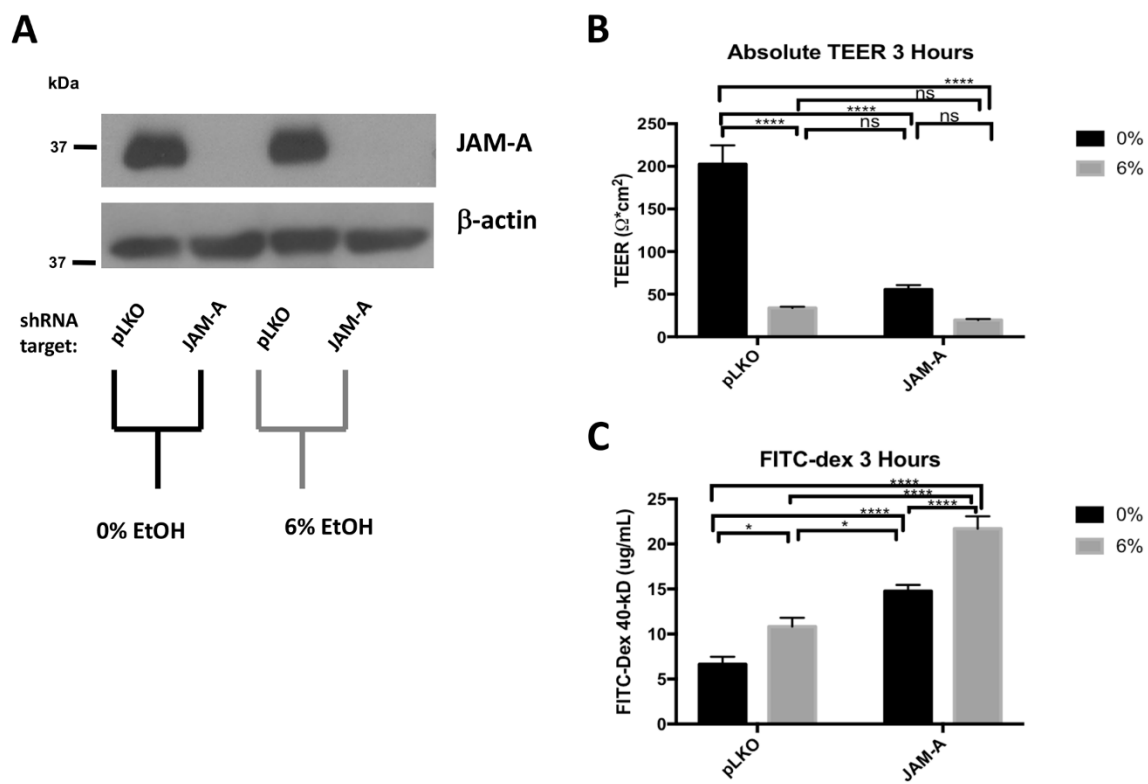


Figure 7

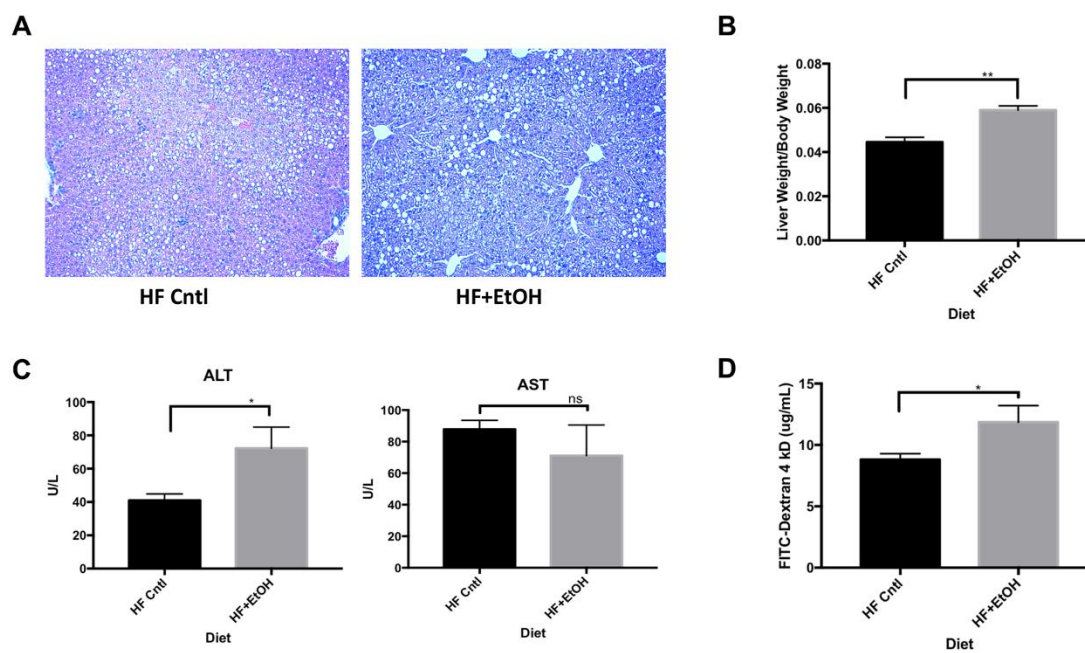


Figure 8

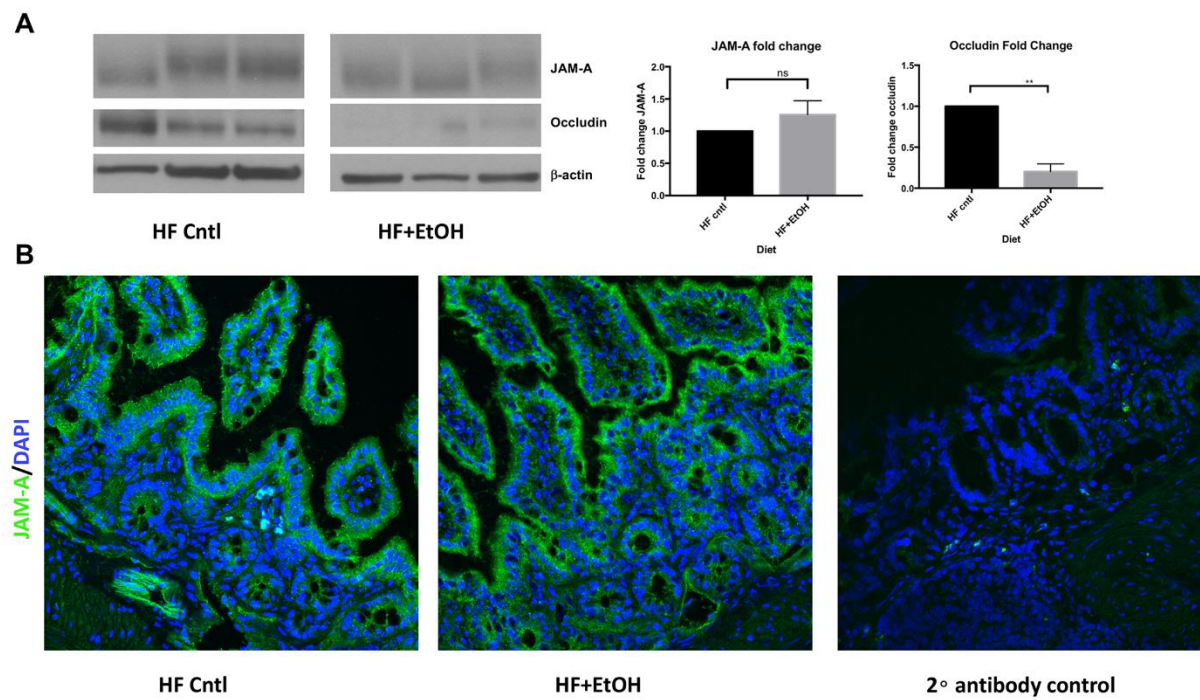


Figure 9

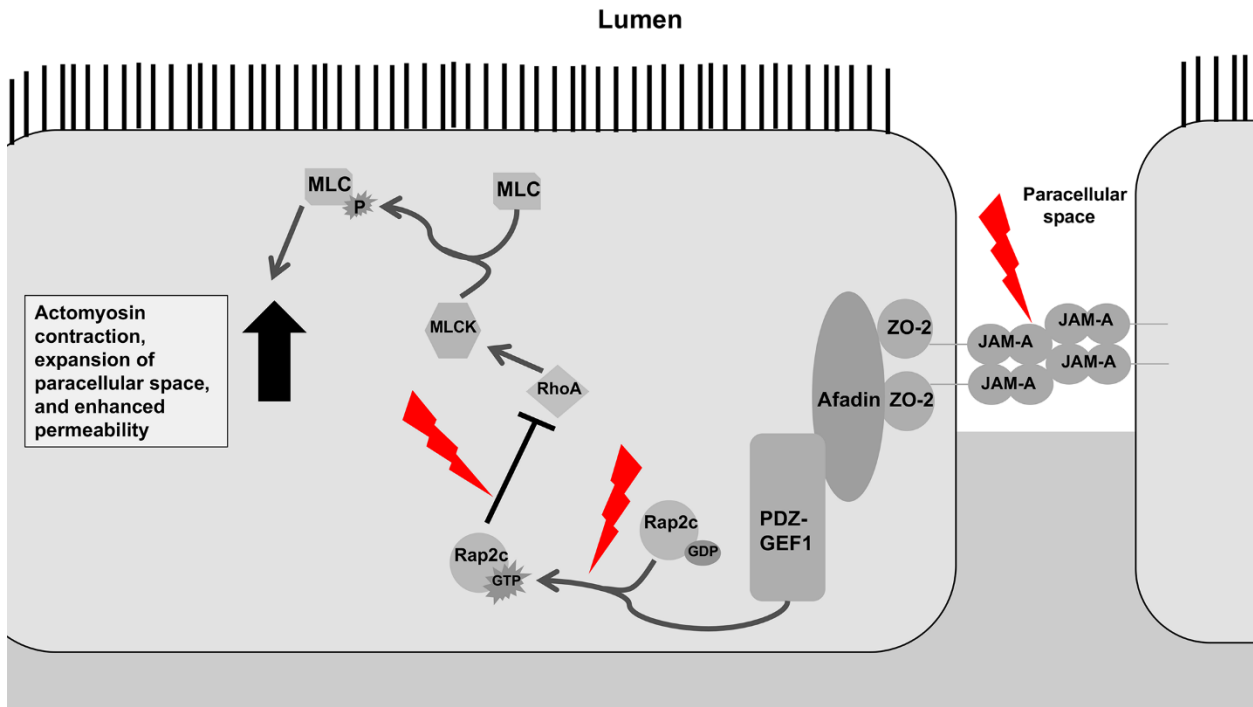


Figure 10

### **Chapter 3: Acetaminophen intoxication rapidly induces apoptosis of intestinal crypt stem cells and enhances intestinal permeability**

Daniel M. Chopyk<sup>1</sup>, Johnasha D. Stuart<sup>1</sup>, Matthew G. Zimmerman<sup>3,4</sup>, Mehul S. Suthar<sup>3,4</sup>, Manoj Thapa<sup>1</sup>, Arash Grakoui<sup>\*1,2</sup>

#### **Author contributions**

D.M.C., M.T., and A.G. conception and design of research; D.M.C. and J.D.S., performed experiments and analyzed data; M.G.Z. provided advice and support for histological slide preparation and processing; D.M.C, J.D.S., M.S.S., M.T, A.G., interpretation of results; D.M.C. drafted manuscript; D.M.C. prepared figures; D.M.C., J.D.S., M.T., A.G., edited and revised manuscript; all authors reviewed and approved the final version of manuscript

#### **Affiliations**

<sup>1</sup>Emory Vaccine Center, Division of Microbiology and Immunology, Yerkes Research Primate Center, Emory University School of Medicine, Atlanta, GA.

<sup>2</sup>Division of Infectious Diseases, Department of Medicine, Emory University School of Medicine, Atlanta, Georgia 30329, USA

<sup>3</sup>Division of Infectious Disease, Department of Pediatrics, Emory University School of Medicine, Atlanta, GA 30322, USA

<sup>4</sup>Emory Vaccine Center, Yerkes National Primate Research Center, Atlanta, GA 30329, USA.

#### **Running Head**

Acetaminophen-induced death of intestinal crypt stem cells

#### **Keywords**

Ileum; PARP; caspase-3; LGR5; TNFR

#### **\*Corresponding Author**

Arash Grakoui, PhD  
Division of Infectious diseases,  
Yerkes National Primate Research Center,  
Division of Microbiology and Immunology,  
Emory Vaccine Center,  
Emory University School of Medicine,  
Atlanta, GA 30329  
Telephone: (404) 727-5850; Fax: (404) 727-7768;  
Email: [arash.grakoui@emory.edu](mailto:arash.grakoui@emory.edu)

## Abbreviations

### APAP

acetaminophen

### NSAIDs

nonsteroidal anti-inflammatory drugs

### ALF

Acute liver failure

### NAPQI

N-acetyl-p-benzoquinone imine

### NAC

N-acetylcysteine

### ALT

Alanine aminotransferase

### FITC

fluorescein isothiocyanate

### LGR5

leucine-rich repeat-containing G-protein coupled receptor 5

### TNFR

Tumor necrosis factor receptor signaling

### WT

Wild-type

### PARP

poly (ADP-ribose) polymerase

### IP

Intraperitoneal

### TNF $\alpha$

Tumor necrosis factor- $\alpha$

### ROS

Reactive oxygen species

## Funding

This project was supported by NIH grants R01AI124680, R01AI126890, and R01AI136533 to A.G., and ORIP/OD P51OD011132 (formerly NCRR P51RR000165) to the Yerkes National Primate Research Center (AG). D.M.C. is supported by National Institute of Alcohol Abuse and Alcoholism (NIAAA) Ruth L. Kirschstein National Research Service Award (NRSA) Individual Predoctoral Fellowship (F31AA024960). J.D.S. is supported by the National Institute of General Medical Sciences (NIGMS) Physician Scientist Award (2K12GM000680-16). M.T. is supported by National Institute of Diabetes, and Digestive and Kidney Diseases (NIDDK) Mentored Career Development Award (K01DK109025). Its contents are solely the responsibility of the authors and do not necessarily represent the official views of the NIH

## Abstract

Acetaminophen (APAP)-induced liver injury is the most common cause of acute liver failure in the western world. APAP toxicity progresses to multiorgan dysfunction and thus has broader whole-body implications. Importantly, greater 30-day mortality has been observed in liver transplant recipients following acute liver failure (ALF) due to APAP versus non-APAP related causes. Reasons for this discrepancy have yet to be determined. Extrahepatic toxicities of APAP overdose may represent underappreciated and unaddressed comorbidities within this patient population. In the present study, rapid induction of apoptosis following APAP overdose was observed in the intestine, an organ which greatly influences the physiology of the liver. Strikingly, apoptotic cells appeared to be strictly restricted to the intestinal crypts. The use of leucine-rich repeat-containing G-protein coupled receptor 5 (*LGR5*) reporter mice confirmed that the *LGR5*<sup>+</sup> crypt base stem cells were disproportionately affected by APAP-induced cell death. While the apoptotic cells were cleared within 24-hr after APAP treatment, potentially long-lived consequences on the intestine due to APAP exposure were indicated by prolonged deficits in gut barrier function. Moreover, the intestinal cell death was found to be independent of tumor necrosis factor receptor signaling and may represent a direct toxic insult to the intestine by exposure to high concentrations of APAP. *Conclusion:* APAP induces intestinal injury via a regulated process of apoptotic cell death that disproportionately affects *LGR5*<sup>+</sup> stem cells. This work advances our understanding of the consequences of APAP toxicity in a novel organ that was not previously considered as a significant site of injury and thus presents potential new considerations for patient management.

Acetaminophen (APAP) is an extensively used analgesic both in over-the-counter and prescription medication formulations due to its generally favorable side effect profile in comparison to non-steroidal anti-inflammatory drugs (NSAIDs) and opiates. At therapeutic doses, APAP is primarily metabolized via glucuronidation and sulfonation pathways and therefore is safely tolerated by most individuals (197). However, clearance of excessive amounts of APAP relies upon cytochrome-mediated oxidative metabolism primarily by hepatocytes, which involves generation of the highly reactive and toxic metabolite N-acetyl-p-benzoquinone imine (NAPQI) (197). Thus, at high doses, APAP causes significant liver injury and necrosis due to overwhelming oxidative stress, protein adduct formation, and cellular malfunction (195, 197).

APAP overdose as a result of either a “therapeutic misadventure” or intentional self-harm represents the leading cause of acute liver failure in the U.S., Canada, and the United Kingdom (250). Despite posing a widespread clinical issue, there is a lack of effective therapies for APAP-induced hepatotoxicity to date. Currently, the standard of care is supplementation with N-acetylcysteine (NAC), which limits hepatic accumulation of NAPQI by replenishing antioxidant glutathione stores. Although it is readily available, NAC supplementation is often started too late as the clinical symptoms of APAP-induced liver failure often do not manifest until the peak of liver injury has been reached (197).

While some patients are able to survive the toxic insult and eventually recover due to the natural regenerative capacity of liver tissue, emergent liver transplantation is indicated for approximately 20-30% of patients due to excessive liver injury (197, 251). Even for those fortunate enough to procure a transplantable liver on an urgent notice, transplanted patients that had developed acute liver failure (ALF) due to APAP-toxicity versus ALF from non-APAP related causes were found to suffer from a lower 30-day survival (252). Explanations for this

discrepancy are remain unknown, but poorer medical compliance and greater adverse events related to psychological comorbidities were speculated causes.

Undoubtedly, the major life-threatening concern for APAP-overdose is widespread liver cell death that rapidly progresses to ALF. However, APAP toxicity can also result in eventual multi-organ dysfunction. Thus, there are likely overlooked pathological effects of APAP overdose on target organs other than the liver that potentially contribute to the increased morbidity and mortality observed in transplanted APAP-induced ALF patients. For example, a few studies have highlighted this possibility by identifying injury and inflammation in the brain, lung, and kidney following APAP overdose (253-255). The intestine is an organ with a particularly important role in both regulating and itself being modulated by liver disease due to the close physiological connections via the portal circulation and hepatic biliary output (1). Critically, the intestine must maintain a tightly regulated and efficient barrier to entry for the countless species of bacteria, fungi, and viruses that comprise the gut microbiome. As has now been well established, loss of intestinal barrier function is a major contributor to various modes of liver injury and potentially other disorders (1), including those considered to be of neurologic origin such as Parkinson's disease (224). Importantly, while a few studies have focused on potential contributions of the gut microbiota on APAP-induced liver injury (205, 206), APAP-induced intestinal damage has not been fully explored (201, 202).

In this study we found that in addition to the well-characterized liver injury following APAP intoxication, damage also occurs within the intestine. Using a murine model of APAP hepatotoxicity, we demonstrate that intestinal apoptotic cell death occurs in the acute phases following APAP intoxication independent of tumor necrosis factor receptor signaling.

Specifically, our findings indicate that death of intestinal cells is an early event following APAP intoxication, is strictly limited to the crypts, and predominantly affected epithelial stem cell populations. However, we found that hepatocyte cell death occurred via an apoptosis-independent mechanism, a finding that is consistent with previous reports (256). Together, these observations indicate that APAP intoxication can induce differential modes of injury across the intestine and liver and suggest that intestinal injury may be a neglected complication suffered by patients during APAP-induced ALF with potential implications on overall outcome.

## Experimental Procedures

### *Mice:*

Six- to eight-week old C57BL6/J wild-type (WT) and heterozygous *LGR5-EGFP-IRES-creERT2* males were purchased from Jackson Laboratories (Bar Harbor, ME). Age-matched and sex-matched B6.129S-*Tnfrsf1a*<sup>tm1lmx</sup>*Tnfrsf1b*<sup>tm1lmx</sup>/J mice were originally purchased from Jackson Laboratories but were bred and maintained in-house. All animals were housed in specific pathogen-free housing in compliance with the Emory Institutional Animal Care and Use Committee (IACUC) and NIH guidelines.

### *Acetaminophen (APAP) treatment:*

Mice were fasted for 12-hr prior to treatment with 500 mg/kg APAP (Sigma-Aldrich; St. Louis, MO) or an equivalent volume of phosphate buffered saline (PBS) vehicle via intraperitoneal (IP) injection. APAP solution was prepared fresh on the day of injection by heating 25 mg/mL APAP in PBS at 75°C until fully dissolved (approximately 5-min). APAP solutions were, sterile filtered, and cooled to 37°C. APAP and PBS control solutions were kept in a 37°C water bath during injections to prevent precipitation. Food was returned to mice immediately after treatment and heating pads were provided in cages to prevent hypothermia. Animals were euthanized 4-hr or 24-hr post-treatment by CO<sub>2</sub> inhalation.

Following euthanasia, blood was collected via cardiac puncture. Livers were gently perfused with ice-cold sterile PBS via the portal vein and were harvested for further analysis. Ileum tissue (approximated as the most distal third of the small intestine) was excised and trimmed of associated mesenteric fat. Ileum samples were opened by a longitudinal cut, and fecal contents were removed by gently shaking the tissue while immersed in cold, sterile PBS. Portions of liver and ileum were frozen on dry ice and placed in long-term storage at -80°C.

*In vivo Intestinal permeability assay:*

To assess intestinal permeability at 4-hr post APAP treatment, mice were restricted from access to food and water for 12-hr prior to APAP injection. At the time of APAP injection, mice were also orally gavaged with 1 g of 4-kDa fluorescein isothiocyanate (FITC)-dextran (Sigma) per kg body weight. FITC-dextran solution was dissolved at 160 mg/mL in PBS. Food and water were returned to mice immediately following gavage and 4-hr later mice were euthanized and blood was collected. To assess intestinal permeability at 24-hr post APAP treatment, mice were restricted from access to food but had free access to water for 12-hr prior to APAP injection. After APAP injection, food was returned to the mice. Mice were restricted from access to water starting 8-hr after APAP treatment. The animals were then gavaged with FITC-dextran as described above at 20-hr after APAP treatment. Water was returned to the animals until 4-hr later, at 24-hr after APAP injection, mice were euthanized and blood was collected.

Blood samples were protected from light the entire time following harvest. Blood was incubated at RT for at least 1-hr to clot and serum was separated by high speed centrifugation for 10-min. Serum aliquots were diluted 1:1 with PBS and were analyzed in duplicate for fluorescence readings at 488/530 nm. FITC-dextran concentration in serum samples was determined according to standard curve values generated from serially diluting (in PBS) the FITC-dextran solution used at the time of oral gavage. All serum samples were normalized to control mouse serum without FITC-dextran whereas standard curve wells were normalized to PBS alone.

*Tissue homogenization and western blot analysis:*

Small portions of frozen animal tissue were lysed in a modification of Abcam's intestinal lysis buffer recipe consisting of 150 mM NaCl, 50 mM Tris-HCl pH 7.4, 1% Triton X-100, 1% sodium-

deoxycholic acid and 0.1% sodium dodecylsulfate reconstituted with 1X protease inhibitor cocktail (Sigma). Tissues were homogenized either via a hand-held rotary homogenizer (Biospec Products #985370; Bartlesville, OK) or with Lysing Matrix D ceramic beads in a FastPrep™-24 5G grinder (MP Biomedicals; Santa Ana, CA) utilized at the pre-registered settings specified for the respective tissues. All samples within each experimental set were homogenized via the same method to ensure equivalent comparison of protein contents. Upon homogenization, samples were cleared of solid debris by centrifugation in a table-top centrifuge at maximum speed for 20-min at 4°C. Controls for apoptotic activation markers were generated by acquiring whole cell lysates from Raw264.7 macrophages (ATCC) incubated with media only or with 10 µg/mL puromycin for ~18-hr. Protein concentration of lysates were quantified by DC™ Protein assay (BioRad; Hercules, CA). Equal amounts of protein were diluted in 1X sample loading buffer containing 5% β-mercaptoethanol and were heated at 95°C for 5- to 10-min. Upon reduction, 25-30 µg of each protein sample was used for SDS-PAGE and western blot analysis. Blots were incubated overnight at 4°C in primary antibody solutions at the following concentrations in 5% BSA/TBST: rabbit anti-PARP 1:1000 (Cell Signaling Technology #9532; Danvers, MA), mouse anti-β-actin 1:5000 (Sigma #A2228), mouse anti-β-tubulin 1:5000 (Sigma #T8328), rabbit anti-caspase-9 1:1000 (Novus Biologicals #NBP2-67362; Centennial, CO), rabbit anti-cleaved caspase-8 1:1000 (Cell Signaling Technology #8592). Secondary antibody solutions consisting of goat anti-rabbit IgG or goat anti-mouse IgG (Jackson ImmunoResearch; West Grove, PA) were applied for 1-hr at RT both at 1:10,000 dilution in 5% milk/TBST. Western blots were developed using Clarity™ Western ECL blotting substrate (BioRad) and were read using a ChemiDoc™ XRS+ System and Image Lab™ software v6.0.1 (BioRad).

*Histology and Immunohistochemistry:*

At time of animal sacrifice, mouse ileums were cleaned as described above and excess fluid was absorbed by placing ileums on paper towels. Ileums were adhered to a flat tooth-pick, gently rolled along their length from proximal to distal end, and were then transferred into 10% phosphate-buffered formalin for fixation overnight. Harvested livers were cut into small sections and were also fixed by overnight incubation in 10% formalin. Tissues were transferred into 70% ethanol for long-term storage and were later paraffin embedded for sectioning. Sections 10  $\mu\text{m}$  thick were used for hematoxylin and eosin (H&E) staining and immunohistochemistry (IHC) analysis of cleaved caspase-3 (Cell Signaling Technology #9661, 1:200). All staining and IHC on tissue sections were performed by the Pathology Core, Yerkes National Primate Research Center, Emory University.

#### *Tissue Cryosections and immunofluorescence*

Ileum tissue was harvested as described above and were immediately frozen in VWR<sup>®</sup> frozen section compound (VWR; Radnor, PA) for sectioning. Frozen ileum sections were fixed in 4% paraformaldehyde in PBS for 15-min at RT and were stained with rabbit anti-cleaved caspase-3 (Cell Signaling Technology, 1:400) and biotinylated mouse anti-GFP tag (Thermo Fisher Scientific #MA515256BTIN, 1:500; Waltham, MA). Goat anti-rabbit IgG (H+L)-AlexaFluor<sup>®</sup> 594 (Jackson ImmunoResearch, 1:500) and FITC-conjugated streptavidin (BD Biosciences; San Jose, CA) were used for secondary staining. Staining, mounting, and imaging of slides was done as previously described (257).

#### *Serological measurements:*

Serum levels of alanine aminotransferase (ALT) were measured by the Pathology Core, Yerkes National Primate Research Center, Emory University. Quantification of tumor necrosis factor- $\alpha$

(TNF $\alpha$ ) in serum was determined using a mouse TNF $\alpha$  ELISA kit (R&D Systems; Minneapolis, MN) according to the manufacturer's instructions. Serum samples were diluted 1:1 with reagent diluent for TNF $\alpha$  ELISA analysis. Cytokine array analysis of serum harvested from mice 4-Hr after APAP or PBS treatment was conducted according to the manufacturer's instructions (Abcam #ab133993; Cambridge, UK).

*Statistical analysis:*

Data are presented as sample means  $\pm$  SEM. Two-tailed student's *t*-test were performed using GraphPad Prism<sup>®</sup> 7.0a software (GraphPad Software; La Jolla, CA) with statistical significance considered as  $p < 0.05$ .

## Results

### Acute acetaminophen toxicity rapidly increases intestinal permeability and apoptosis of crypt cells in small intestine

Several recent studies in diverse models of injury such as sepsis and radiation injury demonstrate that intestinal injury occurs within remarkably quick timeframes post-insult (258, 259). Thus, we sought to better understand the early pathological events that occur following APAP-intoxication. To this end, we treated fasted mice with a toxic dose of acetaminophen and harvested liver and intestinal tissue 4-hr later for analysis. This acute 4-hr time point was selected based off the likely presence of significant early liver injury. Consistent with previous observations, serum ALT levels were significantly elevated in APAP-treated animals versus controls (**Fig. 1A**,  $8391 \pm 2375$  vs  $105.7 \pm 5.69$  U/L). Animals were concurrently administered FITC-dextran at the time of APAP treatment to determine whether early changes in gut permeability occurred during APAP toxicity. Surprisingly, we observed a roughly 2.5-fold increase in serum recovery of FITC-dextran by 4-hrs after APAP treatment compared to controls (**Fig. 1B**,  $2.36 \pm 0.24$  vs  $0.89 \pm 0.13$   $\mu\text{g/mL}$ ). Therefore, these data indicate that acetaminophen impacted intestinal physiology within the same time frame as induction of liver injury.

We postulated that the enhanced gut permeability that occurred in response to APAP intoxication was due to intestinal injury. Therefore, we next investigated protein tissue lysates for cleavage of poly (ADP-ribose) polymerase (PARP) as marker for apoptotic cell death (260). Despite the high serum ALT levels that were consistent with severe liver injury, western blots of liver tissue revealed the absence of PARP cleavage above trace detection levels (**Fig. 1C**). However, whole ileum lysates unexpectedly revealed a significant increase of cleaved-PARP signal in APAP-treated mice when compared to the baseline amounts detected in controls (**Fig. 1D**). As there was no consequent reduction in the expression levels of total PARP within ileum lysates, this potentially suggested that the increased in PARP cleavage arose from a relatively

small population of cells. Thus, in order to clarify these differential observations between the liver and ileum we next examined histopathological tissue sections by H&E staining. As expected, in comparison to PBS-treated mice, liver sections from APAP-treated animals displayed significant areas of liver cell death occurring primarily around the central vein (**Fig. 2A**). Corroborating our western blot analyses, intestinal sections revealed the appearance of small, condensed vesicles consistent with the appearance of apoptotic bodies that were present only within the crypts of APAP-treated but not control mice (**Fig. 2A**). To further confirm whether these vesicles represent apoptotic cells, we performed immunohistochemistry for cleaved/activated caspase-3, the effector molecule and well-verified marker for apoptosis (256). Consistent with the lack of detectable PARP cleavage by western blot, both control and APAP-treated liver tissues displayed an absence of caspase-3 staining (**Fig. 2B**). However, ample positive cleaved caspase-3 staining was observed within the intestinal crypts of APAP-treated mice, supporting the hypothesis that the vesicles observed by H&E staining were derived from apoptotic cells (**Fig. 2B**).

### **Acetaminophen-induced intestinal apoptosis occurs early following the onset of intoxication**

The appearance of apoptotic cells within the intestine following acute APAP overdose was strictly limited to cells within the crypts (**Fig. 2**). As the intestinal crypts are home to various populations of adult stem cells that are responsible for regulating the physiological turnover of enterocytes (107), we questioned what changes may occur to the intestine within a longer period of time post-APAP treatment. Therefore, we similarly assessed gut barrier function and investigated PARP cleavage in liver and ileum lysates at 24-hr post-intoxication. In comparison to control animals, ALT levels remained significantly elevated in APAP-treated mice (**Fig. 3A**,  $24276 \pm 2593$  vs  $96.67 \pm 2.64$  U/L). Serum FITC-dextran recovery was also significantly higher

in APAP-treated animals compared to controls (**Fig. 3B**,  $2.62 \pm 0.71$  vs  $0.60 \pm 0.08$   $\mu\text{g/mL}$ ). PARP cleavage was still undetected in liver lysates suggesting that apoptosis was not playing a significant role in APAP-induced liver cell death and injury (**Fig. 3C**). However, while an increase in PARP cleavage was still observed at 24-hr in APAP-treated mice ileums versus controls, the effect was less pronounced compared to results seen at 4-hr (**Fig. 3D, 1D**). Therefore, in order to determine whether there were any changes at the tissue structure level, we again examined histopathological sections at 24-hr after APAP treatment. By this time, livers demonstrated extensive regions of late necrotic death. However, only sparse apoptotic bodies remained within ileum sections without any gross alteration of crypt-villus structure (**Fig. 4A**). Cleaved caspase-3 staining was similarly sparse within ileum sections at 24-hr after APAP treatment (**Fig. 4B**). As was the case during the earlier phases of APAP hepatotoxicity, liver sections were negative for cleaved caspase-3 staining at 24-hr. Together these data suggest that death of APAP-sensitive intestinal cell populations occurs early after overdose and that clearance of these apoptotic cells is largely complete within 24-hr. Further, apoptosis does not appear to be a significant contributor to direct APAP hepatotoxicity.

### **Acetaminophen-induced intestinal apoptosis occurs independent of TNFR signaling**

The appearance of apoptotic bodies within the ileum was observed alongside significant liver injury (**Fig. 1A, 2B**). It was unclear whether the intestinal injury occurred as a result from the systemic release of soluble mediators from the damaged liver tissue, or if it occurred due to a direct mechanism localized at the intestine. For instance, previous studies have demonstrated that APAP-induced liver injury results in the release of inflammatory and cytotoxic cytokines into the serum such as  $\text{TNF}\alpha$  and HMGB1 (201, 261).  $\text{TNF}\alpha$  itself has been shown to play a role in inducing intestinal injury and increasing intestinal permeability in various disease models (175, 262, 263). For these reasons we first focused on investigating potential roles of  $\text{TNF}\alpha$  signaling

in APAP-induced intestinal toxicity. As previously reported (261), we detected greater concentrations of  $TNF\alpha$  in the serum of mice 4-Hr after APAP treatment in comparison to PBS-treated controls (**Fig. 5A**,  $64.75 \pm 22.88$  vs  $0.43 \pm 0.43$  pg/mL  $TNF\alpha$ ). However, some variability was noted in this observation as  $TNF\alpha$  remained undetectable in the serum from ~35% of APAP-treated mice. In order to directly investigate a potential role of  $TNF\alpha$  signaling in mediating APAP-induced intestinal crypt cell death either via systemic or localized mechanisms, we employed knockout mice for both the  $TNFR\alpha$  chain and  $TNFR\beta$  chain ( $TNFR^{-/-}$ ). We examined PARP expression in liver lysates of WT and  $TNFR^{-/-}$  mice following treatment with APAP. PARP cleavage was absent in both APAP-treated WT and  $TNFR^{-/-}$  mice as anticipated (**Fig 5B**). However, ileum lysates demonstrated that an increase in PARP cleavage occurred even in the absence of  $TNFR$  signaling (**Fig. 5C**). Furthermore, the appearance of apoptotic bodies by H&E and immunohistochemical staining for cleaved/activated caspase-3 was identical between APAP-treated WT and  $TNFR^{-/-}$  ileum sample sections (**Fig. 5D**). These results indicate that apoptosis of intestinal crypt cells due to APAP overdose occurred independently from  $TNF\alpha$  signaling.

### **Intestinal crypt stem cells are disproportionately susceptible to acetaminophen-induced cell death**

Both WT and  $TNFR^{-/-}$  mice suffered widespread intestinal apoptosis 4-hr after APAP treatment, yet all cell death remained restricted to the intestinal crypts. The intestinal crypt base houses the epithelial stem cell populations, most notably the rapidly dividing leucine-rich repeat-containing G-protein coupled receptor 5+ ( $LGR5^+$ ) crypt base columnar cells (107).  $LGR5^+$  cells and other subsets of intestinal crypt cells are highly susceptible to cytotoxic stressors such as radiation and numerous chemotherapeutics (108, 114, 264). Therefore, we hypothesized that the APAP-

induced death we observed was disproportionately affecting *LGR5*<sup>+</sup> stem cell populations. To test this hypothesis, we treated heterozygous *LGR5-EGFP-IRES-creERT2* reporter mice with APAP or PBS and harvested their ileums 4-hr later. Immunofluorescence analysis of fresh frozen ileum revealed diffuse expression of GFP in the intestinal crypts of control animals that was reduced in APAP-treated mice (**Fig. 6**). Consistent with the IHC staining, apoptotic bodies were detected in the intestinal crypts of APAP-treated animals that had strong staining for cleaved caspase-3. Merging of these two channels demonstrated that the majority of these apoptotic bodies co-localized with strong, condensed GFP<sup>+</sup> signals (**Fig. 6**). Together, these data demonstrate that intestinal toxicity due to high-dose acetaminophen exposure disproportionately induced death of *LGR5*<sup>+</sup> stem cells.

## Discussion

Widespread liver cell death that rapidly progresses to acute liver failure is without question the definitive threat posed by acetaminophen toxicity. However, the specific kinetic progression and mechanistic nature of APAP liver injury remains incompletely characterized. For instance, a somewhat controversial topic is the relative contributions the various forms of cell death (apoptosis, necrosis, pyroptosis, etc.) (195, 198). Even to this day, publications report conflicting evidence either in favor or against a role of hepatic apoptosis in APAP hepatotoxicity (256, 265, 266). Though this topic was not the focus of the current study, our data provides the strongest support to the argument that direct hepatic injury due to APAP toxicity is primarily driven by necrotic cell death. Instead, we surprisingly found that widespread apoptosis occurred throughout the crypts of the small intestine rapidly after APAP overdose. Interestingly this observation confirms the speculations made by Possamai *et al* that serum markers of apoptotic injury measured in human patient samples were derived from dying gut cells (202). Though a few studies have demonstrated potential toxicity of APAP on intestinal cell lines and organoids *in vitro* (203, 204, 267), to our knowledge, this study provides the first direct evidence that APAP induces regulated cell death to intestinal cells *in vivo*.

Our observations highlight the fact that APAP toxicity is a whole-body issue with pathological effects beyond liver injury. Previous reports have indicated APAP induces inflammation and injury of the kidney, lung, and brain (253-255). For this study, we focused on the gut due to critical role the intestinal physiology and the microbiome play in regulating chronic conditions of the liver (1), and potentially other organs (224). Currently, the role that intestinal barrier function and intestinal microbiota play in APAP-induced liver injury is somewhat unclear. On one hand, germ-free mice were found to be equally susceptible to APAP liver injury as conventionally housed animals (205). On the other hand, antibiotic-treated mice were found to be protected

from APAP hepatotoxicity, which was linked to the contribution of the bacterial metabolite 1-phenyl-1,2-propanedione enhancing liver injury (206). However, because liver injury is the immediate and acute concern with APAP toxicity, an overlooked and unexplained observation is that transplanted APAP-ALF patients have been found to have higher short-term mortality rates than patients transplanted for other etiologies of ALF (252). While the causes for this observation are currently unclear, greater non-compliance to treatment regimens amongst transplanted APAP-ALF patients was one speculated cause. However, it is entirely possible that this increased short-term mortality may in fact be in part caused by other toxic implications of APAP overdose beyond those directly on the liver that are left unaddressed by liver transplantation alone. To this end, we hypothesize that these toxic insults on target organs beside the liver are comorbid events with health implications that will become more important to consider as management of APAP ALF improves in the future.

In our present observations, APAP-induced intestinal cell death was strictly limited to populations of cells found within the crypts, which is a pattern of cell death that is strikingly similar to that induced by radiation exposure, cancer chemotherapy, and some forms of sepsis (108, 259, 268). This topographical location along the crypt-villus structure is enriched in various intestinal epithelial stem cell populations, such as rapidly dividing *LGR5*<sup>+</sup> cells and quiescent *BMI-1*<sup>+</sup> cells. Indeed, use *LGR5-EGFP-IRES-creERT2* reporter mice demonstrated that the majority of these dying cells were *LGR5*<sup>+</sup> cells. However, it is currently unclear what percentage of *LGR5*<sup>+</sup> cells survive APAP toxicity, and whether the apoptotic bodies that did not co-localize with the GFP reporter tag represent late remnants of *LGR5*<sup>+</sup> cells or death of small subsets of *LGR5* cellular populations. Regardless, the specificity of APAP-induced death to intestinal stem cells implies that APAP intestinal injury is likely to have longer last effects on overall intestinal physiology (107, 269). While this remains to be fully determined, our observations at least

indicate that enhanced gut permeability is also triggered at an early stage of APAP toxicity but persists even after apoptotic cells are cleared from the crypts.

Unfortunately, the direct mechanism of APAP-induced apoptotic death remains unclear. While we originally hypothesized that the intestinal injury occurred as a secondary result of massive hepatic necrosis, our evidence suggests that these events are likely independent from each other. Our initial focus for testing this hypothesis was  $TNF\alpha$ , which has been shown both in the present work and by previous studies to be rapidly elevated in the serum following APAP overdose (261). However, a significant subset of animals did not have elevated serum  $TNF\alpha$  levels at a time point at which intestinal apoptosis was widespread. Furthermore, intestinal apoptosis was highly prominent prior to the peak of liver injury as suggested by our ALT and histological analyses. By 24-hr after APAP overdose, a time by which liver injury had further progressed, apoptosis of intestinal stem cells was no longer present. Therefore, it seems most likely that acetaminophen induced a direct toxic insult localized to the intestine itself in which  $TNFR^{-/}$  signaling does not play a role. Whether other members of the death receptor family such as Fas/FasL play a role in APAP-induced intestinal injury remains to be determined. It is also distinctly possible that APAP may induce cytotoxic-stress related intrinsic cell death in intestinal stem cells, as the gut does express CYP2E1, the predominant metabolic enzyme for production of APAP-related reactive oxygen species (ROS) (195, 270-272). Elucidating the relative roles of intrinsic vs extrinsically induced cell death will have to be a focus of future work on extrahepatic APAP toxicity, including intestinal injury.

In conclusion, we provide the novel observation that acetaminophen overdose induces rapid apoptosis of intestine stem cells, predominantly of the  $LGR5^{+}$  population at the base of the

crypts. The pattern of this intestinal cell death mimics that observed by radiation-induced injury and has potentially long-lived consequences. Characterizing the mechanism of this death and the potential contributions APAP-induced intestinal injury has on overall morbidity and mortality will be an important advancement towards improving the management of patients suffering from APAP toxicity and ALF.

### **Acknowledgements**

We thank Dr. Pratyusha Mandal for the helpful scientific discussions and technical support in guiding this work, and Krystal Chopyk for assistance in final preparation of figures. We additionally thank Drs. Brian Evavold, Mark Czaja, Joshy Jacob, and Malú Tansey as critical sources of feedback and scientific critique. We are grateful to the Pathology Cores of Emory Vaccine Center, and to the veterinary and animal care staff of Yerkes National Primate Research Center, Emory University for their assistance. This research project was supported in part by the Emory University Integrated Cellular Imaging Microscopy Core of the Emory and Children's Pediatric Research Center.

### **Disclosures**

The authors have no conflicts of interest related to this research.

## Figure Legend

**Figure 1. Increased intestinal permeability and enhanced PARP cleavage is detected within the ileum during the acute response to acetaminophen overdose.** Six- to eight-week old male C57BL/6J mice were fasted and restricted from water for 12-hr. Mice were then treated with 500 mg/kg APAP by IP injection and with 1 g/kg 4-kDa FITC-dextran by oral gavage. Water and food were returned to the animals until they were sacrificed 4-hr later. Serum was analyzed for levels of ALT (**A**) and recovery of FITC-dextran (**B**). Data are represented as means  $\pm$  SEM and are representative of 10-15 mice per group from at least 3-independent experiments. Statistical analyses were made by students-*t* test, \*\**p* < 0.01, \*\*\*\**p* < 0.0001. Total protein lysates (25-30  $\mu$ g) of liver (**C**) and distal ileum (**D**) tissue were analyzed by western blot for PARP cleavage. Lysates of Raw 264.7 macrophages treated with or without 10  $\mu$ g/mL puromycin for 18-hr were included as controls. Arrows indicate cleaved PARP. Breaks in the depicted ileum image represent non-adjacent wells on the same gel. Western blot images are representative of 10-12 mice per group from at least 3-independent experiments.

**Figure 2. Apoptosis is induced in the ileum but not liver during the acute response to acetaminophen intoxication.** Six- to eight-week old male C57BL/6J mice were fasted for 12-hr and were treated with 500 mg/kg APAP by IP injection. Food was returned to the animals and they were euthanized 4-hr later. Formalin-fixed, paraffin embedded sections of liver and distal ileum tissue were analyzed by hematoxylin and eosin staining (**A**) and by immunohistochemical staining for cleaved caspase-3 (**B**). All provided images were taken at 200x magnification and are representative of at least 3 mice per group. Scale bars represent 150  $\mu$ m. Arrows indicate apoptotic bodies (**A**).

**Figure 3. Intestinal barrier deficits persist at 24-hr after acetaminophen overdose despite a reduction in ileum PARP cleavage.** Six- to eight-week old male C57BL/6J mice were fasted for 12-hr and were treated with 500 mg/kg APAP by IP injection. Food was returned to the animals, and they were restricted from water access starting from 8-hrs after APAP injection. After an additional 12-hr, mice were gavaged with 1 g/kg 4-kDa FITC-dextran. Water was then returned to the animals until they were sacrificed 4-hr later (A total of 24-hr after APAP treatment). Serum was analyzed for levels of ALT (**A**) and recovery of FITC-dextran (**B**). Data are represented as means  $\pm$  SEM and are representative of 9-15 mice per group from at least 3-independent experiments. Statistical analyses were made by students-*t* test, \*\**p* < 0.01, \*\*\*\**p* < 0.0001. Total protein lysates (25-30  $\mu$ g) of liver (**C**) and distal ileum (**D**) tissue were analyzed by western blot for PARP cleavage. Lysates of Raw 264.7 macrophages treated with or without 10  $\mu$ g/mL puromycin for 18-hr were included as controls. Arrows indicate cleaved PARP. Western blot images are representative of 10-15 mice per group from at least 3-independent experiments.

**Figure 4. Intestinal apoptotic bodies are cleared within 24-hr after acetaminophen overdose.** Six- to eight-week old male C57BL/6J mice were fasted for 12-hr and were treated with 500 mg/kg APAP by IP injection. Food was returned to the animals and they were euthanized 24-hr later. Formalin-fixed, paraffin embedded sections of liver and distal ileum tissue were analyzed by hematoxylin and eosin staining (**A**) and by immunohistochemical staining for cleaved caspase-3 (**B**). All provided images were taken at 200x magnification and are representative of at least 3 mice per group. Scale bars represent 150  $\mu$ m. Arrows indicate apoptotic bodies (**A**) and cells with positive staining for cleaved caspase-3 (**B**).

**Figure 5. Apoptotic death of intestinal crypt cells following acetaminophen overdose****occurs independent of TNFR signaling.**

Six- to eight-week old male C57BL/6J and age-matched *TNFR<sup>-/-</sup>* male mice were fasted for 12-hr and treated with 500 mg/kg APAP by IP injection. Food was returned to the animals and they were euthanized 4-hr later. Serum was analyzed for concentration of TNF $\alpha$  by sandwich ELISA (**A**). Concentrations are represented as means  $\pm$  SEM and are representative of 18-20 mice per group from at least 6-independent experiments. Statistical analyses were made by students-*t* test, \*\*\**p* < 0.001. Total protein lysates (25-30  $\mu$ g) of liver (**B**) and distal ileum (**C**) tissue were also analyzed by western blot for PARP cleavage. Lysates of Raw 264.7 macrophages treated with or without 10  $\mu$ g/mL puromycin for 18-hr were included as controls. Arrows indicate cleaved PARP. Western blot images are representative of 10-11 mice per group from at least 3-independent experiments. Formalin-fixed, paraffin embedded sections of liver and distal ileum tissue were analyzed by hematoxylin and eosin staining and immunohistochemical staining for cleaved caspase-3 (**D**). All provided images were taken at 200x magnification and are representative of at least 3 mice per group. Scale bars represent 150  $\mu$ m. Arrows indicate apoptotic bodies.

**Figure 6. Acetaminophen-induced intestinal apoptosis disproportionately affects *LGR5*<sup>+</sup>****stem cells.**

Six- to eight-week old male heterozygous *LGR5-EGFP-IRES-creERT2* reporter mice were fasted for 12-hr and were treated with 500 mg/kg APAP by IP injection. Food was returned to the animals and they were euthanized 4-hr later. Frozen ileum sections were stained for expression of GFP and cleaved caspase-3 and were analyzed by confocal immunofluorescence microscopy. All images except the secondary antibody control are representative of n = 3 mice per group and are 400x magnification. Scale bars represent 75  $\mu$ m. White arrowheads indicate sites of co-localization of GFP with cleaved caspase-3.

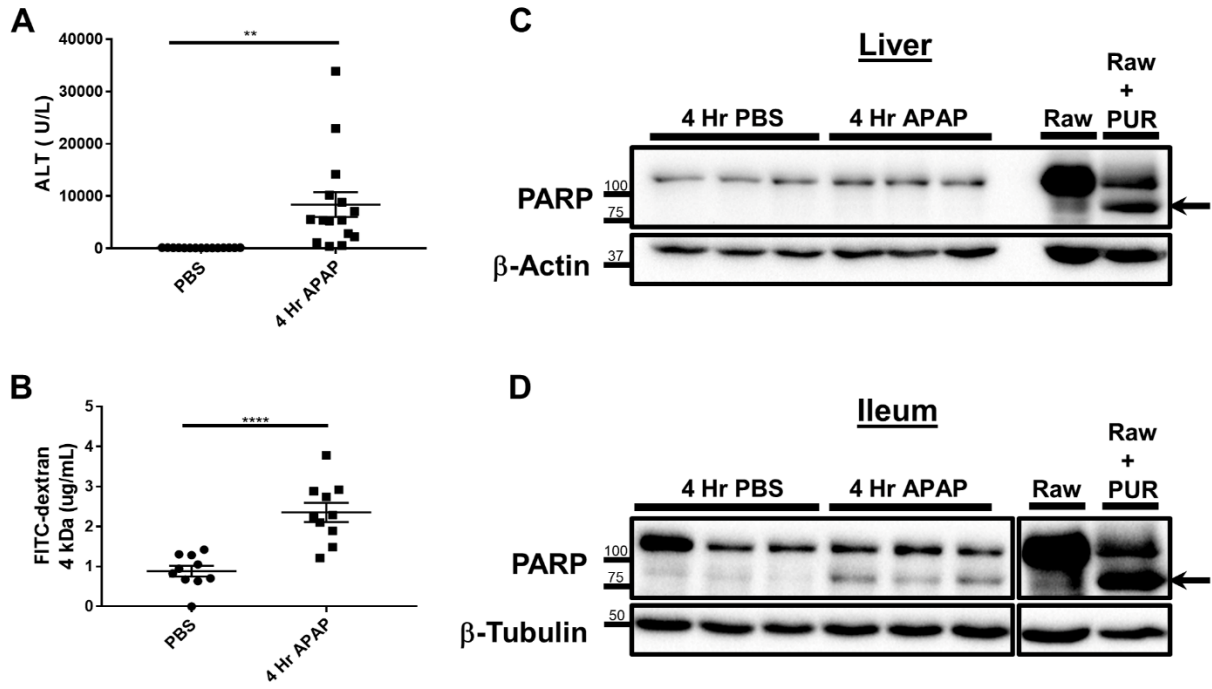


Figure 1

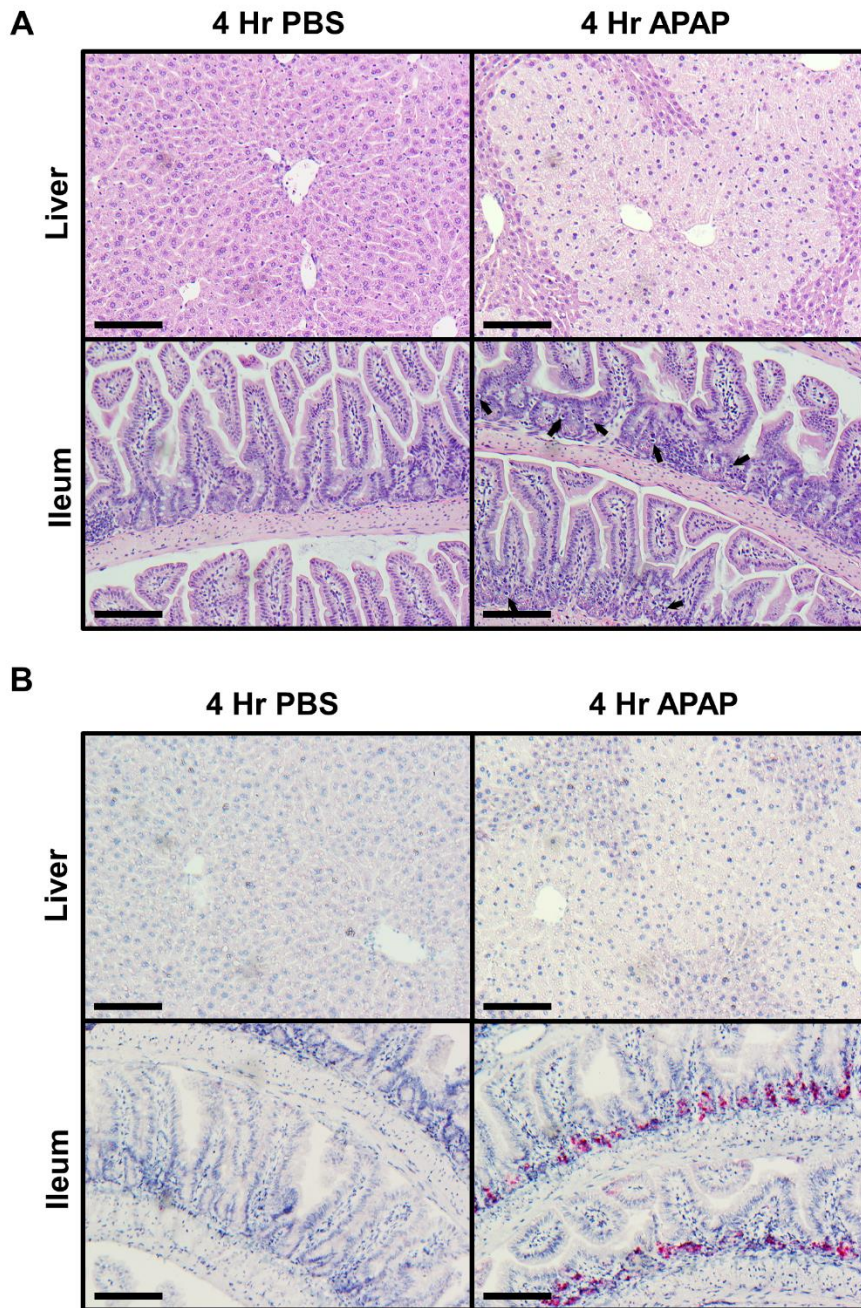


Figure 2

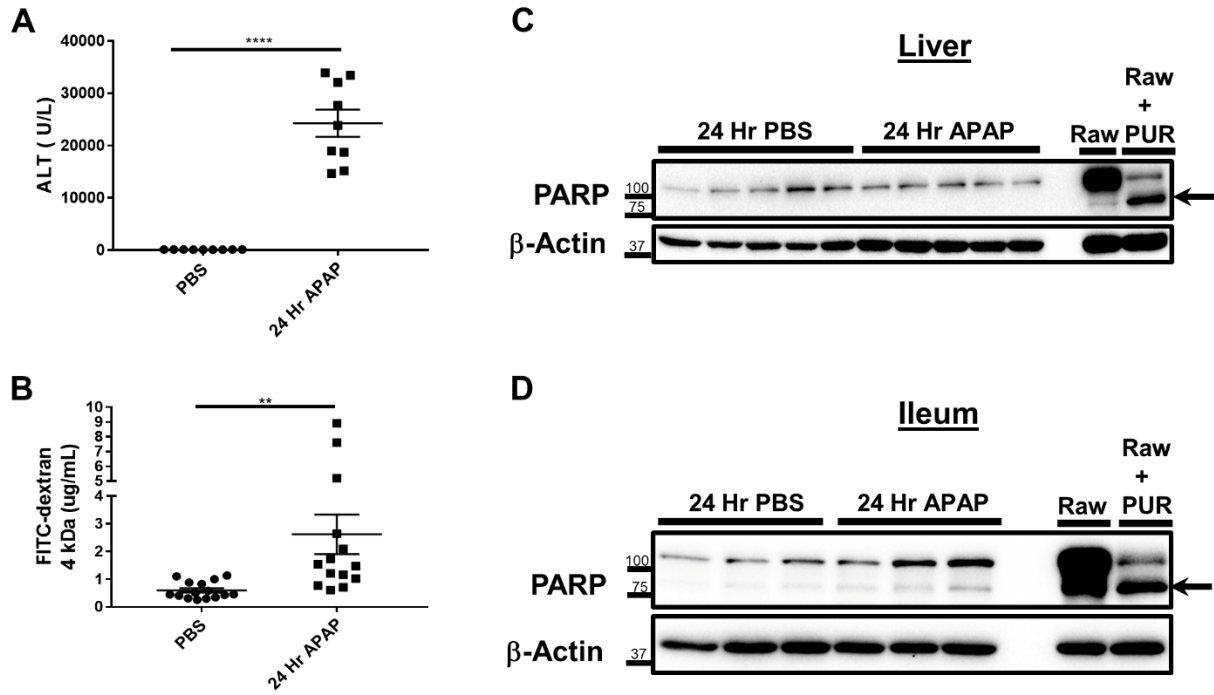


Figure 3

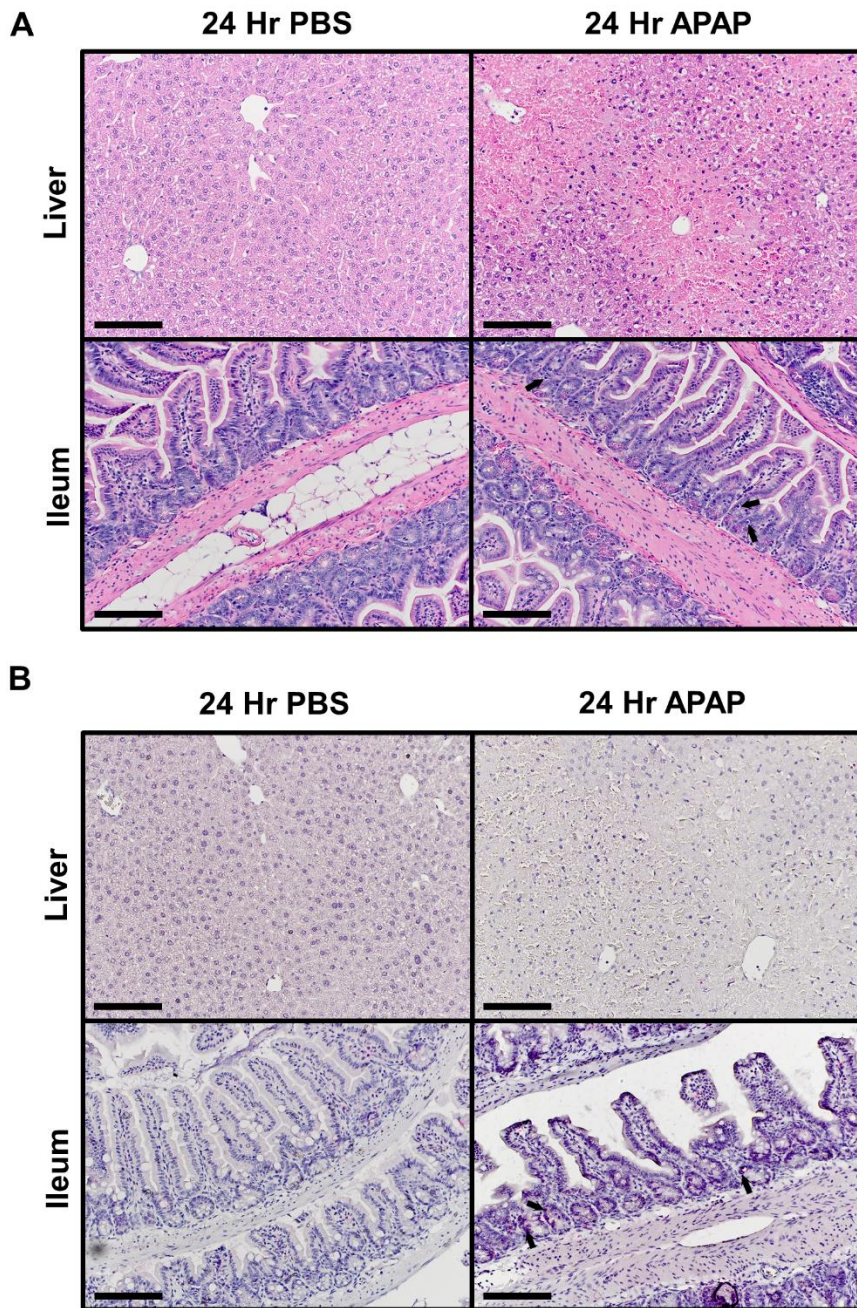


Figure 4

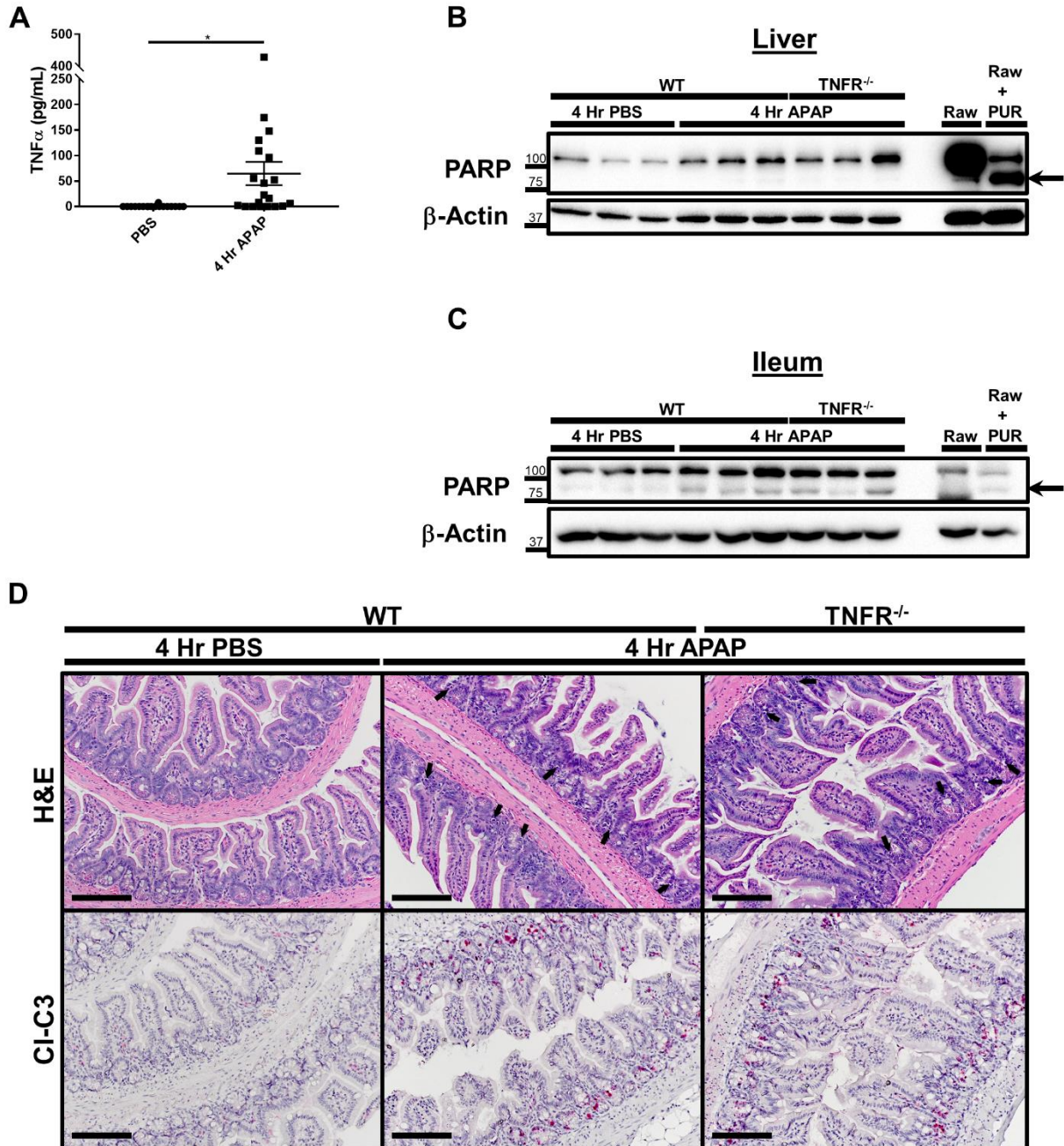


Figure 5

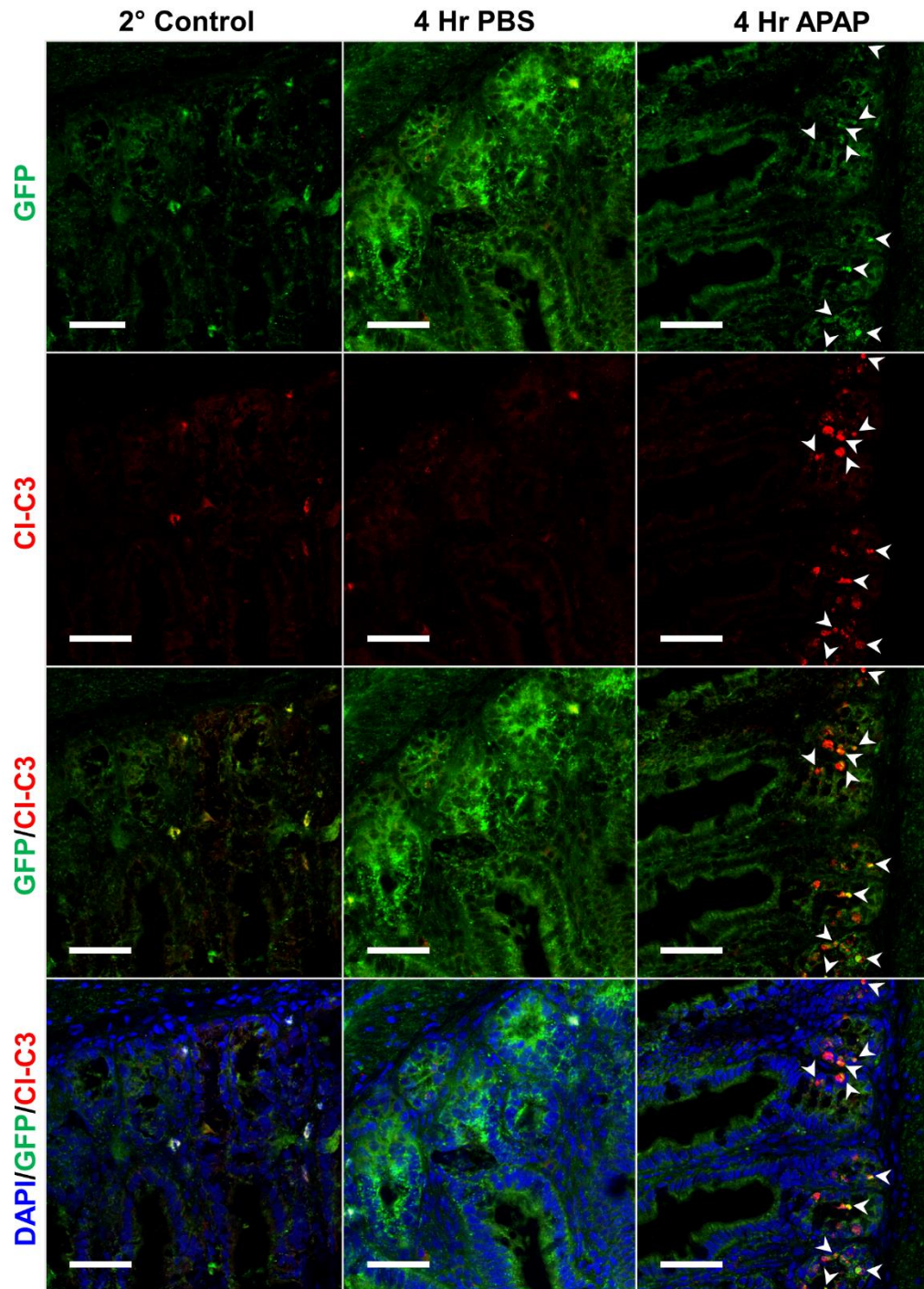


Figure 6

## Chapter 4: Discussion

Recent years have seen increasing excitement and investment of research funds in the area of gut-liver axis research. The largest movements in this collective endeavor are currently focused on unraveling the complex, intertwined web of the intestinal microbiome. However, fundamental understanding of intestinal barrier physiology and the specific mechanisms by which this barrier is disrupted in different disease settings is similarly lacking. The gut barrier is a complex multi-tiered conglomerate of its epithelial, mucus, immune, and microbial components that are held in a finely balanced state. Each distinct layer of this system consists of a host of individual cellular and molecular components with distinct yet overlapping functions.

The collective work of this dissertation specifically sought to characterize previously unexplored aspects of gut epithelial barrier dysfunction under environmental contexts that were relevant to chronic and acute liver injury. However, all work that I conducted outlined in **Chapters 2 and 3** took a basic approach, and it is likely that the conclusions that can be drawn from these data have broader implications on intestinal epithelial and TJ physiology. Much of my work is descriptive rather than mechanistic, and as such raises many more questions than I initially sought to address. It is my hope that my publications will indeed stir up such discussion amongst the scientific community and serve as a foundation for new investigations based upon lines of thought that had not existed prior to my work. In this final chapter I will briefly summarize how the conclusions drawn from **Chapters 2 and 3** fit into the larger scientific environment in relation to the advancements made by my colleagues across the globe within the same time frame that this dissertation work was conducted.

### Tight junction dysfunction in ALD:

As discussed in **Chapters 1 and 2**, evidence indicating a role of TJ dysfunction in ethanol-induced intestinal permeabilization has existed for several decades. This conclusion was drawn from several lines of associative evidence that primarily pertained to reduced protein expression of occludin and ZO-1 following exposure to ethanol or acetaldehyde (178, 273). However, the functional role that occludin plays in regulating paracellular permeability is still poorly understood. It is somewhat controversial amongst different TJ scholars whether occludin plays a primary or accessory role in barrier function. This controversy largely stems from the fact that occludin by itself cannot form TJs, and that *occludin*<sup>-/-</sup> mice do not display enhanced gut permeability compared to WT animals (34). Although it was recently demonstrated that *occludin*<sup>-/-</sup> mice are more susceptible to alcohol-induced liver injury, the same study reconfirmed that without alcohol as an offending stimulus, these animals had equivalent barrier function compared to the WT controls (180).

Contrary to *occludin*<sup>-/-</sup> animals, *JAM-A*<sup>-/-</sup> mice were shown to have impaired intestinal barrier function under baseline conditions (77). JAM-A has also been proposed to play a key role in regulating the paracellular permeability via a non-selective “leak” pathway, which permits the diffusion of relatively large molecules such as bacterial LPS (75). These observations provided the justification for questioning whether JAM-A dysfunction contributed to gut barrier dysfunction in ALD (**Chapter 2**), a chronic condition which is often associated with endotoxemia (11). I found that JAM-A protein expression is indeed reduced across two separate intestinal epithelial cell lines, though only to a modest extent (**Chapter 2, Fig. 3**). Combined JAM-A overexpression and knockdown studies raise further interesting questions regarding the functionality of this molecule (**Chapter 2, Fig. 6, 7**). These two complementary approaches most strongly indicated that JAM-A plays a minimal role in the mechanisms by which ethanol reduces epithelial TEER, at least at a concentration of 6% v/v. However, on the contrary, the reduction in 40-kDa FITC-

dextran flux brought about by JAM-A overexpression even within the presence of alcohol supports that it may play a role in regulating leak pathway flux. Additional work by the Anania lab further demonstrated that *JAM-A*<sup>-/-</sup> mice fed a HFD develop enhanced endotoxemia than control animals (190). Together, the *in vitro* data presented in **Chapter 2 Fig. 6** and the *JAM-A*<sup>-/-</sup> mouse data generated other Anania lab members lend further support to the functionality of JAM-A in regulating paracellular diffusion of large molecules. This potential delineation of epithelial resistance (ion flux) and large-molecular flux should be further explored by more comprehensive analyses of the whole epithelial TJ network.

My dissertation work also demonstrated that short-term alcohol exposure was associated with a reduction in the active form of Rap2 GTPase, an inhibitor of MLCK (**Chapter 2, Fig. 5**). To my knowledge, this is the first evidence that Rap2 activation status is altered by ethanol treatment, and it provides a potential link to the well-substantiated observation that alcohol causes MLCK activation. While JAM-A is a known regulator of Rap2c, these data do not identify which specific isoform(s) of Rap2 are affected by ethanol treatment, and this question will need to be addressed by future work. Due to the differential kinetics of Rap2 inhibition after 30-min exposure, and reduced JAM-A protein at 6-hr exposure to ethanol, it is unclear whether the mechanism of Rap2 inhibition is directly on Rap2 itself or via upstream inhibition of JAM-A function. Nevertheless, my data suggest that preventing the inhibitory action of ethanol on Rap2 may serve as a novel therapeutic target. However, a small-molecule activator of Rap2 does not currently exist, so this was unable to be directly explored. As a proof of principle experiment, additional studies could take a molecular biology approach and generate a Rap2c mutant that lacks GTPase function and would thus be constitutively active.

It was recently confirmed by Fan *et al.* that phosphorylation of JAM-A amino acid residue Y280 occurs in the presence of inflammatory cytokines and results in the redistribution of JAM-A from the TJ and contributes to barrier collapse (274). These new data provide a possible explanation

for my contradicting observations that JAM-A localization was maintained following ethanol exposure *in vitro*, while intestinal JAM-A localization was disrupted in alcohol fed-mice (**Chapter 2 Fig. 4, Fig 9**). Specifically, it possible that the reduction in TJ localization of JAM-A requires inflammatory signals that would be absent or reduced *in vitro* but would be provided by activated immune cells *in vivo*. Furthermore, it was also found that phosphorylation of JAM-A reduced its association with active Rap2 (274). Therefore, the approach of using constitutively active Rap2c mutant as described above is held back by the fact that ethanol may still prevent the association of this mutant with JAM-A. A suitable correlative approach for future studies would be to also test the effects of preventing JAM-A phosphorylation by using Src2 kinase inhibitor PP2 in combination with ethanol treatment.

The TJ is highly complex, with multiple members of each integral membrane protein family (MAGUKS, JAMs, claudins) that have overlapping yet distinct functionality. However, we still know surprisingly little about JAM-A function in comparison to other TJ proteins. My work has reinforced the hypothesis that JAM-A contributes to TJ function primarily through regulating the paracellular permeability of large solutes. Furthermore, my observations suggest that electrical resistance and permeability to large solutes may not be fully correlated. Given our current knowledge it is most likely that the claudin family plays the largest role in regulating epithelial TEER, but even within that family, some isoforms (i.e., claudin-1) are associated with increased resistance, whereas others (i.e., claudin-2) are associated with reduced resistance. Therefore, I believe that future studies TJ function, particularly in the setting of alcohol exposure, will have to take a more holistic approach in order to get a clearer understanding of the complex physiology of this system. Ideally this work will incorporate larger scale proteomics approaches such as stable isotope labeling with amino acids in cell culture (SILAC) (275). Techniques such as SILAC followed by quantitation and interaction pathway network analysis could serve as a strong basis for unraveling the associative changes ethanol causes to the TJ. This would also

serve as a strong foundation for future mechanistic studies which remain relatively sparse in the literature but are the most critical need for uncovering potential new therapeutics for ALD and other disorders by targeting gut permeability.

### **Intestinal permeability in APAP-induced ALF and intestinal epithelial stem cell physiology**

The role in compromised intestinal barrier function in modulating disease has primarily focused on chronic conditions. The reason for this is partially due to the greater public health burden that chronic diseases pose in comparison to acute organ injury. Furthermore, the predominant issue posed by gut barrier dysfunction and bacterial translocation is persistent, long-lived inflammation in the liver and other target organs. The chronicity of even low-grade inflammatory insults to the liver and distant organs is what drives gradual transition from silent injury to symptomatic disease of worsening phenotype.

Leakage of bacteria and PAMPS into the portal and systemic circulation will have immediate immunological consequences. However, the magnitude of the body's acute inflammatory response to gut leakiness is not well characterized. It is therefore uncertain to what extent gut barrier dysfunction contributes to acute organ injury, if at all. To this end I sought to identify if any physiological derangements occurred within the intestine during APAP toxicity, which serves as a predictable, clinically relevant model of acute liver injury (**Chapter 3**). APAP is a known hepatotoxin when consumed at high doses but is an often preferred analgesic due to its otherwise low side-effect profile in comparison to NSAIDs, steroids, and opiates (197). This model was of particular interest for two reasons: 1) Unlike NSAIDs, APAP is widely believed to not cause gastrointestinal injury; 2) APAP injury is thought to follow two different phases – initial injury driven by APAP metabolism alone, and a secondary phase of host immune-mediated

exacerbation of organ damage. We sought to characterize whether the intestine suffered direct injury during APAP intoxication, and if such intestinal injury could have potential consequences on either APAP liver injury or overall morbidity and mortality.

As demonstrated in **Chapter 3 Fig. 1** and **Fig. 3**, intestinal permeability was significantly increased in APAP-treated mice within an acute time frame and persisted through later periods of liver injury. These findings reinforced previous work in the APAP ALF literature that had demonstrated intestinal permeability following APAP intoxication (201). However, these previous reports were unable to convincingly demonstrate direct intestinal injury that may be an underlying cause for the enhanced gut leakiness (201, 202). For instance, Yang *et al.* were able to demonstrate bacterial translocation into the mesenteric lymph nodes during APAP liver injury. The same study indicated some potential signs of histologic injury to the intestinal villi, but the data were of questionable significance and left the character of this potential injury undefined (201). Our collective data in **Chapter 3** extensively demonstrates that APAP induces direct intestinal injury by triggering apoptosis of enterocytes with a predilection for the *LGR5*<sup>+</sup> crypt base stem cells.

This is the first inarguable *in vivo* evidence of APAP enterotoxicity, which confirms previous speculations by Possamai *et al.* based upon human clinical data (202). Though my work represents a critical step in changing how we think about the consequences of APAP toxicity there are a few notable questions that it leaves apparent. First is that the direct mechanisms that involved in triggering epithelial cell apoptosis remain uncharacterized. This is a deceptively difficult problem to address to the highly intertwined and overlapping nature of cell death pathways combined with the fact that only a relatively small population of cells is affected in this setting of injury. More robust means of probing cell death pathways, such as antibodies specific for cleaved caspase-9, could perhaps facilitate more in-depth histological studies in the future. A second glaring question is what the specific consequences of intestinal injury and enhanced gut

permeability during APAP toxicity are. For instance, it is unclear whether or not gut permeability modulates APAP-induced liver injury. As mentioned in **Chapter 3**, the contribution of the intestinal microbiome to APAP hepatotoxicity is somewhat unclear in itself. However, recent work by Gong *et al.* demonstrate a contribution of microbial metabolites in susceptibility APAP hepatotoxicity, and that depletion of gut microbiota by antibiotic treatment prevents APAP liver injury (206). This observation is likely more informative to APAP liver injury in humans compared to GF mouse studies, as the immune system of GF mice lacks the “education” provided by commensal organisms (205). Therefore, I speculate that further contributory roles of gut microbiota to APAP hepatotoxicity exist and will soon come to light, and that gut permeability likely does play a role in this pathophysiology. Moreover, it is also very likely that ingestion of excessive amounts of APAP has a direct consequence on gut microbial populations and metabolic activities, which are questions that need to be addressed by future work. Such potential persistent changes in gut microbial content and lasting gut permeability brought about by APAP enterotoxicity may thus be reasons for longer-term morbidity in this patient population.

That *LGR5*<sup>+</sup> stem cells were the predominant cellular population to be sensitive to APAP-induced intestinal injury is an intriguing finding that should be separately discussed due to its potential implications beyond APAP ALF. Intestinal stem cell biology is still a developing field which is currently experiencing rapid expansion of knowledge. As discussed in **Chapter 1**, much of this has to do with the identification of novel stem cell markers such as *LGR5* and the development of new tools with which to study them. The intestinal epithelial monolayer is indeed one of the most critical components of the gut barrier as evidenced by the drastic consequences attributed to TJ dysfunction in mediating gut permeability. Therefore, regulation of epithelial cell shedding and renewal have been overlooked aspects of intestinal barrier function, particularly in studies of the gut-liver axis. I suspect that this will change rather imminently amongst liver scholars, now that we have access to tools to more directly probe intestinal stem cell biology.

Just recently two papers were published indicating a reduction in intestinal stem cell populations in models of alcoholic and cholestatic liver injury (183, 215). While these are pioneering studies in their areas of investigation, they are still limited by use of older, less specific technologies such as qRT-PCR, in comparison to the *LGR5-EGFP-IRES-creERT2* reporter mice utilized in my dissertational work. These mice are an incredibly powerful tool that have thus far seen use primarily amongst stem cell biologists (276). Thus, I firmly believe that the descriptive studies summed in **Chapter 3** will be a significant contribution to our knowledge in not only APAP toxicity, but intestinal stem cell biology and gut-liver axis research as a whole.

### **Final reflections**

Intestinal barrier physiology is a complex topic that can be approached from practically any angle of academic study. It is therefore fitting that this dissertation applied broad *in vitro* and *in vivo* methodological techniques to study gut barrier disruption in contexts relevant to acute (APAP ALF) and chronic (ALD) liver injury. In doing so, I feel personally accomplished in what I set out to do – to gain the confidence in my own skills and knowledge. More importantly, this dissertation should contribute significantly to our understanding of general gut barrier physiology, as well as pathophysiological mechanisms specific to the settings of ALD and APAP ALF. Thus, the work summed herein serves as a reminder that TJ protein signaling pathways and epithelial stem cell numbers and function are significant targets to consider in studying gut barrier physiology and its impact on whole-body health.

## References

1. Tripathi A, Debelius J, Brenner DA, Karin M, Loomba R, Schnabl B, Knight R. 2018. The gut-liver axis and the intersection with the microbiome. *Nat Rev Gastroenterol Hepatol* 15: 397-411
2. Houser MC, Tansey MG. 2017. The gut-brain axis: is intestinal inflammation a silent driver of Parkinson's disease pathogenesis? *NPJ Parkinsons Dis* 3: 3
3. Powell N, Walker MM, Talley NJ. 2017. The mucosal immune system: master regulator of bidirectional gut-brain communications. *Nat Rev Gastroenterol Hepatol* 14: 143-59
4. Pasini E, Aquilani R, Testa C, Baiardi P, Angioletti S, Boschi F, Verri M, Dioguardi F. 2016. Pathogenic Gut Flora in Patients With Chronic Heart Failure. *JACC Heart Fail* 4: 220-7
5. Yang J, Lim SY, Ko YS, Lee HY, Oh SW, Kim MG, Cho WY, Jo SK. 2019. Intestinal barrier disruption and dysregulated mucosal immunity contribute to kidney fibrosis in chronic kidney disease. *Nephrol Dial Transplant* 34: 419-28
6. Hiippala K, Jouhten H, Ronkainen A, Hartikainen A, Kainulainen V, Jalanka J, Satokari R. 2018. The Potential of Gut Commensals in Reinforcing Intestinal Barrier Function and Alleviating Inflammation. *Nutrients* 10
7. Cervantes-Barragan L, Chai JN, Tianero MD, Di Luccia B, Ahern PP, Merriman J, Cortez VS, Caparon MG, Donia MS, Gilfillan S, Cella M, Gordon JI, Hsieh CS, Colonna M. 2017. Lactobacillus reuteri induces gut intraepithelial CD4(+)CD8alphaalpha(+) T cells. *Science* 357: 806-10
8. Yap YA, Marino E. 2018. An Insight Into the Intestinal Web of Mucosal Immunity, Microbiota, and Diet in Inflammation. *Front Immunol* 9: 2617
9. Adak A, Khan MR. 2019. An insight into gut microbiota and its functionalities. *Cell Mol Life Sci* 76: 473-93
10. Wells JM, Brummer RJ, Derrien M, MacDonald TT, Troost F, Cani PD, Theodorou V, Dekker J, Meheust A, de Vos WM, Mercenier A, Nauta A, Garcia-Rodenas CL. 2017. Homeostasis of the gut barrier and potential biomarkers. *Am J Physiol Gastrointest Liver Physiol* 312: G171-G93
11. Wang HJ, Gao B, Zakhari S, Nagy LE. 2012. Inflammation in alcoholic liver disease. *Annu Rev Nutr* 32: 343-68
12. Rao M, Gershon MD. 2016. The bowel and beyond: the enteric nervous system in neurological disorders. *Nat Rev Gastroenterol Hepatol* 13: 517-28
13. Chairatana P, Nolan EM. 2017. Defensins, lectins, mucins, and secretory immunoglobulin A: microbe-binding biomolecules that contribute to mucosal immunity in the human gut. *Crit Rev Biochem Mol Biol* 52: 45-56
14. Farquhar MG, Palade GE. 1963. Junctional complexes in various epithelia. *J Cell Biol* 17: 375-412
15. Claude P, Goodenough DA. 1973. Fracture faces of zonulae occludentes from "tight" and "leaky" epithelia. *J Cell Biol* 58: 390-400
16. Martinez-Palomo A, Erij D, Bracho H. 1971. Localization of permeability barriers in the frog skin epithelium. *J Cell Biol* 50: 277-87
17. Machen TE, Erij D, Wooding FB. 1972. Permeable junctional complexes. The movement of lanthanum across rabbit gallbladder and intestine. *J Cell Biol* 54: 302-12
18. Shen L, Weber CR, Raleigh DR, Yu D, Turner JR. 2011. Tight junction pore and leak pathways: a dynamic duo. *Annu Rev Physiol* 73: 283-309
19. Sasaki H, Matsui C, Furuse K, Mimori-Kiyosue Y, Furuse M, Tsukita S. 2003. Dynamic behavior of paired claudin strands within apposing plasma membranes. *Proc Natl Acad Sci U S A* 100: 3971-6
20. Van Itallie CM, Anderson JM. 2014. Architecture of tight junctions and principles of molecular composition. *Semin Cell Dev Biol* 36: 157-65

21. Furuse M, Hirase T, Itoh M, Nagafuchi A, Yonemura S, Tsukita S, Tsukita S. 1993. Occludin: a novel integral membrane protein localizing at tight junctions. *J Cell Biol* 123: 1777-88
22. Ando-Akatsuka Y, Saitou M, Hirase T, Kishi M, Sakakibara A, Itoh M, Yonemura S, Furuse M, Tsukita S. 1996. Interspecies diversity of the occludin sequence: cDNA cloning of human, mouse, dog, and rat-kangaroo homologues. *J Cell Biol* 133: 43-7
23. Furuse M, Itoh M, Hirase T, Nagafuchi A, Yonemura S, Tsukita S, Tsukita S. 1994. Direct association of occludin with ZO-1 and its possible involvement in the localization of occludin at tight junctions. *J Cell Biol* 127: 1617-26
24. Fanning AS, Jameson BJ, Jesaitis LA, Anderson JM. 1998. The tight junction protein ZO-1 establishes a link between the transmembrane protein occludin and the actin cytoskeleton. *J Biol Chem* 273: 29745-53
25. Van Itallie CM, Anderson JM. 1997. Occludin confers adhesiveness when expressed in fibroblasts. *J Cell Sci* 110 ( Pt 9): 1113-21
26. Cording J, Berg J, Kading N, Bellmann C, Tscheik C, Westphal JK, Milatz S, Gunzel D, Wolburg H, Piontek J, Huber O, Blasig IE. 2013. In tight junctions, claudins regulate the interactions between occludin, tricellulin and marvelD3, which, inversely, modulate claudin oligomerization. *J Cell Sci* 126: 554-64
27. Fujimoto K. 1995. Freeze-fracture replica electron microscopy combined with SDS digestion for cytochemical labeling of integral membrane proteins. Application to the immunogold labeling of intercellular junctional complexes. *J Cell Sci* 108 ( Pt 11): 3443-9
28. Wong V. 1997. Phosphorylation of occludin correlates with occludin localization and function at the tight junction. *Am J Physiol* 273: C1859-67
29. Sakakibara A, Furuse M, Saitou M, Ando-Akatsuka Y, Tsukita S. 1997. Possible involvement of phosphorylation of occludin in tight junction formation. *J Cell Biol* 137: 1393-401
30. Matter K, Balda MS. 1998. Biogenesis of tight junctions: the C-terminal domain of occludin mediates basolateral targeting. *J Cell Sci* 111 ( Pt 4): 511-9
31. McCarthy KM, Skare IB, Stankewich MC, Furuse M, Tsukita S, Rogers RA, Lynch RD, Schneeberger EE. 1996. Occludin is a functional component of the tight junction. *J Cell Sci* 109 ( Pt 9): 2287-98
32. Balda MS, Whitney JA, Flores C, Gonzalez S, Cereijido M, Matter K. 1996. Functional dissociation of paracellular permeability and transepithelial electrical resistance and disruption of the apical-basolateral intramembrane diffusion barrier by expression of a mutant tight junction membrane protein. *J Cell Biol* 134: 1031-49
33. Wong V, Gumbiner BM. 1997. A synthetic peptide corresponding to the extracellular domain of occludin perturbs the tight junction permeability barrier. *J Cell Biol* 136: 399-409
34. Saitou M, Furuse M, Sasaki H, Schulzke JD, Fromm M, Takano H, Noda T, Tsukita S. 2000. Complex phenotype of mice lacking occludin, a component of tight junction strands. *Mol Biol Cell* 11: 4131-42
35. Sanchez-Pulido L, Martin-Belmonte F, Valencia A, Alonso MA. 2002. MARVEL: a conserved domain involved in membrane apposition events. *Trends Biochem Sci* 27: 599-601
36. Ikenouchi J, Furuse M, Furuse K, Sasaki H, Tsukita S, Tsukita S. 2005. Tricellulin constitutes a novel barrier at tricellular contacts of epithelial cells. *J Cell Biol* 171: 939-45
37. Steed E, Rodrigues NT, Balda MS, Matter K. 2009. Identification of MarvelD3 as a tight junction-associated transmembrane protein of the occludin family. *BMC Cell Biol* 10: 95
38. Raleigh DR, Marchiando AM, Zhang Y, Shen L, Sasaki H, Wang Y, Long M, Turner JR. 2010. Tight junction-associated MARVEL proteins marvelD3, tricellulin, and occludin have distinct but overlapping functions. *Mol Biol Cell* 21: 1200-13

39. Furuse M, Fujita K, Hiiragi T, Fujimoto K, Tsukita S. 1998. Claudin-1 and -2: novel integral membrane proteins localizing at tight junctions with no sequence similarity to occludin. *J Cell Biol* 141: 1539-50
40. Mineta K, Yamamoto Y, Yamazaki Y, Tanaka H, Tada Y, Saito K, Tamura A, Igarashi M, Endo T, Takeuchi K, Tsukita S. 2011. Predicted expansion of the claudin multigene family. *FEBS Lett* 585: 606-12
41. Morita K, Furuse M, Fujimoto K, Tsukita S. 1999. Claudin multigene family encoding four-transmembrane domain protein components of tight junction strands. *Proc Natl Acad Sci U S A* 96: 511-6
42. Itoh M, Furuse M, Morita K, Kubota K, Saitou M, Tsukita S. 1999. Direct binding of three tight junction-associated MAGUKs, ZO-1, ZO-2, and ZO-3, with the COOH termini of claudins. *J Cell Biol* 147: 1351-63
43. Furuse M, Sasaki H, Fujimoto K, Tsukita S. 1998. A single gene product, claudin-1 or -2, reconstitutes tight junction strands and recruits occludin in fibroblasts. *J Cell Biol* 143: 391-401
44. Kubota K, Furuse M, Sasaki H, Sonoda N, Fujita K, Nagafuchi A, Tsukita S. 1999. Ca<sup>2+</sup>-independent cell-adhesion activity of claudins, a family of integral membrane proteins localized at tight junctions. *Curr Biol* 9: 1035-8
45. Niimi T, Nagashima K, Ward JM, Minoo P, Zimonjic DB, Popescu NC, Kimura S. 2001. claudin-18, a novel downstream target gene for the T/EBP/NKX2.1 homeodomain transcription factor, encodes lung- and stomach-specific isoforms through alternative splicing. *Mol Cell Biol* 21: 7380-90
46. Simon DB, Lu Y, Choate KA, Velazquez H, Al-Sabban E, Praga M, Casari G, Bettinelli A, Colussi G, Rodriguez-Soriano J, McCredie D, Milford D, Sanjad S, Lifton RP. 1999. Paracellin-1, a renal tight junction protein required for paracellular Mg<sup>2+</sup> resorption. *Science* 285: 103-6
47. Rahner C, Mitic LL, Anderson JM. 2001. Heterogeneity in expression and subcellular localization of claudins 2, 3, 4, and 5 in the rat liver, pancreas, and gut. *Gastroenterology* 120: 411-22
48. Morita K, Sasaki H, Fujimoto K, Furuse M, Tsukita S. 1999. Claudin-11/OSP-based tight junctions of myelin sheaths in brain and Sertoli cells in testis. *J Cell Biol* 145: 579-88
49. Furuse M, Sasaki H, Tsukita S. 1999. Manner of interaction of heterogeneous claudin species within and between tight junction strands. *J Cell Biol* 147: 891-903
50. Gow A, Southwood CM, Li JS, Pariali M, Riordan GP, Brodie SE, Danias J, Bronstein JM, Kachar B, Lazzarini RA. 1999. CNS myelin and sertoli cell tight junction strands are absent in Osp/claudin-11 null mice. *Cell* 99: 649-59
51. Morita K, Sasaki H, Furuse M, Tsukita S. 1999. Endothelial claudin: claudin-5/TMVCF constitutes tight junction strands in endothelial cells. *J Cell Biol* 147: 185-94
52. Furuse M, Hata M, Furuse K, Yoshida Y, Haratake A, Sugitani Y, Noda T, Kubo A, Tsukita S. 2002. Claudin-based tight junctions are crucial for the mammalian epidermal barrier: a lesson from claudin-1-deficient mice. *J Cell Biol* 156: 1099-111
53. Furuse M, Furuse K, Sasaki H, Tsukita S. 2001. Conversion of zonulae occludentes from tight to leaky strand type by introducing claudin-2 into Madin-Darby canine kidney I cells. *J Cell Biol* 153: 263-72
54. Van Itallie C, Rahner C, Anderson JM. 2001. Regulated expression of claudin-4 decreases paracellular conductance through a selective decrease in sodium permeability. *J Clin Invest* 107: 1319-27
55. Stevenson BR, Anderson JM, Goodenough DA, Mooseker MS. 1988. Tight junction structure and ZO-1 content are identical in two strains of Madin-Darby canine kidney cells which differ in transepithelial resistance. *J Cell Biol* 107: 2401-8

56. Colegio OR, Van Itallie C, Rahner C, Anderson JM. 2003. Claudin extracellular domains determine paracellular charge selectivity and resistance but not tight junction fibril architecture. *Am J Physiol Cell Physiol* 284: C1346-54
57. Van Itallie CM, Fanning AS, Anderson JM. 2003. Reversal of charge selectivity in cation or anion-selective epithelial lines by expression of different claudins. *Am J Physiol Renal Physiol* 285: F1078-84
58. Capaldo CT, Nusrat A. 2015. Claudin switching: Physiological plasticity of the Tight Junction. *Semin Cell Dev Biol* 42: 22-9
59. Tanaka H, Takechi M, Kiyonari H, Shioi G, Tamura A, Tsukita S. 2015. Intestinal deletion of Claudin-7 enhances paracellular organic solute flux and initiates colonic inflammation in mice. *Gut* 64: 1529-38
60. Kinugasa T, Sakaguchi T, Gu X, Reinecker HC. 2000. Claudins regulate the intestinal barrier in response to immune mediators. *Gastroenterology* 118: 1001-11
61. Martin-Padura I, Lostaglio S, Schneemann M, Williams L, Romano M, Fruscella P, Panzeri C, Stoppacciaro A, Ruco L, Villa A, Simmons D, Dejana E. 1998. Junctional adhesion molecule, a novel member of the immunoglobulin superfamily that distributes at intercellular junctions and modulates monocyte transmigration. *J Cell Biol* 142: 117-27
62. Williams LA, Martin-Padura I, Dejana E, Hogg N, Simmons DL. 1999. Identification and characterisation of human Junctional Adhesion Molecule (JAM). *Mol Immunol* 36: 1175-88
63. Cunningham SA, Arrate MP, Rodriguez JM, Bjercke RJ, Vanderslice P, Morris AP, Brock TA. 2000. A novel protein with homology to the junctional adhesion molecule. Characterization of leukocyte interactions. *J Biol Chem* 275: 34750-6
64. Palmeri D, van Zante A, Huang CC, Hemmerich S, Rosen SD. 2000. Vascular endothelial junction-associated molecule, a novel member of the immunoglobulin superfamily, is localized to intercellular boundaries of endothelial cells. *J Biol Chem* 275: 19139-45
65. Arrate MP, Rodriguez JM, Tran TM, Brock TA, Cunningham SA. 2001. Cloning of human junctional adhesion molecule 3 (JAM3) and its identification as the JAM2 counter-receptor. *J Biol Chem* 276: 45826-32
66. Aurrand-Lions M, Duncan L, Ballestrem C, Imhof BA. 2001. JAM-2, a novel immunoglobulin superfamily molecule, expressed by endothelial and lymphatic cells. *J Biol Chem* 276: 2733-41
67. Luissint AC, Nusrat A, Parkos CA. 2014. JAM-related proteins in mucosal homeostasis and inflammation. *Semin Immunopathol* 36: 211-26
68. Ebnet K, Suzuki A, Ohno S, Vestweber D. 2004. Junctional adhesion molecules (JAMs): more molecules with dual functions? *J Cell Sci* 117: 19-29
69. Itoh M, Sasaki H, Furuse M, Ozaki H, Kita T, Tsukita S. 2001. Junctional adhesion molecule (JAM) binds to PAR-3: a possible mechanism for the recruitment of PAR-3 to tight junctions. *J Cell Biol* 154: 491-7
70. Kostrewa D, Brockhaus M, D'Arcy A, Dale GE, Nelboeck P, Schmid G, Mueller F, Bazzoni G, Dejana E, Bartfai T, Winkler FK, Hennig M. 2001. X-ray structure of junctional adhesion molecule: structural basis for homophilic adhesion via a novel dimerization motif. *EMBO J* 20: 4391-8
71. Bazzoni G, Martinez-Estrada OM, Mueller F, Nelboeck P, Schmid G, Bartfai T, Dejana E, Brockhaus M. 2000. Homophilic interaction of junctional adhesion molecule. *J Biol Chem* 275: 30970-6
72. Severson EA, Parkos CA. 2009. Mechanisms of outside-in signaling at the tight junction by junctional adhesion molecule A. *Ann N Y Acad Sci* 1165: 10-8
73. Ebnet K, Schulz CU, Meyer Zu Brickwedde MK, Pendl GG, Vestweber D. 2000. Junctional adhesion molecule interacts with the PDZ domain-containing proteins AF-6 and ZO-1. *J Biol Chem* 275: 27979-88

74. Bazzoni G, Martinez-Estrada OM, Orsenigo F, Cordenonsi M, Citi S, Dejana E. 2000. Interaction of junctional adhesion molecule with the tight junction components ZO-1, cingulin, and occludin. *J Biol Chem* 275: 20520-6
75. Monteiro AC, Sumagin R, Rankin CR, Leoni G, Mina MJ, Reiter DM, Stehle T, Dermody TS, Schaefer SA, Hall RA, Nusrat A, Parkos CA. 2013. JAM-A associates with ZO-2, afadin, and PDZ-GEF1 to activate Rap2c and regulate epithelial barrier function. *Mol Biol Cell* 24: 2849-60
76. Nomme J, Fanning AS, Caffrey M, Lye MF, Anderson JM, Lavie A. 2011. The Src homology 3 domain is required for junctional adhesion molecule binding to the third PDZ domain of the scaffolding protein ZO-1. *J Biol Chem* 286: 43352-60
77. Laukoetter MG, Nava P, Lee WY, Severson EA, Capaldo CT, Babbitt BA, Williams IR, Koval M, Peatman E, Campbell JA, Dermody TS, Nusrat A, Parkos CA. 2007. JAM-A regulates permeability and inflammation in the intestine in vivo. *J Exp Med* 204: 3067-76
78. Khandoga A, Kessler JS, Meissner H, Hanschen M, Corada M, Motoike T, Enders G, Dejana E, Krombach F. 2005. Junctional adhesion molecule-A deficiency increases hepatic ischemia-reperfusion injury despite reduction of neutrophil transendothelial migration. *Blood* 106: 725-33
79. Ebnet K, Suzuki A, Horikoshi Y, Hirose T, Meyer Zu Brickwedde MK, Ohno S, Vestweber D. 2001. The cell polarity protein ASIP/PAR-3 directly associates with junctional adhesion molecule (JAM). *EMBO J* 20: 3738-48
80. Del Maschio A, De Luigi A, Martin-Padura I, Brockhaus M, Bartfai T, Fruscella P, Adorini L, Martino G, Furlan R, De Simoni MG, Dejana E. 1999. Leukocyte recruitment in the cerebrospinal fluid of mice with experimental meningitis is inhibited by an antibody to junctional adhesion molecule (JAM). *J Exp Med* 190: 1351-6
81. Flemming S, Luissint AC, Nusrat A, Parkos CA. 2018. Analysis of leukocyte transepithelial migration using an in vivo murine colonic loop model. *JCI Insight* 3
82. Mandell KJ, Babbitt BA, Nusrat A, Parkos CA. 2005. Junctional adhesion molecule 1 regulates epithelial cell morphology through effects on beta1 integrins and Rap1 activity. *J Biol Chem* 280: 11665-74
83. Monteiro AC, Parkos CA. 2012. Intracellular mediators of JAM-A-dependent epithelial barrier function. *Ann N Y Acad Sci* 1257: 115-24
84. Monteiro AC, Luissint AC, Sumagin R, Lai C, Vielmuth F, Wolf MF, Laur O, Reiss K, Spindler V, Stehle T, Dermody TS, Nusrat A, Parkos CA. 2014. Trans-dimerization of JAM-A regulates Rap2 and is mediated by a domain that is distinct from the cis-dimerization interface. *Mol Biol Cell* 25: 1574-85
85. Stevenson BR, Siliciano JD, Mooseker MS, Goodenough DA. 1986. Identification of ZO-1: a high molecular weight polypeptide associated with the tight junction (zonula occludens) in a variety of epithelia. *J Cell Biol* 103: 755-66
86. Gumbiner B, Lowenkopf T, Apatira D. 1991. Identification of a 160-kDa polypeptide that binds to the tight junction protein ZO-1. *Proc Natl Acad Sci U S A* 88: 3460-4
87. Jesaitis LA, Goodenough DA. 1994. Molecular characterization and tissue distribution of ZO-2, a tight junction protein homologous to ZO-1 and the Drosophila discs-large tumor suppressor protein. *J Cell Biol* 124: 949-61
88. Haskins J, Gu L, Wittchen ES, Hibbard J, Stevenson BR. 1998. ZO-3, a novel member of the MAGUK protein family found at the tight junction, interacts with ZO-1 and occludin. *J Cell Biol* 141: 199-208
89. Willott E, Balda MS, Fanning AS, Jameson B, Van Itallie C, Anderson JM. 1993. The tight junction protein ZO-1 is homologous to the Drosophila discs-large tumor suppressor protein of septate junctions. *Proc Natl Acad Sci U S A* 90: 7834-8

90. Fanning AS, Ma TY, Anderson JM. 2002. Isolation and functional characterization of the actin binding region in the tight junction protein ZO-1. *FASEB J* 16: 1835-7
91. Fanning AS, Anderson JM. 2009. Zonula occludens-1 and -2 are cytosolic scaffolds that regulate the assembly of cellular junctions. *Ann N Y Acad Sci* 1165: 113-20
92. Adachi M, Inoko A, Hata M, Furuse K, Umeda K, Itoh M, Tsukita S. 2006. Normal establishment of epithelial tight junctions in mice and cultured cells lacking expression of ZO-3, a tight-junction MAGUK protein. *Mol Cell Biol* 26: 9003-15
93. Xu J, Kausalya PJ, Phua DC, Ali SM, Hossain Z, Hunziker W. 2008. Early embryonic lethality of mice lacking ZO-2, but Not ZO-3, reveals critical and nonredundant roles for individual zonula occludens proteins in mammalian development. *Mol Cell Biol* 28: 1669-78
94. Citi S, Sabanay H, Jakes R, Geiger B, Kendrick-Jones J. 1988. Cingulin, a new peripheral component of tight junctions. *Nature* 333: 272-6
95. D'Atri F, Nadalutti F, Citi S. 2002. Evidence for a functional interaction between cingulin and ZO-1 in cultured cells. *J Biol Chem* 277: 27757-64
96. Guillemot L, Citi S. 2006. Cingulin regulates claudin-2 expression and cell proliferation through the small GTPase RhoA. *Mol Biol Cell* 17: 3569-77
97. Yano T, Matsui T, Tamura A, Uji M, Tsukita S. 2013. The association of microtubules with tight junctions is promoted by cingulin phosphorylation by AMPK. *J Cell Biol* 203: 605-14
98. Guillemot L, Hammar E, Kaister C, Ritz J, Caille D, Jond L, Bauer C, Meda P, Citi S. 2004. Disruption of the cingulin gene does not prevent tight junction formation but alters gene expression. *J Cell Sci* 117: 5245-56
99. Mandai K, Nakanishi H, Satoh A, Obaishi H, Wada M, Nishioka H, Itoh M, Mizoguchi A, Aoki T, Fujimoto T, Matsuda Y, Tsukita S, Takai Y. 1997. Afadin: A novel actin filament-binding protein with one PDZ domain localized at cadherin-based cell-to-cell adherens junction. *J Cell Biol* 139: 517-28
100. Yamamoto T, Harada N, Kano K, Taya S, Canaani E, Matsuura Y, Mizoguchi A, Ide C, Kaibuchi K. 1997. The Ras target AF-6 interacts with ZO-1 and serves as a peripheral component of tight junctions in epithelial cells. *J Cell Biol* 139: 785-95
101. Yamada T, Kuramitsu K, Rikitsu E, Kurita S, Ikeda W, Takai Y. 2013. Nectin and junctional adhesion molecule are critical cell adhesion molecules for the apico-basal alignment of adherens and tight junctions in epithelial cells. *Genes Cells* 18: 985-98
102. Severson EA, Lee WY, Capaldo CT, Nusrat A, Parkos CA. 2009. Junctional adhesion molecule A interacts with Afadin and PDZ-GEF2 to activate Rap1A, regulate beta1 integrin levels, and enhance cell migration. *Mol Biol Cell* 20: 1916-25
103. Tanaka-Okamoto M, Hori K, Ishizaki H, Itoh Y, Onishi S, Yonemura S, Takai Y, Miyoshi J. 2011. Involvement of afadin in barrier function and homeostasis of mouse intestinal epithelia. *J Cell Sci* 124: 2231-40
104. Campbell HK, Maiers JL, DeMali KA. 2017. Interplay between tight junctions & adherens junctions. *Exp Cell Res* 358: 39-44
105. Niessen CM. 2007. Tight junctions/adherens junctions: basic structure and function. *J Invest Dermatol* 127: 2525-32
106. Barker N. 2014. Adult intestinal stem cells: critical drivers of epithelial homeostasis and regeneration. *Nat Rev Mol Cell Biol* 15: 19-33
107. Barker N, van Oudenaarden A, Clevers H. 2012. Identifying the stem cell of the intestinal crypt: strategies and pitfalls. *Cell Stem Cell* 11: 452-60
108. Yu J. 2013. Intestinal stem cell injury and protection during cancer therapy. *Transl Cancer Res* 2: 384-96

109. Barker N, van Es JH, Kuipers J, Kujala P, van den Born M, Cozijnsen M, Haegebarth A, Korving J, Begthel H, Peters PJ, Clevers H. 2007. Identification of stem cells in small intestine and colon by marker gene Lgr5. *Nature* 449: 1003-7
110. Sato T, Vries RG, Snippert HJ, van de Wetering M, Barker N, Stange DE, van Es JH, Abo A, Kujala P, Peters PJ, Clevers H. 2009. Single Lgr5 stem cells build crypt-villus structures in vitro without a mesenchymal niche. *Nature* 459: 262-5
111. Bhanja P, Norris A, Gupta-Saraf P, Hoover A, Saha S. 2018. BCN057 induces intestinal stem cell repair and mitigates radiation-induced intestinal injury. *Stem Cell Res Ther* 9: 26
112. Yan KS, Chia LA, Li X, Ootani A, Su J, Lee JY, Su N, Luo Y, Heilshorn SC, Amieva MR, Sangiorgi E, Capecchi MR, Kuo CJ. 2012. The intestinal stem cell markers Bmi1 and Lgr5 identify two functionally distinct populations. *Proc Natl Acad Sci U S A* 109: 466-71
113. Tian H, Biehs B, Warming S, Leong KG, Rangell L, Klein OD, de Sauvage FJ. 2011. A reserve stem cell population in small intestine renders Lgr5-positive cells dispensable. *Nature* 478: 255-9
114. Metcalfe C, Kljavin NM, Ybarra R, de Sauvage FJ. 2014. Lgr5+ stem cells are indispensable for radiation-induced intestinal regeneration. *Cell Stem Cell* 14: 149-59
115. Hua G, Thin TH, Feldman R, Haimovitz-Friedman A, Clevers H, Fuks Z, Kolesnick R. 2012. Crypt base columnar stem cells in small intestines of mice are radioresistant. *Gastroenterology* 143: 1266-76
116. Cornick S, Tawiah A, Chadee K. 2015. Roles and regulation of the mucus barrier in the gut. *Tissue Barriers* 3: e982426
117. Faderl M, Noti M, Corazza N, Mueller C. 2015. Keeping bugs in check: The mucus layer as a critical component in maintaining intestinal homeostasis. *IUBMB Life* 67: 275-85
118. Johansson ME, Ambort D, Pelaseyed T, Schutte A, Gustafsson JK, Ermund A, Subramani DB, Holmen-Larsson JM, Thomsson KA, Bergstrom JH, van der Post S, Rodriguez-Pineiro AM, Sjoval H, Backstrom M, Hansson GC. 2011. Composition and functional role of the mucus layers in the intestine. *Cell Mol Life Sci* 68: 3635-41
119. Petersson J, Schreiber O, Hansson GC, Gendler SJ, Velcich A, Lundberg JO, Roos S, Holm L, Phillipson M. 2011. Importance and regulation of the colonic mucus barrier in a mouse model of colitis. *Am J Physiol Gastrointest Liver Physiol* 300: G327-33
120. Pelaseyed T, Bergstrom JH, Gustafsson JK, Ermund A, Birchenough GM, Schutte A, van der Post S, Svensson F, Rodriguez-Pineiro AM, Nyström EE, Wising C, Johansson ME, Hansson GC. 2014. The mucus and mucins of the goblet cells and enterocytes provide the first defense line of the gastrointestinal tract and interact with the immune system. *Immunol Rev* 260: 8-20
121. Sonnenburg JL, Xu J, Leip DD, Chen CH, Westover BP, Weatherford J, Buhler JD, Gordon JI. 2005. Glycan foraging in vivo by an intestine-adapted bacterial symbiont. *Science* 307: 1955-9
122. Schroeder BO. 2019. Fight them or feed them: how the intestinal mucus layer manages the gut microbiota. *Gastroenterol Rep (Oxf)* 7: 3-12
123. Sicard JF, Le Bihan G, Vogelee P, Jacques M, Harel J. 2017. Interactions of Intestinal Bacteria with Components of the Intestinal Mucus. *Front Cell Infect Microbiol* 7: 387
124. Ho SB, Dvorak LA, Moor RE, Jacobson AC, Frey MR, Corredor J, Polk DB, Shekels LL. 2006. Cysteine-rich domains of muc3 intestinal mucin promote cell migration, inhibit apoptosis, and accelerate wound healing. *Gastroenterology* 131: 1501-17
125. Mowat AM, Agace WW. 2014. Regional specialization within the intestinal immune system. *Nat Rev Immunol* 14: 667-85
126. Okumura R, Takeda K. 2016. Maintenance of gut homeostasis by the mucosal immune system. *Proc Jpn Acad Ser B Phys Biol Sci* 92: 423-35
127. Walker JA, Barlow JL, McKenzie AN. 2013. Innate lymphoid cells--how did we miss them? *Nat Rev Immunol* 13: 75-87

128. Kurioka A, Walker LJ, Klenerman P, Willberg CB. 2016. MAIT cells: new guardians of the liver. *Clin Transl Immunology* 5: e98
129. Nielsen MM, Witherden DA, Havran WL. 2017. gammadelta T cells in homeostasis and host defence of epithelial barrier tissues. *Nat Rev Immunol* 17: 733-45
130. Mukherjee S, Hooper LV. 2015. Antimicrobial defense of the intestine. *Immunity* 42: 28-39
131. Nakamura K, Sakuragi N, Takakuwa A, Ayabe T. 2016. Paneth cell alpha-defensins and enteric microbiota in health and disease. *Biosci Microbiota Food Health* 35: 57-67
132. Ganz T. 2004. Antimicrobial polypeptides. *J Leukoc Biol* 75: 34-8
133. Ganz T. 2003. Defensins: antimicrobial peptides of innate immunity. *Nat Rev Immunol* 3: 710-20
134. Mukherjee S, Zheng H, Derebe MG, Callenberg KM, Partch CL, Rollins D, Propheter DC, Rizo J, Grabe M, Jiang QX, Hooper LV. 2014. Antibacterial membrane attack by a pore-forming intestinal C-type lectin. *Nature* 505: 103-7
135. Gallo RL, Kim KJ, Bernfield M, Kozak CA, Zanetti M, Merluzzi L, Gennaro R. 1997. Identification of CRAMP, a cathelin-related antimicrobial peptide expressed in the embryonic and adult mouse. *J Biol Chem* 272: 13088-93
136. Fabisiak A, Murawska N, Fichna J. 2016. LL-37: Cathelicidin-related antimicrobial peptide with pleiotropic activity. *Pharmacol Rep* 68: 802-8
137. Lopez-Garcia B, Lee PH, Yamasaki K, Gallo RL. 2005. Anti-fungal activity of cathelicidins and their potential role in *Candida albicans* skin infection. *J Invest Dermatol* 125: 108-15
138. Xhindoli D, Pacor S, Benincasa M, Scocchi M, Gennaro R, Tossi A. 2016. The human cathelicidin LL-37--A pore-forming antibacterial peptide and host-cell modulator. *Biochim Biophys Acta* 1858: 546-66
139. Vaishnava S, Behrendt CL, Ismail AS, Eckmann L, Hooper LV. 2008. Paneth cells directly sense gut commensals and maintain homeostasis at the intestinal host-microbial interface. *Proc Natl Acad Sci U S A* 105: 20858-63
140. Loonen LM, Stolte EH, Jaklofsky MT, Meijerink M, Dekker J, van Baarlen P, Wells JM. 2014. REG3gamma-deficient mice have altered mucus distribution and increased mucosal inflammatory responses to the microbiota and enteric pathogens in the ileum. *Mucosal Immunol* 7: 939-47
141. Macpherson AJ, Geuking MB, McCoy KD. 2012. Homeland security: IgA immunity at the frontiers of the body. *Trends Immunol* 33: 160-7
142. Inamine T, Schnabl B. 2018. Immunoglobulin A and liver diseases. *J Gastroenterol* 53: 691-700
143. Mantis NJ, Rol N, Corthesy B. 2011. Secretory IgA's complex roles in immunity and mucosal homeostasis in the gut. *Mucosal Immunol* 4: 603-11
144. Phalipon A, Cardona A, Kraehenbuhl JP, Edelman L, Sansonetti PJ, Corthesy B. 2002. Secretory component: a new role in secretory IgA-mediated immune exclusion in vivo. *Immunity* 17: 107-15
145. Stokes CR, Soothill JF, Turner MW. 1975. Immune exclusion is a function of IgA. *Nature* 255: 745-6
146. Donaldson GP, Ladinsky MS, Yu KB, Sanders JG, Yoo BB, Chou WC, Conner ME, Earl AM, Knight R, Bjorkman PJ, Mazmanian SK. 2018. Gut microbiota utilize immunoglobulin A for mucosal colonization. *Science* 360: 795-800
147. Vaerman JP, Derijck-Langendries A, Rits M, Delacroix D. 1985. Neutralization of cholera toxin by rat bile secretory IgA antibodies. *Immunology* 54: 601-3
148. Yel L. 2010. Selective IgA deficiency. *J Clin Immunol* 30: 10-6
149. Harriman GR, Bogue M, Rogers P, Finegold M, Pacheco S, Bradley A, Zhang Y, Mbawuike IN. 1999. Targeted deletion of the IgA constant region in mice leads to IgA deficiency with alterations in expression of other Ig isotypes. *J Immunol* 162: 2521-9

150. Suzuki K, Meek B, Doi Y, Muramatsu M, Chiba T, Honjo T, Fagarasan S. 2004. Aberrant expansion of segmented filamentous bacteria in IgA-deficient gut. *Proc Natl Acad Sci U S A* 101: 1981-6
151. Langford TD, Housley MP, Boes M, Chen J, Kagnoff MF, Gillin FD, Eckmann L. 2002. Central importance of immunoglobulin A in host defense against *Giardia* spp. *Infect Immun* 70: 11-8
152. Wei M, Shinkura R, Doi Y, Maruya M, Fagarasan S, Honjo T. 2011. Mice carrying a knock-in mutation of *Aicda* resulting in a defect in somatic hypermutation have impaired gut homeostasis and compromised mucosal defense. *Nat Immunol* 12: 264-70
153. Bauer MA, Kainz K, Carmona-Gutierrez D, Madeo F. 2018. Microbial wars: Competition in ecological niches and within the microbiome. *Microb Cell* 5: 215-9
154. Litvak Y, Mon KKZ, Nguyen H, Chanthavixay G, Liou M, Velazquez EM, Kutter L, Alcantara MA, Byndloss MX, Tiffany CR, Walker GT, Faber F, Zhu Y, Bronner DN, Byndloss AJ, Tsolis RM, Zhou H, Baumler AJ. 2019. Commensal Enterobacteriaceae Protect against Salmonella Colonization through Oxygen Competition. *Cell Host Microbe* 25: 128-39 e5
155. Derrien M, Van Baarlen P, Hooiveld G, Norin E, Muller M, de Vos WM. 2011. Modulation of Mucosal Immune Response, Tolerance, and Proliferation in Mice Colonized by the Mucin-Degrader *Akkermansia muciniphila*. *Front Microbiol* 2: 166
156. Shin NR, Lee JC, Lee HY, Kim MS, Whon TW, Lee MS, Bae JW. 2014. An increase in the *Akkermansia* spp. population induced by metformin treatment improves glucose homeostasis in diet-induced obese mice. *Gut* 63: 727-35
157. Peng L, Li ZR, Green RS, Holzman IR, Lin J. 2009. Butyrate enhances the intestinal barrier by facilitating tight junction assembly via activation of AMP-activated protein kinase in Caco-2 cell monolayers. *J Nutr* 139: 1619-25
158. Hajjar AM, Ernst RK, Tsai JH, Wilson CB, Miller SI. 2002. Human Toll-like receptor 4 recognizes host-specific LPS modifications. *Nat Immunol* 3: 354-9
159. Di Lorenzo F, De Castro C, Silipo A, Molinaro A. 2019. Lipopolysaccharide structures of Gram-negative populations in the Gut Microbiota and effects on host interactions. *FEMS Microbiol Rev*
160. Wexler AG, Goodman AL. 2017. An insider's perspective: *Bacteroides* as a window into the microbiome. *Nat Microbiol* 2: 17026
161. Lopez-Siles M, Duncan SH, Garcia-Gil LJ, Martinez-Medina M. 2017. *Faecalibacterium prausnitzii*: from microbiology to diagnostics and prognostics. *ISME J* 11: 841-52
162. Turrone F, Milani C, Duranti S, Mahony J, van Sinderen D, Ventura M. 2018. Glycan Utilization and Cross-Feeding Activities by Bifidobacteria. *Trends Microbiol* 26: 339-50
163. Wexler HM. 2007. *Bacteroides*: the good, the bad, and the nitty-gritty. *Clin Microbiol Rev* 20: 593-621
164. Meijers B, Farre R, Dejongh S, Vicario M, Evenepoel P. 2018. Intestinal Barrier Function in Chronic Kidney Disease. *Toxins (Basel)* 10
165. Pastori D, Carnevale R, Nocella C, Novo M, Santulli M, Cammisotto V, Menichelli D, Pignatelli P, Violi F. 2017. Gut-Derived Serum Lipopolysaccharide is Associated With Enhanced Risk of Major Adverse Cardiovascular Events in Atrial Fibrillation: Effect of Adherence to Mediterranean Diet. *J Am Heart Assoc* 6
166. Hendriks T, Schnabl B. 2019. Antimicrobial proteins: intestinal guards to protect against liver disease. *J Gastroenterol* 54: 209-17
167. Coyte KZ, Schluter J, Foster KR. 2015. The ecology of the microbiome: Networks, competition, and stability. *Science* 350: 663-6
168. !!! INVALID CITATION !!! {}.
169. WHO. 2018. Global status report on alcohol and health 2018.
170. Bala S, Marcos M, Gattu A, Catalano D, Szabo G. 2014. Acute binge drinking increases serum endotoxin and bacterial DNA levels in healthy individuals. *PLoS One* 9: e96864

171. Prytz H, Bjerneboe M, Orskov F, Hilden M. 1973. Antibodies to Escherichia coli in alcoholic and non-alcoholic patients with cirrhosis of the liver or fatty liver. *Scand J Gastroenterol* 8: 433-8
172. Simjee AE, Hamilton-Miller JM, Thomas HC, Brumfitt W, Sherlock S. 1975. Antibodies to Escherichia coli in chronic liver diseases. *Gut* 16: 871-5
173. Llopis M, Cassard AM, Wrzosek L, Boschat L, Bruneau A, Ferrere G, Puchois V, Martin JC, Lepage P, Le Roy T, Lefevre L, Langelier B, Cailleux F, Gonzalez-Castro AM, Rabot S, Gaudin F, Agostini H, Prevot S, Berrebi D, Ciocan D, Jousse C, Naveau S, Gerard P, Perlemuter G. 2016. Intestinal microbiota contributes to individual susceptibility to alcoholic liver disease. *Gut* 65: 830-9
174. Hartmann P, Chu H, Duan Y, Schnabl B. 2019. Gut microbiota in liver disease: Too much is harmful, nothing at all is not helpful either. *Am J Physiol Gastrointest Liver Physiol*
175. Chen P, Starkel P, Turner JR, Ho SB, Schnabl B. 2015. Dysbiosis-induced intestinal inflammation activates tumor necrosis factor receptor I and mediates alcoholic liver disease in mice. *Hepatology* 61: 883-94
176. Adachi Y, Moore LE, Bradford BU, Gao W, Thurman RG. 1995. Antibiotics prevent liver injury in rats following long-term exposure to ethanol. *Gastroenterology* 108: 218-24
177. Chen P, Miyamoto Y, Mazagova M, Lee KC, Eckmann L, Schnabl B. 2015. Microbiota Protects Mice Against Acute Alcohol-Induced Liver Injury. *Alcohol Clin Exp Res* 39: 2313-23
178. Patel S, Behara R, Swanson GR, Forsyth CB, Voigt RM, Keshavarzian A. 2015. Alcohol and the Intestine. *Biomolecules* 5: 2573-88
179. Cho YE, Yu LR, Abdelmegeed MA, Yoo SH, Song BJ. 2018. Apoptosis of enterocytes and nitration of junctional complex proteins promote alcohol-induced gut leakiness and liver injury. *J Hepatol* 69: 142-53
180. Mir H, Meena AS, Chaudhry KK, Shukla PK, Gangwar R, Manda B, Padala MK, Shen L, Turner JR, Dietrich P, Dragatsis I, Rao R. 2015. Occludin deficiency promotes ethanol-induced disruption of colonic epithelial junctions, gut barrier dysfunction and liver damage in mice. *Biochim Biophys Acta*
181. Yan AW, Fouts DE, Brandl J, Starkel P, Torralba M, Schott E, Tsukamoto H, Nelson KE, Brenner DA, Schnabl B. 2011. Enteric dysbiosis associated with a mouse model of alcoholic liver disease. *Hepatology* 53: 96-105
182. Wang L, Fouts DE, Starkel P, Hartmann P, Chen P, Llorente C, DePew J, Moncera K, Ho SB, Brenner DA, Hooper LV, Schnabl B. 2016. Intestinal REG3 Lectins Protect against Alcoholic Steatohepatitis by Reducing Mucosa-Associated Microbiota and Preventing Bacterial Translocation. *Cell Host Microbe* 19: 227-39
183. Lu R, Voigt RM, Zhang Y, Kato I, Xia Y, Forsyth CB, Keshavarzian A, Sun J. 2017. Alcohol Injury Damages Intestinal Stem Cells. *Alcohol Clin Exp Res* 41: 727-34
184. Safari Z, Gerard P. 2019. The links between the gut microbiome and non-alcoholic fatty liver disease (NAFLD). *Cell Mol Life Sci* 76: 1541-58
185. Younossi ZM. 2019. Non-alcoholic fatty liver disease - A global public health perspective. *J Hepatol* 70: 531-44
186. Cui Y, Wang Q, Chang R, Zhou X, Xu C. 2019. Intestinal Barrier Function-Non-alcoholic Fatty Liver Disease Interactions and Possible Role of Gut Microbiota. *J Agric Food Chem* 67: 2754-62
187. Brun P, Castagliuolo I, Di Leo V, Buda A, Pinzani M, Palu G, Martines D. 2007. Increased intestinal permeability in obese mice: new evidence in the pathogenesis of nonalcoholic steatohepatitis. *Am J Physiol Gastrointest Liver Physiol* 292: G518-25
188. Yang SQ, Lin HZ, Lane MD, Clemens M, Diehl AM. 1997. Obesity increases sensitivity to endotoxin liver injury: implications for the pathogenesis of steatohepatitis. *Proc Natl Acad Sci U S A* 94: 2557-62

189. Miele L, Valenza V, La Torre G, Montalto M, Cammarota G, Ricci R, Masciana R, Forgione A, Gabrieli ML, Perotti G, Vecchio FM, Rapaccini G, Gasbarrini G, Day CP, Grieco A. 2009. Increased intestinal permeability and tight junction alterations in nonalcoholic fatty liver disease. *Hepatology* 49: 1877-87
190. Rahman K, Desai C, Iyer SS, Thorn NE, Kumar P, Liu Y, Smith T, Neish AS, Li H, Tan S, Wu P, Liu X, Yu Y, Farris AB, Nusrat A, Parkos CA, Anania FA. 2016. Loss of Junctional Adhesion Molecule A Promotes Severe Steatohepatitis in Mice on a Diet High in Saturated Fat, Fructose, and Cholesterol. *Gastroenterology* 151: 733-46 e12
191. Saltzman ET, Palacios T, Thomsen M, Vitetta L. 2018. Intestinal Microbiome Shifts, Dysbiosis, Inflammation, and Non-alcoholic Fatty Liver Disease. *Front Microbiol* 9: 61
192. Wang B, Jiang X, Cao M, Ge J, Bao Q, Tang L, Chen Y, Li L. 2016. Altered Fecal Microbiota Correlates with Liver Biochemistry in Nonobese Patients with Non-alcoholic Fatty Liver Disease. *Sci Rep* 6: 32002
193. Zhou D, Pan Q, Xin FZ, Zhang RN, He CX, Chen GY, Liu C, Chen YW, Fan JG. 2017. Sodium butyrate attenuates high-fat diet-induced steatohepatitis in mice by improving gut microbiota and gastrointestinal barrier. *World J Gastroenterol* 23: 60-75
194. Cani PD, Amar J, Iglesias MA, Poggi M, Knauf C, Bastelica D, Neyrinck AM, Fava F, Tuohy KM, Chabo C, Waget A, Delmee E, Cousin B, Sulpice T, Chamontin B, Ferrieres J, Tanti JF, Gibson GR, Casteilla L, Delzenne NM, Alessi MC, Burcelin R. 2007. Metabolic endotoxemia initiates obesity and insulin resistance. *Diabetes* 56: 1761-72
195. Iorga A, Dara L, Kaplowitz N. 2017. Drug-Induced Liver Injury: Cascade of Events Leading to Cell Death, Apoptosis or Necrosis. *Int J Mol Sci* 18
196. Garcia-Cortes M, Ortega-Alonso A, Lucena MI, Andrade RJ, Spanish Group for the Study of Drug-Induced Liver Disease I. 2018. Drug-induced liver injury: a safety review. *Expert Opin Drug Saf* 17: 795-804
197. Yoon E, Babar A, Choudhary M, Kutner M, Pysropoulos N. 2016. Acetaminophen-Induced Hepatotoxicity: a Comprehensive Update. *J Clin Transl Hepatol* 4: 131-42
198. Krenkel O, Mossanen JC, Tacke F. 2014. Immune mechanisms in acetaminophen-induced acute liver failure. *Hepatobiliary Surg Nutr* 3: 331-43
199. Su GL, Gong KQ, Fan MH, Kelley WM, Hsieh J, Sun JM, Hemmila MR, Arbabi S, Remick DG, Wang SC. 2005. Lipopolysaccharide-binding protein modulates acetaminophen-induced liver injury in mice. *Hepatology* 41: 187-95
200. Su GL, Hoesel LM, Bayliss J, Hemmila MR, Wang SC. 2010. Lipopolysaccharide binding protein inhibitory peptide protects against acetaminophen-induced hepatotoxicity. *Am J Physiol Gastrointest Liver Physiol* 299: G1319-25
201. Yang R, Zou X, Tenhunen J, Zhu S, Kajander H, Koskinen ML, Tonnessen TI. 2014. HMGB1 neutralization is associated with bacterial translocation during acetaminophen hepatotoxicity. *BMC Gastroenterol* 14: 66
202. Possamai LA, McPhail MJ, Quaglia A, Zingarelli V, Abeles RD, Tidswell R, Puthuchery Z, Rawal J, Karvellas CJ, Leslie EM, Hughes RD, Ma Y, Jassem W, Shawcross DL, Bernal W, Dharwan A, Heaton ND, Thursz M, Wendon JA, Mitry RR, Antoniadis CG. 2013. Character and temporal evolution of apoptosis in acetaminophen-induced acute liver failure\*. *Crit Care Med* 41: 2543-50
203. Schafer C, Schroder KR, Hoglinger O, Tollabimazraehno S, Lornejad-Schafer MR. 2013. Acetaminophen changes intestinal epithelial cell membrane properties, subsequently affecting absorption processes. *Cell Physiol Biochem* 32: 431-47
204. Li AP, Alam N, Amaral K, Ho MD, Loretz C, Mitchell W, Yang Q. 2018. Cryopreserved Human Intestinal Mucosal Epithelium: A Novel In Vitro Experimental System for the Evaluation of

- Enteric Drug Metabolism, Cytochrome P450 Induction, and Enterotoxicity. *Drug Metab Dispos* 46: 1562-71
205. Possamai LA, McPhail MJ, Khamri W, Wu B, Concas D, Harrison M, Williams R, Cox RD, Cox IJ, Anstee QM, Thursz MR. 2015. The role of intestinal microbiota in murine models of acetaminophen-induced hepatotoxicity. *Liver Int* 35: 764-73
  206. Gong S, Lan T, Zeng L, Luo H, Yang X, Li N, Chen X, Liu Z, Li R, Win S, Liu S, Zhou H, Schnabl B, Jiang Y, Kaplowitz N, Chen P. 2018. Gut microbiota mediates diurnal variation of acetaminophen induced acute liver injury in mice. *J Hepatol* 69: 51-9
  207. Fricker ZP, Lichtenstein DR. 2019. Primary Sclerosing Cholangitis: A Concise Review of Diagnosis and Management. *Dig Dis Sci* 64: 632-42
  208. Liao L, Schneider KM, Galvez EJC, Frissen M, Marschall HU, Su H, Hatting M, Wahlstrom A, Haybaeck J, Puchas P, Mohs A, Peng J, Bergheim I, Nier A, Hennings J, Reissing J, Zimmermann HW, Longerich T, Strowig T, Liedtke C, Cubero FJ, Trautwein C. 2019. Intestinal dysbiosis augments liver disease progression via NLRP3 in a murine model of primary sclerosing cholangitis. *Gut*
  209. Loftus EV, Jr., Harewood GC, Loftus CG, Tremaine WJ, Harmsen WS, Zinsmeister AR, Jewell DA, Sandborn WJ. 2005. PSC-IBD: a unique form of inflammatory bowel disease associated with primary sclerosing cholangitis. *Gut* 54: 91-6
  210. Nakamoto N, Sasaki N, Aoki R, Miyamoto K, Suda W, Teratani T, Suzuki T, Koda Y, Chu PS, Taniki N, Yamaguchi A, Kanamori M, Kamada N, Hattori M, Ashida H, Sakamoto M, Atarashi K, Narushima S, Yoshimura A, Honda K, Sato T, Kanai T. 2019. Gut pathobionts underlie intestinal barrier dysfunction and liver T helper 17 cell immune response in primary sclerosing cholangitis. *Nat Microbiol* 4: 492-503
  211. O'Toole A, Alakkari A, Keegan D, Doherty G, Mulcahy H, O'Donoghue D. 2012. Primary sclerosing cholangitis and disease distribution in inflammatory bowel disease. *Clin Gastroenterol Hepatol* 10: 439-41
  212. Sasatomi K, Noguchi K, Sakisaka S, Sata M, Tanikawa K. 1998. Abnormal accumulation of endotoxin in biliary epithelial cells in primary biliary cirrhosis and primary sclerosing cholangitis. *J Hepatol* 29: 409-16
  213. Tornai T, Palyu E, Vitalis Z, Tornai I, Tornai D, Antal-Szalmas P, Norman GL, Shums Z, Veres G, Dezsofi A, Par G, Par A, Orosz P, Szalay F, Lakatos PL, Papp M. 2017. Gut barrier failure biomarkers are associated with poor disease outcome in patients with primary sclerosing cholangitis. *World J Gastroenterol* 23: 5412-21
  214. Dhillon AK, Kummen M, Troseid M, Akra S, Liaskou E, Moum B, Vesterhus M, Karlsen TH, Seljeflot I, Hov JR. 2019. Circulating markers of gut barrier function associated with disease severity in primary sclerosing cholangitis. *Liver Int* 39: 371-81
  215. Liu R, Li X, Huang Z, Zhao D, Ganesh BS, Lai G, Pandak WM, Hylemon PB, Bajaj JS, Sanyal AJ, Zhou H. 2018. C/EBP homologous protein-induced loss of intestinal epithelial stemness contributes to bile duct ligation-induced cholestatic liver injury in mice. *Hepatology* 67: 1441-57
  216. Tedesco D, Thapa M, Chin CY, Ge Y, Gong M, Li J, Gumber S, Speck P, Elrod EJ, Burd EM, Kitchens WH, Magliocca JF, Adams AB, Weiss DS, Mohamadzadeh M, Grakoui A. 2018. Alterations in Intestinal Microbiota Lead to Production of Interleukin 17 by Intrahepatic gammadelta T-Cell Receptor-Positive Cells and Pathogenesis of Cholestatic Liver Disease. *Gastroenterology* 154: 2178-93
  217. Fuchs CD, Paumgartner G, Mlitz V, Kunczer V, Halilbasic E, Leditznig N, Wahlstrom A, Stahlman M, Thuringer A, Kashofer K, Stojakovic T, Marschall HU, Trauner M. 2018. Colesevelam attenuates cholestatic liver and bile duct injury in Mdr2(-/-) mice by modulating composition, signalling and excretion of faecal bile acids. *Gut*

218. Lopez-Ramirez MA, Fischer R, Torres-Badillo CC, Davies HA, Logan K, Pfizenmaier K, Male DK, Sharrack B, Romero IA. 2012. Role of caspases in cytokine-induced barrier breakdown in human brain endothelial cells. *J Immunol* 189: 3130-9
219. Grainger J, Daw R, Wemyss K. 2018. Systemic instruction of cell-mediated immunity by the intestinal microbiome. *F1000Res* 7
220. Benakis C, Brea D, Caballero S, Faraco G, Moore J, Murphy M, Sita G, Racchumi G, Ling L, Pamer EG, Iadecola C, Anrather J. 2016. Commensal microbiota affects ischemic stroke outcome by regulating intestinal gammadelta T cells. *Nat Med* 22: 516-23
221. Sudo N, Chida Y, Aiba Y, Sonoda J, Oyama N, Yu XN, Kubo C, Koga Y. 2004. Postnatal microbial colonization programs the hypothalamic-pituitary-adrenal system for stress response in mice. *J Physiol* 558: 263-75
222. Houser MC, Chang J, Factor SA, Molho ES, Zabetian CP, Hill-Burns EM, Payami H, Hertzberg VS, Tansey MG. 2018. Stool Immune Profiles Evince Gastrointestinal Inflammation in Parkinson's Disease. *Mov Disord* 33: 793-804
223. Forsyth CB, Shannon KM, Kordower JH, Voigt RM, Shaikh M, Jaglin JA, Estes JD, Dodiya HB, Keshavarzian A. 2011. Increased intestinal permeability correlates with sigmoid mucosa alpha-synuclein staining and endotoxin exposure markers in early Parkinson's disease. *PLoS One* 6: e28032
224. Sampson TR, Debelius JW, Thron T, Janssen S, Shastri GG, Ilhan ZE, Challis C, Schretter CE, Rocha S, Gradinaru V, Chesselet MF, Keshavarzian A, Shannon KM, Krajmalnik-Brown R, Wittung-Stafshede P, Knight R, Mazmanian SK. 2016. Gut Microbiota Regulate Motor Deficits and Neuroinflammation in a Model of Parkinson's Disease. *Cell* 167: 1469-80 e12
225. McGettigan BM, McMahan RH, Luo Y, Wang XX, Orlicky DJ, Porsche C, Levi M, Rosen HR. 2016. Sevelamer Improves Steatohepatitis, Inhibits Liver and Intestinal Farnesoid X Receptor (FXR), and Reverses Innate Immune Dysregulation in a Mouse Model of Non-alcoholic Fatty Liver Disease. *J Biol Chem* 291: 23058-67
226. Velayudham A, Dolganiuc A, Ellis M, Petrasek J, Kodys K, Mandrekar P, Szabo G. 2009. VSL#3 probiotic treatment attenuates fibrosis without changes in steatohepatitis in a diet-induced nonalcoholic steatohepatitis model in mice. *Hepatology* 49: 989-97
227. Braun T, Di Segni A, BenShoshan M, Neuman S, Levhar N, Bubis M, Picard O, Sosnovski K, Efroni G, Farage Barhom S, Glick Saar E, Lahad A, Weiss B, Yablecovitch D, Lahat A, Eliakim R, Kopylov U, Ben-Horin S, Haberman Y. 2019. Individualized Dynamics in the Gut Microbiota Precede Crohn's Disease Flares. *Am J Gastroenterol*
228. World Health Organization. 2014. *Global status report on alcohol and health 2014*. Geneva: World Health Organization. xiv, 376 p. pp.
229. Keshavarzian A, Holmes EW, Patel M, Iber F, Fields JZ, Pethkar S. 1999. Leaky gut in alcoholic cirrhosis: a possible mechanism for alcohol-induced liver damage. *Am J Gastroenterol* 94: 200-7
230. Bode C, Kugler V, Bode JC. 1987. Endotoxemia in patients with alcoholic and non-alcoholic cirrhosis and in subjects with no evidence of chronic liver disease following acute alcohol excess. *J Hepatol* 4: 8-14
231. Fukui H, Brauner B, Bode JC, Bode C. 1991. Plasma endotoxin concentrations in patients with alcoholic and non-alcoholic liver disease: reevaluation with an improved chromogenic assay. *J Hepatol* 12: 162-9
232. Parlesak A, Schafer C, Schutz T, Bode JC, Bode C. 2000. Increased intestinal permeability to macromolecules and endotoxemia in patients with chronic alcohol abuse in different stages of alcohol-induced liver disease. *J Hepatol* 32: 742-7
233. Szabo G. 2015. Gut-Liver Axis in Alcoholic Liver Disease. *Gastroenterology* 148: 30-6
234. Nagy LE. 2015. The Role of Innate Immunity in Alcoholic Liver Disease. *Alcohol Res* 37: 237-50

235. Lingaraju A, Long TM, Wang Y, Austin JR, 2nd, Turner JR. 2015. Conceptual barriers to understanding physical barriers. *Semin Cell Dev Biol* 42: 13-21
236. Koval M. 2015. The expanding diversity of roles for claudins. *Semin Cell Dev Biol* 42: 1-2
237. Samak G, Gangwar R, Meena AS, Rao RG, Shukla PK, Manda B, Narayanan D, Jaggar JH, Rao R. 2016. Calcium Channels and Oxidative Stress Mediate a Synergistic Disruption of Tight Junctions by Ethanol and Acetaldehyde in Caco-2 Cell Monolayers. *Sci Rep* 6: 38899
238. Tong J, Wang Y, Chang B, Zhang D, Liu P, Wang B. 2013. Activation of RhoA in alcohol-induced intestinal barrier dysfunction. *Inflammation* 36: 750-8
239. Tong J, Wang Y, Chang B, Zhang D, Wang B. 2013. Evidence for the Involvement of RhoA Signaling in the Ethanol-Induced Increase in Intestinal Epithelial Barrier Permeability. *Int J Mol Sci* 14: 3946-60
240. Elamin E, Masclee A, Dekker J, Jonkers D. 2014. Ethanol disrupts intestinal epithelial tight junction integrity through intracellular calcium-mediated Rho/ROCK activation. *Am J Physiol Gastrointest Liver Physiol* 306: G677-85
241. Ma TY, Nguyen D, Bui V, Nguyen H, Hoa N. 1999. Ethanol modulation of intestinal epithelial tight junction barrier. *Am J Physiol* 276: G965-74
242. Rubbens J, Brouwers J, Wolfs K, Adams E, Tack J, Augustijns P. 2016. Ethanol concentrations in the human gastrointestinal tract after intake of alcoholic beverages. *Eur J Pharm Sci* 86: 91-5
243. Rodriguez FD, Simonsson P, Alling C. 1992. A method for maintaining constant ethanol concentrations in cell culture media. *Alcohol Alcohol* 27: 309-13
244. Hidalgo IJ, Raub TJ, Borchardt RT. 1989. Characterization of the human colon carcinoma cell line (Caco-2) as a model system for intestinal epithelial permeability. *Gastroenterology* 96: 736-49
245. Yu Q, Wang Z, Li P, Yang Q. 2013. The effect of various absorption enhancers on tight junction in the human intestinal Caco-2 cell line. *Drug Dev Ind Pharm* 39: 587-92
246. Thomes PG, Osna NA, Bligh SM, Tuma DJ, Kharbanda KK. 2015. Role of defective methylation reactions in ethanol-induced dysregulation of intestinal barrier integrity. *Biochem Pharmacol* 96: 30-8
247. Mitzscherling K, Volynets V, Parlesak A. 2009. Phosphatidylcholine reverses ethanol-induced increase in transepithelial endotoxin permeability and abolishes transepithelial leukocyte activation. *Alcohol Clin Exp Res* 33: 557-62
248. Koivisto T, Salaspuro M. 1997. Effects of acetaldehyde on brush border enzyme activities in human colon adenocarcinoma cell line Caco-2. *Alcohol Clin Exp Res* 21: 1599-605
249. Ki SH, Park O, Zheng M, Morales-Ibanez O, Kolls JK, Bataller R, Gao B. 2010. Interleukin-22 treatment ameliorates alcoholic liver injury in a murine model of chronic-binge ethanol feeding: role of signal transducer and activator of transcription 3. *Hepatology* 52: 1291-300
250. Bernal W, Wendon J. 2013. Acute liver failure. *N Engl J Med* 369: 2525-34
251. Bunchorntavakul C, Reddy KR. 2013. Acetaminophen-related hepatotoxicity. *Clin Liver Dis* 17: 587-607, viii
252. Cooper SC, Aldridge RC, Shah T, Webb K, Nightingale P, Paris S, Gunson BK, Mutimer DJ, Neuberger JM. 2009. Outcomes of liver transplantation for paracetamol (acetaminophen)-induced hepatic failure. *Liver Transpl* 15: 1351-7
253. Neff SB, Neff TA, Kunkel SL, Hogaboam CM. 2003. Alterations in cytokine/chemokine expression during organ-to-organ communication established via acetaminophen-induced toxicity. *Exp Mol Pathol* 75: 187-93
254. da Silva MH, da Rosa EJ, de Carvalho NR, Dobrachinski F, da Rocha JB, Mauriz JL, Gonzalez-Gallego J, Soares FA. 2012. Acute brain damage induced by acetaminophen in mice: effect of diphenyl diselenide on oxidative stress and mitochondrial dysfunction. *Neurotox Res* 21: 334-44

255. Kennon-McGill S, McGill MR. 2018. Extrahepatic Toxicity of Acetaminophen: Critical Evaluation of the Evidence and Proposed Mechanisms. *J Clin Transl Res* 3
256. Jaeschke H, Duan L, Akakpo JY, Farhood A, Ramachandran A. 2018. The role of apoptosis in acetaminophen hepatotoxicity. *Food Chem Toxicol* 118: 709-18
257. Chopyk DM, Kumar P, Raeman R, Liu Y, Smith T, Anania FA. 2017. Dysregulation of junctional adhesion molecule-A contributes to ethanol-induced barrier disruption in intestinal epithelial cell monolayers. *Physiol Rep* 5
258. Mandal P, Feng Y, Lyons JD, Berger SB, Otani S, DeLaney A, Tharp GK, Maner-Smith K, Burd EM, Schaeffer M, Hoffman S, Capriotti C, Roback L, Young CB, Liang Z, Ortlund EA, DiPaolo NC, Bosinger S, Bertin J, Gough PJ, Brodsky IE, Coopersmith CM, Shayakhmetov DM, Mocarski ES. 2018. Caspase-8 Collaborates with Caspase-11 to Drive Tissue Damage and Execution of Endotoxic Shock. *Immunity* 49: 42-55 e6
259. Qiu W, Leibowitz B, Zhang L, Yu J. 2010. Growth factors protect intestinal stem cells from radiation-induced apoptosis by suppressing PUMA through the PI3K/AKT/p53 axis. *Oncogene* 29: 1622-32
260. Elmore S. 2007. Apoptosis: a review of programmed cell death. *Toxicol Pathol* 35: 495-516
261. Simpson KJ, Lukacs NW, McGregor AH, Harrison DJ, Strieter RM, Kunkel SL. 2000. Inhibition of tumour necrosis factor alpha does not prevent experimental paracetamol-induced hepatic necrosis. *J Pathol* 190: 489-94
262. Van Hauwermeiren F, Armaka M, Karagianni N, Kranidioti K, Vandenbroucke RE, Loges S, Van Roy M, Staelens J, Puimege L, Palagani A, Berghe WV, Victoratos P, Carmeliet P, Libert C, Kollias G. 2013. Safe TNF-based antitumor therapy following p55TNFR reduction in intestinal epithelium. *J Clin Invest* 123: 2590-603
263. Schulzke JD, Bojarski C, Zeissig S, Heller F, Gitter AH, Fromm M. 2006. Disrupted barrier function through epithelial cell apoptosis. *Ann N Y Acad Sci* 1072: 288-99
264. Ijiri K, Potten CS. 1987. Further studies on the response of intestinal crypt cells of different hierarchical status to eighteen different cytotoxic agents. *Br J Cancer* 55: 113-23
265. Du K, Ramachandran A, Weemhoff JL, Woolbright BL, Jaeschke AH, Chao X, Ding WX, Jaeschke H. 2019. Mito-tempo protects against acute liver injury but induces limited secondary apoptosis during the late phase of acetaminophen hepatotoxicity. *Arch Toxicol* 93: 163-78
266. Li X, Lin J, Lin Y, Huang Z, Pan Y, Cui P, Yu C, Cai C, Xia J. 2019. Hydrogen sulfide protects against acetaminophen-induced acute liver injury by inhibiting apoptosis via the JNK/MAPK signaling pathway. *J Cell Biochem* 120: 4385-97
267. Bundscherer AC, Malsy M, Gruber MA, Graf BM, Sinner B. 2018. Acetaminophen and Metamizole Induce Apoptosis in HT 29 and SW 480 Colon Carcinoma Cell Lines In Vitro. *Anticancer Res* 38: 745-51
268. Coopersmith CM, Stromberg PE, Dunne WM, Davis CG, Amiot DM, 2nd, Buchman TG, Karl IE, Hotchkiss RS. 2002. Inhibition of intestinal epithelial apoptosis and survival in a murine model of pneumonia-induced sepsis. *JAMA* 287: 1716-21
269. Bull-Otterson L, Feng W, Kirpich I, Wang Y, Qin X, Liu Y, Gobejishvili L, Joshi-Barve S, Ayvaz T, Petrosino J, Kong M, Barker D, McClain C, Barve S. 2013. Metagenomic analyses of alcohol induced pathogenic alterations in the intestinal microbiome and the effect of Lactobacillus rhamnosus GG treatment. *PLoS One* 8: e53028
270. Bergheim I, Bode C, Parlesak A. 2005. Distribution of cytochrome P450 2C, 2E1, 3A4, and 3A5 in human colon mucosa. *BMC Clin Pharmacol* 5: 4
271. Forsyth CB, Voigt RM, Shaikh M, Tang Y, Cederbaum AI, Turek FW, Keshavarzian A. 2013. Role for intestinal CYP2E1 in alcohol-induced circadian gene-mediated intestinal hyperpermeability. *Am J Physiol Gastrointest Liver Physiol* 305: G185-95

272. Ding X, Kaminsky LS. 2003. Human extrahepatic cytochromes P450: function in xenobiotic metabolism and tissue-selective chemical toxicity in the respiratory and gastrointestinal tracts. *Annu Rev Pharmacol Toxicol* 43: 149-73
273. Neuman MG, Malnick S, Maor Y, Nanau RM, Melzer E, Ferenci P, Seitz HK, Mueller S, Mell H, Samuel D, Cohen L, Kharbanda KK, Osna NA, Ganesan M, Thompson KJ, McKillop IH, Bautista A, Bataller R, French SW. 2015. Alcoholic liver disease: Clinical and translational research. *Exp Mol Pathol*
274. Fan S, Weight CM, Luissint AC, Hilgarth RS, Brazil JC, Ettl M, Nusrat A, Parkos CA. 2019. Role of JAM-A tyrosine phosphorylation in epithelial barrier dysfunction during intestinal inflammation. *Mol Biol Cell* 30: 566-78
275. Kamal AHM, Chakrabarty JK, Udden SMN, Zaki MH, Chowdhury SM. 2018. Inflammatory Proteomic Network Analysis of Statin-treated and Lipopolysaccharide-activated Macrophages. *Sci Rep* 8: 164
276. Yan KS, Janda CY, Chang J, Zheng GXY, Larkin KA, Luca VC, Chia LA, Mah AT, Han A, Terry JM, Ootani A, Roelf K, Lee M, Yuan J, Li X, Bolen CR, Wilhelmy J, Davies PS, Ueno H, von Furstenberg RJ, Belgrader P, Ziraldo SB, Ordonez H, Henning SJ, Wong MH, Snyder MP, Weissman IL, Hsueh AJ, Mikkelsen TS, Garcia KC, Kuo CJ. 2017. Non-equivalence of Wnt and R-spondin ligands during Lgr5(+) intestinal stem-cell self-renewal. *Nature* 545: 238-42